Quantum Superposition Phenomena in Chemistry within the Perspective of Quantum Information Theory

by

Mahir Hüseyin Yeşiller

A Dissertation Submitted to the
Graduate School of Sciences and Engineering
in Partial Fulfillment of the Requirements for
the Degree of

Master of Science

in

Physics

September, 2023

Quantum Superposition Phenomena in Chemistry within the Perspective of Quantum Information Theory

Koç University

Graduate School of Sciences and Engineering

This is to certify that I have examined this copy of a master's thesis by

Mahir Hüseyin Yeşiller

and have found that it is complete and satisfactory in all respects,
and that any and all revisions required by the final
examining committee have been made.

Committee Members:

_____

Prof. Dr. Özgür Müstecaplıoğlu (Advisor)

_____

Dr. Onur Pusuluk (Co-advisor)

_____

Assoc. Prof. Özgür Çakır

_____

Asst. Prof. Dr. Osman Barış Malcıoğlu

_____

Prof. Dr. Ahmet Levent Subaşı

Date: _____

ABSTRACT

Quantum Superposition Phenomena in Chemistry
within the Perspective of Quantum Information Theory
Mahir Hüseyin Yeşiller
Master of Science in Physics
September, 2023

In light of the first quantum revolution, our understanding of chemical bonding was enhanced by explaining covalent bonds through a quantum superposition of overlapping atomic orbitals between two atoms. On the other hand, the second quantum revolution showed that quantum superposition and its special forms, such as quantum correlations, are essential for the deep understanding of some physical processes, and they can also be used as a resource, like energy, in emerging quantum technologies. This thesis aims to delve into understanding chemical phenomena using the latest tools of quantum information theory that drive the second quantum revolution. In the first part, we introduced the concept of orbital discord from the perspective of the fermionic quantum information theory, which enables us to present the first proper and additive decomposition of the total orbital correlations into its classical and quantum parts. Our analysis of three representative molecules showed that in some instances, quantum orbital correlations can surpass their classical counterparts and survive even without orbital entanglement. In the second part, we investigate the concept of aromaticity, a multi-atom bonding phenomenon arising from the delocalization of electrons in closed-loop atom structures. To do that, we describe the delocalization of electrons in the π-electronic structures of archetypal monocyclic aromatic molecules as the superposition in overlapping atomic orbitals. Our findings reveal that the biorthogonal representation of atomic orbitals accurately captures the aromaticity order of these molecules, whereas its superposition in nonorthogonal representation mostly falls short due to neglecting the overlaps between atomic orbitals.

ÖZETÇE

Kuantum Enformasyon Teorisi Perspektifinde Kimyada Kuantum Üst Üste Binme Olayları
Mahir Hüseyin Yeşiller
Fizik, Yüksek Lisans
Eylül, 2023

İlk kuantum devriminin ışığında, iki atom arasında örtüşen atomik orbitallerin kuantum üst üste binmeleri ile kovalent bağları açıklayarak kimyasal bağlama hakkındaki anlayışımızı geliştirdik. Öte yandan, ikinci kuantum devrimi, kuantum üst üste binme olgusunun ve onun özel bir hali olan kuantum ilintilerin, bazı fiziksel olayların derinlemesine anlaşılması için esas olduğunu ve yeni kuantum teknolojilerinde, enerji gibi, kaynak olarak kullanılabileceğini gösterdi. Bu tez, ikinci kuantum devrimini süren kuantum enformasyon teorisinin güncel araçlarını kullanarak kimyasal olayları derinlemesine anlamakta yeni bir perspektif sunmayı hedeflemektedir. İlk bölümde, orbital uyuşmazlığı kavramını gelişme aşamasında olan fermiyonik kuantum enformasyon teorisi perspektifinden tanıtarak, toplam orbital ilintilerini klasik ve kuantum parçalarına uygun bir şekilde ayrıştırdık. Üç arketipik molekül üzerindeki analizimiz, bazı durumlarda kuantum orbital ilintilerin klasik karşılıklarını aşabileceğini ve orbital dolaşıklığı olmadan bile var olabileceğini gösterdi. İkinci bölümde, kapalı bir çevrim oluşturan atom yapılarındaki elektronların delokalizyonundan kaynaklanan çok atomlu bir bağlama olayı olan aromatikliği araştırıyoruz. Bunun için, en basit tek halkalı aromatik moleküllerin π-elektronik yapılarındaki elektronların delokalizyonunu, örtüşen atomik orbitallerdeki üst üste binmenin bir nicellemesi olarak tanımlıyoruz. Bulgularımız, atomik orbitallerin biortogonal temsilinin bu moleküllerin aromatiklik sırasını doğru bir şekilde yakaladığını, ancak nonortogonal temsilin orbital örtüşmelerindeki üst üste binmeleri göz ardı ederek çoğunlukla yetersiz kaldığını gösteriyor.

ACKNOWLEDGMENTS

Foremost, I extend my gratitude to Prof. Özgür E. Müstecaplıoğlu for his support and kindness throughout my master's journey. I am also thankful to all members of the QUEST group for their friendship.

I would like to express my deep appreciation to Prof. Ersin Yurtsever for the invaluable guidance and patience he exhibited in our quantum chemistry learning process during our TÜBİTAK project. I also want to thank my thesis committee: Prof. Levent Subaşı, Asst. Prof. Barış Malcıoğlu, and Assoc. Prof. Özgür Çakır for their insightful comments and constructive feedback on my thesis.

I wish to thank all the members of $\langle qX|Bio\rangle$ group, especially Dr. Gökhan Torun, Hasan Tunçer, and Doruk Can Alyürük, with whom I had the chance to work together in the project.

I want to express my gratitude to my family for their unconditional support and many thanks to my girlfriend, Ceren Bayraktar, for her support and patience, which I sometimes find hard to comprehend.

Last but certainly not least, I extend my deepest thanks to Dr. Onur Pusuluk. Words fall short in expressing my gratitude for not just being an inspiring supervisor with endless energy and curiosity but also for his enduring friendship.

TABLE OF CONTENTS

LIST OF TABLES

LIST OF FIGURES

ABBREVIATIONS

AO	Atomic orbital
BLW	Block localized wavefunction
CAS	Complete active space
CASSCF	Complete active space self-consistent field
cc-pVTZ	Correlation consistent-polarized valence triple zeta
CI	Configuration interaction
CISD	Configuration interaction singles and doubles
DI	Delocalization index
ESI	Electron share index
FLU	Fluctuation index
HF	Hartree-Fock
HOMA	Harmonic oscillator model of aromaticity
HOMO	Highest occupied molecular orbital
LOCC	Local operations and classical correlations
LUMO	Lowest unoccupied molecular orbital
MCI	Multicenter index
MO	Molecular orbital
MSCF	Multi-configurational self-consistent field
N-SSR	Number superselection rule
NICS	Nucleus-independent chemical shift
PDI	Para-delocalization index
P-SSR	Parity superselection rule
POVM	Positive operator-valued measure
RE	Resonance energy
RTS	Resource theory of superposition

STO	Slater-type orbital
VB	Valence bond
X-MR	X-Membered ring

Chapter 1

INTRODUCTION

The first quantum revolution fundamentally advanced our understanding of chemical bonding. The quantum mechanical description explains the formation of a covalent bond between two atoms as a consequence of overlapping atomic orbitals. The valence bond theory provides this explanation through the notion of localized *hybrid orbitals*, which arise from the superposition of atomic orbitals within the same atoms [1, 2]. On the other hand, the molecular orbital theory offers a complementary perspective: it introduces the superposition of atomic orbitals from distinct atoms, resulting in the generation of *molecular orbitals* that can span the entire molecule [3, 4]. Constructive superpositions lead to bonding molecular orbitals, whereas destructive superpositions give rise to antibonding molecular orbitals. Interestingly, despite their distinctive conceptual frameworks, both theories eventually align in their interpretation of chemical bonding at the limit of full configuration interaction [5–7].

In light of the second quantum revolution [8, 9], quantum states began to be viewed as resources for new quantum technologies. Herein, quantum correlations are the characteristic traits of such states, leading to the entire departure of quantum materials from classical lines of thought. An exemplary manifestation of quantum correlations is quantum entanglement [10]. Its role as a pivotal resource in the several quantum processes is undeniable, especially in quantum information processing tasks, including quantum teleportation [11–13], and quantum cryptography [14–16].

Over the past decade, several work has been done to gain a deeper understanding of chemical systems and processes using the toolbox of quantum information theory that drives the second quantum revolution. Specifically, findings from study-

ing two-orbital entanglement patterns in molecular electronic structures indicate that strong two-orbital entanglement frequently emerges between orbitals engaged in a specific bond [17–27]. However, from the first proposed study until Ref. [28], orbital entanglement was misidentified by measuring quantum mutual information which quantifies total correlations between orbitals including classical and quantum parts [29, 30]. Despite this misidentification, studies have demonstrated the practical utility of understanding orbital correlations. For instance, the computational efficiency of the quantum chemical density matrix renormalization group (DMRG) algorithm [31, 32] can be enhanced using knowledge of these correlations [33–35]. Furthermore, it has been shown that the computational efficiency of the complete active space method benefits from selecting active orbitals based on orbital correlations [36].

Lexin et al. [28] was the first to point out the misidentification of orbital entanglement and also to attempt for decomposition of total orbital-orbital correlations into classical and quantum parts. Even if they suggested a proper measure for orbital entanglement by a distance-based measure [29], their desegregation for classical and quantum correlations was not accurate since the classical correlation measure they used quantifies both classical and quantum correlations beyond entanglement [37], so their definition of quantum correlations was restricted to entanglement.

It's essential to recognize that quantum entanglement is a subset of broader quantum correlations, known as quantum discord [29, 30, 38]. Quantum discord is an important concept on its own because it is regarded as a resource in some tasks that are otherwise impossible, even in the absence of entanglement. Examples include the detection of quantum phase transitions [39], remote state preparation for quantum information processing [40], secure quantum key distribution in quantum [41] interferometric schemes in quantum metrology [42, 43], and controlling micro- and nanoscale heat flow in quantum thermodynamics [44, 45].

Consequently, if one wishes to dissect total orbital correlations into classical and quantum parts properly, quantum correlations must be defined and measured using the concept of orbital discord. Following this, in Chap. 3, we present the first comprehensive decomposition of total orbital correlations into classical and quantum

correlation by defining orbital discord. Also, the orbital-orbital correlations in the electronic ground states of some prototypical molecules are discussed to study the relationship between chemical bonding and orbital discord in the realm of molecular orbital theory.

Besides this, the orbital correlations have been previously analyzed based on the DMRG algorithm in the literature. Molecular orbitals were treated as two-qubit systems in most of these calculations, though each of them consists of two fermionic modes [46]. Here, we develop a fermionic information theoretical approach compatible with all conventional post-Hartree-Fock quantum chemistry algorithms [47].

Simple covalent bonds align well with the two-orbital correlation framework, allowing them to be analyzed through orbital-orbital correlations. Yet, complex bonding scenarios, where electrons are shared across multiple atoms, demand a multi-orbital correlation approach. For instance, for such phenomena, aromaticity—originating from the delocalization of electrons among more than two atoms forming a closed loop [48, 49]— cannot be reduced to mere two-orbital interactions. Instead, its essence lies in genuine multi-orbital bonds. In our understanding and analysis of aromaticity, multi-orbital correlations are inevitable and enable us to understand it further [24]. Yet, multi-orbital correlations are still an open problem because of the absence of a proper framework for genuine multipartite quantum correlations in quantum information theory [50–54].

Thus, we pursued a different approach to studying the delocalized electrons in aromaticity phenomena. In Chap. 4, we present a quantification method for the non-classicality in π-structures of planar aromatic molecules by measuring the shared quantum superposition within the localized and non-orthogonal atomic orbitals that form these structures.

Chapter 2

BACKGROUND

2.1 Basics of quantum mechanics

Here, we will provide a brief overview of the mathematical formalism pertaining to quantum states. We will abstain from delving into the dynamics of quantum states. Our focus will remain on elucidating the distinction between pure and mixed states, as well as the influence of measurements upon them. This will enable us to discuss the quantum information encapsulated within quantum states in the form of quantum correlations.

2.1.1 Quantum states and observables

A physical system is defined as a segment of the universe that we aim to describe. The *state* of this system contains the current information regarding the properties of interest. This information is generally obtained through the measurement of specific physical quantities, known as *observables*. In the quantum world, these concepts, as well as related physical notions, are associated with mathematical objects, such as vectors in a linear vector space and operators acting upon this space.

The state of a closed quantum system is represented by *a state vector* in a complex vector space that is equipped with an inner product. In Dirac's bra-ket notation, a state can be denoted by a *ket* $|\psi\rangle$. The corresponding vector space is known as a *Hilbert space* $\mathcal{H}$ containing all the required information about our system of interest.

The closure of the Hilbert space $\mathcal{H}$ under vector addition and multiplication reflects the *superposition principle* in the quantum world [55]. This principle indicates that any linear combination of the state vectors in $\mathcal{H}$, such as

$$|\psi\rangle = \alpha|\psi_1\rangle + \beta|\psi_2\rangle + \ldots, \tag{2.1}$$

is another vector belonging to $\mathcal{H}$. Superposed states imply that quantum systems are allowed to exist in multiple states simultaneously. Many unique quantum phenomena, like *entanglement*, arise from this principle.

Any state vector must be a unit vector in $\mathcal{H}$ to guarantee that the system is in a valid physical state. This requirement is known as the *normalization condition* that is expressed as $\langle\psi|\psi\rangle = 1$ for any state vector. Here, the mathematical object $\langle\psi|$—called *bra* in Dirac notation—represents the conjugate transpose of the ket $|\psi\rangle$ that lives in the dual space $\mathcal{H}^*$ of $\mathcal{H}$ and *bra-ket* $\langle\cdot|\cdot\rangle$ corresponds to the inner product of state vectors, mapping them into a complex number.

For discrete systems where the dimension of $\mathcal{H}$ is finite or countably infinite, a basis $\{|i\rangle\}$ of $\mathcal{H}$ comprises an ensemble of state vectors $\{|i\rangle\}$ such that any state vector $|\psi\rangle$ can be written as a coherent superposition of them:

$$|\psi\rangle = \sum_i c_i\,|i\rangle. \tag{2.2}$$

Here, the complex coefficients c_i are components of $|\psi\rangle$ in this basis, and $\{|i\rangle\}$ forms an orthonormal set satisfying the condition $\langle i|j\rangle = \delta_{i,j}$. Within such an orthonormal basis, each coefficient c_i is calculated as $c_i = \langle i|\psi\rangle$, and these coefficients correspond to the *probability amplitudes*. According to the *Born's probability rule* [56], the absolute square of these amplitudes, $|c_i|^2$, gives the probability of obtaining a measurement outcome associated with the basis state $|i\rangle$ upon measuring $|\psi\rangle$, expressed as $P(i) = |\langle i|\psi\rangle|^2$.

Every physical *observable*—that can be empirically measured on quantum systems such as energy, position, and momentum—is represented by a *Hermitian operator*[1], acting on the system's Hilbert space $\mathcal{H}$. For any Hermitian operator $\mathcal{O}$, one can find an orthonormal basis of $\mathcal{H}$ that corresponds to eigenvectors of $\mathcal{O}$, with associating real eigenvalues. Moreover, multiple physical observables can be associated with different Hermitian operators within the same basis, each having different spectra of real eigenvalues[2]. In every case, the Hermiticity of operators ensures that the eigenvalues are real numbers, hence representing possible measurement outcomes.

[1] A linear operator A is Hermitian if it is equal to its own Hermitian conjugate, $A = A^\dagger$.

[2] For instance, the number operator and the Hamiltonian in the quantum harmonic oscillator

Therefore, the spectral decomposition theorem allows us to express an observable in terms of its eigenvalues $\{\epsilon_i\}$ and eigenstates $\{|i\rangle\}$, as follows:

$$\mathcal{O} = \sum \epsilon_i \, |i\rangle\langle i|. \tag{2.3}$$

Here, the set $\{\epsilon_i\}$ represents possible real outcomes upon measuring the observable $\mathcal{O}$. Thus, when the physical quantity associated with operator $\mathcal{O}$ is measured on a quantum system in the state $|\psi\rangle$, the probability of obtaining a specific outcome e_i is $P(\epsilon_i) = |\langle i|\psi\rangle|^2$, in accordance with the Born's rule.

Until now, we have focused on systems described by a single state vector, known as *pure state*. This is because such a state provides complete information about the system of interest. However, in many practical scenarios, complete information about a system's state might not be obtainable. For instance, the polarization state of photons emitted from a source of unpolarized light can only be known statistically, having randomly oriented polarization. In such scenarios, the system could be in state $|\psi_1\rangle$ with classical probability p_1 or in state $|\psi_2\rangle$ with classical probability p_2, and so forth. These probabilities reflect our lack of knowledge about the system. Consequently, the system's state can be characterized as a statistical mixture of state vectors[3], known as *mixed states*.

A more comprehensive representation of a quantum system's state, including mixed states, is provided by the density matrix formalism[4]. In this framework, a generic density operator ρ can be expressed as [59]

$$\rho = \sum_i p_i \, |\psi_i\rangle\langle\psi_i|, \tag{2.4}$$

where $\{|\psi_i\rangle\}$ forms a set of state vectors that are prepared with corresponding

---

are examples of different Hermitian operators within the same basis. The former counts the number of particles while the latter represents the energy of the system.

[3]In some sources, mixed state is defined as an incoherent superposition of state vectors, indicating to distinguish mixed states from coherent superposition states.

[4]The roots of the density matrix framework can be traced back to the early foundational works of John von Neumann on quantum mechanics [57]. However, its practical importance for generalizing the concept of quantum state was overlooked for an extended period [58].

classical probabilities $\{p_i\}$. To represent a physically meaningful state, a density operator should satisfy the following three properties:

i. The trace of ρ equals one, indicating that the probabilities sum up to 1:

$$\mathrm{Tr}[\rho] = \sum_i p_i \underbrace{\mathrm{Tr}[|\psi_i\rangle\langle\psi_i|]}_{\langle\psi_i|\psi_i\rangle=1} = \sum_i p_i = 1. \tag{2.5}$$

ii. As its eigenvalues correspond to probabilities, ρ is a Hermitian operator, i.e., $\rho = \rho^\dagger$ as $|\psi_i\rangle\langle\psi_i|$ are Hermitian.

iii. As all probabilities are between 0 and 1, ρ is a positive-semidefinite operator, meaning that

$$\langle\phi|\rho|\phi\rangle = \sum_i p_i \, |\langle\phi|\psi_i\rangle|^2 \geq 0, \tag{2.6}$$

for any state vector $|\phi\rangle$.

Note that for a pure state $|\psi\rangle$, the density operator ρ is simply $\rho = |\psi\rangle\langle\psi|$. On the contrary, mixed states have more than one non-zero classical probability in Eq. (2.4).

The standard way of discriminating between pure or mixed states can be done via a straightforward criterion: $\mathrm{Tr}[\rho^2] = 1$ for pure states because $\rho^2 = (|\psi\rangle\langle\psi|)(|\psi\rangle\langle\psi|) = \rho$, whereas for mixed states, it is less than 1 since $\sum_i (p_i)^2 < 1$, given that $p_i^2 < p_i$ for any probability $0 < p_i < 1$.

Moreover, the density operator plays an invaluable role in characterizing states of subsystems. This is achieved through the introduction of *reduced density operator* [59]. Consider a composite system composed of two subsystems A and B represented by ρ_{AB} in $\mathcal{H}_{AB} = \mathcal{H}_A \otimes \mathcal{H}_B$. Such systems are called *bipartite*. The state of subsystem A is given by a reduced density operator ρ_A for A:

$$\rho_A = \mathrm{Tr}_B[\rho_{AB}], \tag{2.7}$$

where Tr_B represents the *partial trace* over subsystem B and is defined as $\mathrm{Tr}_B[\rho_A \otimes |\phi\rangle\langle\psi|_B] = \lambda\,\rho_A$ with $\lambda = \mathrm{Tr}[|\phi\rangle\langle\psi|_B] = \langle\psi|\phi\rangle_B$. This operation "traces out" or ignores the degrees of freedom related to subsystem B, thereby leaving solely those relevant to subsystem A.

2.1.2 Measurements

The measurement process in quantum mechanics represents a distinct departure from classical mechanics, showcasing a fundamental shift in how observations are understood and interpreted. Information acquisition becomes an active endeavor capable of altering the system's state. For instance, in quantum measurement, the system can be compelled to transition from a state of superposition to a specific state vector through a collapsing phenomenon. The standard formulation of quantum mechanics does not explain this phenomenon, but it is postulated as a premise [57, 60, 61]. The following subsection presents an overview of quantum measurements, with a focus on *projective measurement* and *positive operator-valued measurement* (POVM), which are commonly utilized in quantum information theory [59, 62].

Projective Measurement

Projective measurement, also called von Neumann measurement, is the primary mathematical construct used to describe the measurement process in quantum mechanics due to its direct connection with the concept of physical observables [57]. It is based on determining the state occupied by a given set of distinguishable (orthogonal) states. For example, consider an atom that can exist in either a lower energy ground state denoted by $|g\rangle$ or an excited state given by $|e\rangle$. Projective measurement lets us determine whether the atom resides in $|g\rangle$ or $|e\rangle$.

A projection measurement Π can be constructed from a complete set of orthogonal projection operators Π_i that satisfy the completeness relation $\sum_i \Pi_i = \mathbb{1}$, orthogonality condition $\Pi_i\Pi_j = \delta_{ij}\Pi_i$, and idempotent condition $\Pi_i^2 = \Pi_i$. In our atom example, we define two projection operators: $\Pi_g = |g\rangle\langle g|$ for $|g\rangle$, and $\Pi_e = |e\rangle\langle e|$ for $|e\rangle$, which fulfill all conditions because $|g\rangle$ and $|e\rangle$ are distinguishable.

One can express the spectral decomposition of a projection measurement Π, as illustrated for a generic physical observable in Eq. (2.3), using projective operators:

$$\Pi = \sum_i \epsilon_i \Pi_i, \tag{2.8}$$

where $\Pi_i = |i\rangle\langle i|$ represent projections onto the eigen-sector associated with the

eigenvalue ϵ_i. Thus, given a system characterized by the density operator ρ, the probability of obtaining result ϵ_i upon measurement with Π is given by

$$Pr(\epsilon_i) = \mathrm{Tr}[\rho\,\Pi_i]. \tag{2.9}$$

Upon performing a projective measurement Π, the quantum system's state "collapses" into a *post-measurement state* ρ'_i, with probability $Pr(\epsilon_i)$. Hence, for the observed outcome ϵ_i, the post-measurement state ρ'_i is given as [59]

$$\rho'_i = \frac{\Pi_i \rho \Pi_i^\dagger}{Pr(\epsilon_i)} = \frac{\Pi_i \rho \Pi_i}{\mathrm{Tr}[\rho \Pi_i]}. \tag{2.10}$$

This equation suggests that after measurement, the system's state can become the normalized projection of its initial (*pre*-measurement) state ρ onto the eigen-sector corresponding to the measurement outcome ϵ_i.

Positive Operator-Valued Measurement (POVM)

Quantum measurements can be performed in the more general framework of *positive operator valued measurement* (POVM) that may not have a one-to-one correspondence with the eigenstates of an observable. The key distinction of POVM, when compared to the projective measurement, is the relaxation of orthogonality and idempotent conditions for the measurement operators.

A POVM is still characterized by a set of positive Hermitian operators, denoted as $\{E_i\}$. While these operators satisfy the completeness relation, $\sum_i E_i = \mathbb{1}$, they aren't necessarily representing orthogonal projectors and might not commute with one another [59]. The probability of obtaining an outcome ϵ_i upon measuring the state ρ is given similarly to projective measurement such that $Pr(\epsilon_i) = \mathrm{Tr}[\rho\, E_i]$.

A distinctive feature of the POVM framework arises due to its flexibility regarding orthogonality. The number of positive operators E_i used to describe a POVM can exceed the dimension of the corresponding Hilbert space. This means a POVM performed on a given Hilbert space can then yield more outcomes than a projective measurement, as the outcomes are not uniquely associated with specific states of the quantum system. This peculiar attribute makes POVMs particularly useful for specific quantum tasks.

For instance, consider two quantum states, $|\psi\rangle$ and $|\phi\rangle$, that are indistinguishable (not orthogonal). Using a POVM, discrimination between these states can be achieved up to a certain success probability by suitably choosing the operators $\{E_i\}$ [63, 64]. However, such imperfect state discrimination can not be performed as a projection measurement because projection operators are mutually orthogonal, no matter which is selected.

2.2 Bipartite correlations in distinguishable systems

In the following section, we aim to provide a broad overview of quantum correlations and their quantification. A comprehensive exploration of the concepts and measures to be discussed can be found in Refs. [10, 38, 65–67].

2.2.1 Total correlations

Von Neumann entropy

Entropy serves as a measure of average uncertainty in the state of a physical system. For a classical system, consider X as a discrete random variable that can take a value x with probability p_x. The entropy of X quantifies the average uncertainty about X before learning the specific value x, or alternatively, how much information is gained upon learning x.

The entropy of X is defined by the *Shannon entropy* H [68], which is directly based on probabilities $\{p_x\}$:

$$H(X) = -\sum_x p_x \log_2 p_x, \tag{2.11}$$

where we assign $0 \log_2 0 \equiv 0$ for mathematical convenience.

Shannon entropy can be viewed as the classical limit of *von Neumann entropy* [57], which measures to the uncertainty of a quantum state. If a quantum state is represented by the density operator ρ, the von Neumann entropy is given by [69]

$$S(\rho) = -\operatorname{Tr}[\rho \log_2 \rho]. \tag{2.12}$$

Expressing ρ in terms of its eigendecomposition $\rho = \sum_i p_i |i\rangle\langle i|$, the von Neumann entropy can be further written as [70]

$$S(\rho) = -\sum_i p_i \log_2 p_i. \tag{2.13}$$

As discussed in Subsec. 2.1.1, pure states represent complete information about a quantum system, leading to a von Neumann entropy of zero. Conversely, maximal uncertainty in a d-dimensional Hilbert space is obtained by the completely mixed density operator, $\rho = \sum_i^d 1/d\, |\psi_i\rangle\langle\psi_i|$, which has the von Neumann entropy of $\log_2 d$.

Quantum mutual information

In classical systems involving two discrete random variables X and Y, the *mutual information* measures the amount of common information shared between the two variables. In terms of the Shannon entropy, the mutual information can be expressed as [59]

$$H(X:Y) = H(X) + H(Y) - H(X,Y), \tag{2.14}$$

where $H(X,Y) = -\sum_{x,y} p(x,y) \log_2 p(x,y)$ denotes the joint entropy of X and Y.

For quantum bipartite systems, the concept of mutual information is extended by replacing Shannon entropy with von Neumann entropy and classical random variables with reduced quantum states of the subsystems. This gives rise to the *quantum mutual information* I of a bipartite state ρ_{AB} which is defined as

$$I(\rho_{AB}) = S(\rho_A) + S(\rho_B) - S(\rho_{AB}). \tag{2.15}$$

While classical mutual information measures correlations between two random variables [71], quantum mutual information allows us to quantify the total correlations in a bipartite system, including quantum and classical parts [29, 30].

An important characteristic of quantum mutual information is that it becomes zero for states that can be represented as product states, $\rho_{AB} = \rho_A \otimes \rho_B$. Such states are therefore termed as *uncorrelated states*. Furthermore, for the pure bipartite states $\rho_{AB} = |\psi\rangle\langle\psi|_{AB}$, the entropies of the subsystems are equal, i.e., $S(\rho_A) = S(\rho_B)$, while the joint system has zero entropy, $S(\rho_{AB}) = 0$. Thus, $I(\rho_{AB}) = 2S(\rho_A) = 2S(\rho_B)$.

Quantum relative entropy

Another important entropy measure in the quantum world is the *quantum relative entropy*. Analogous to the Kullback-Leibler distance in classical information theory [71], the quantum relative entropy quantifies the distinguishability between two quantum states [72, 73]:

$$S(\rho||\sigma) = -\operatorname{Tr}\left[\rho\left(\log_2\rho - \log_2\sigma\right)\right]. \tag{2.16}$$

Thus, $S(\rho||\rho) = 0$ for any quantum state ρ.

One can express the total correlation in Eq. (2.15) by considering the quantum relative entropy between the state ρ of interest and the closest product state σ to ρ [37]:

$$I(\rho) = \min_{\{\sigma\in\mathcal{P}\}} S(\rho||\sigma), \tag{2.17}$$

where the minimum is performed over all product states in the set $\mathcal{P}$, aiming to find the closest one to ρ.

2.2.2 Entanglement

A bipartite pure $|\psi\rangle_{AB}$, living in the total Hilbert space $\mathcal{H}_{AB} = \mathcal{H}_A \otimes \mathcal{H}_B$, can be represented as

$$|\psi\rangle_{AB} = \sum_{ij} c_{ij}\,|i\rangle_A \otimes |j\rangle_B\,, \tag{2.18}$$

where $\{|i\rangle_A\}$ and $\{|j\rangle_B\}$ denote orthonormal bases of the local Hilbert spaces $\mathcal{H}_A$ and $\mathcal{H}_B$ respectively, while the set $\{|i\rangle_A \otimes |j\rangle_B\}$ forms a basis for $\mathcal{H}_{AB}$.

A bipartite state is deemed *separable* if and only if it can be written in the product form:

$$|\psi\rangle_{AB} = \sum_i a_i\,|i\rangle_A \otimes \sum_j b_j\,|j\rangle_B\,, \tag{2.19}$$

which means that $c_{ij} = a_i\,b_j$ in Eq. (2.18). Conversely, any pure state in $\mathcal{H}_{AB}$ is described as *entangled* if it cannot be separated like the above equation [74], i.e., if $c_{ij} \neq a_i\,b_j$.

The *Schmidt decomposition* is one way that allows us to determine whether a bipartite pure state is entangled or separable. Any such state $|\psi\rangle_{AB}$ can be rewritten in its Schmidt form:

$$|\psi\rangle_{AB} = \sum_i \lambda_i |u_i\rangle_A \otimes |w_i\rangle_B , \tag{2.20}$$

where $\{|u_i\rangle\}$ and $\{|w_i\rangle\}$ are respectively orthogonal bases for subsystems A and B, often referred to as the *Schmidt bases*. The expansion coefficients $\{\lambda_i\}$, known as *Schmidt coefficients*, satisfy the conditions $\lambda_i \geq 0$ and $\sum_i \lambda_i^2 = 1$.

The entanglement properties of a pure bipartite state are embedded in its Schmidt coefficients, which are calculated from the eigenvalues of $\mathrm{Tr}_B[|\psi_{AB}\rangle \langle\psi_{AB}|]$. The *Schmidt number*, the count of nonzero Schmidt coefficients λ_i, provides us that a Schmidt number of 1 denotes a separable pure state, while a Schmidt number greater than 1 indicates an entangled pure state.

For mixed bipartite states, a state is considered separable if it can be written as a convex combination of product states [75], as follows:

$$\rho_{AB} = \sum_i p_i \rho_A^i \otimes \rho_A^i, \tag{2.21}$$

where $\{p_i\}$ are classical probabilities satisfying $\sum_i p_i = 1$. If a mixed state cannot adopt this form, it is classified as entangled. Unlike pure separable states, mixed separable states can exhibit both classical and quantum correlations. These quantum correlations are often referred to as *quantum correlations beyond entanglement* and will be discussed in Subsec 2.2.3.

The above definition that extends the concept of entanglement to mixed states was proposed by Werner [75]. His motivation is based on the fact that separable mixed bipartite states can be prepared using *local quantum operations and classical communication* (LOCC) in two laboratories far from each other [76]. These states might also possess classically correlated through classical communication channels, such as telephones. However, entangled states cannot be prepared via local operations, and the amount of entanglement can not be increased by classical communication.

One way to determine the separability of a bipartite mixed state is achievable through the Peres–Horodecki criterion [77, 78]. While the Schmidt decomposition does not extend directly to mixed states, the Peres-Horodecki criterion can be applied to pure and mixed states.

The Peres-Horodecki criterion relies on the *partial transpose* operation. A generic bipartite density operator ρ_{AB} acting on $\mathcal{H}_{AB}$ can be written in the form:

$$\rho_{AB} = \sum_{i,j,k,l} p_{ijkl} \left|i\right\rangle \left\langle j\right| \otimes \left|k\right\rangle \left\langle l\right| . \tag{2.22}$$

The partial transpose of ρ with respect to one of the subsystems (for instance, subsystem B) is defined as

$$\rho_{AB}^{T_B} = (\mathbb{1} \otimes T)\, \rho_{AB} = \sum_{i,j,k,l} p_{ijlk} \left|i\right\rangle \left\langle j\right| \otimes \left|k\right\rangle \left\langle l\right| . \tag{2.23}$$

The *partial transpose operation* T involves transposing the state within one subsystem's space while the other subsystem's state (in this case, subsystem A) remains unaffected. The transpose of ρ_{AB} comprises the swap of the kets and bras within the transposed subsystem's terms.

According to the Peres-Horodecki criterion, a bipartite state ρ_{AB} is separable if all eigenvalues of $\rho_{AB}^{T_B}$ are non-negative. On the contrary, if $\rho_{AB}^{T_B}$ has at least one negative eigenvalue, then the state ρ_{AB} is considered entangled. This criterion serves as a powerful witness for diagnosing entanglement in quantum states.

Entanglement Measures

The "resourcefulness" of a quantum state in accomplishing tasks beyond classical capabilities is evaluated by the amount of entanglement it possesses. Unlike the entanglement witnesses, such as Schmidt number and Peres-Horodecki criterion, entanglement measures, denoted as E, provide to quantify and order the degree of entanglement present in quantum states.

Several entanglement measures have been developed, each exhibiting distinct strengths and weaknesses [10, 65]. In general, a proper measure for any quantum resource must fulfill some rigid mathematical requirements like nonnegativity, con-

vexity, subadditivity [65, 79]. However, without delving deep into too much mathematical detail, it suffices to know that a robust entanglement measure typically satisfies the following two criteria [10]:

1. *Non-increase of E under LOCC.* The most noteworthy property of any entanglement measure, which is proposed by Ref. [72], ensures that under LOCC, separable states can't be converted into entangled ones, and the degree of entanglement within a quantum state does not increase. Measures that adhere to this condition are termed *entanglement monotones*.

2. *Vanishing of E for only separable states.* This implies that a measure E should be zero only for separable states. If it is not, then the state is considered entangled. Although a genuine measure E should satisfy this condition, there exist other measures that do not fulfill this criterion but are still useful. Measures meeting this condition are called *faithful*.

For pure bipartite states, the entanglement is uniquely measured by the *entanglement entropy* E_E [80, 81]:

$$E_E(|\psi\rangle_{AB}) = S(\rho_{A/B}) = -\operatorname{Tr}\left[\rho_{A/B}\log_2\rho_{A/B}\right], \tag{2.24}$$

Quantifying entanglement in a bipartite pure state corresponds to the degree of mixedness in its reduced states. The entanglement entropy E_E is a reliable measure since it vanishes for separable states and attains a maximum value for the Bell states.

For the study of mixed states, the convex roof and distance-based measures are the two primary classes of entanglement measures [10, 65]. The *entanglement of formation* E_F represents one of the most popular and operationally meaningful convex roof measures. Because it extends the concept of entanglement entropy to mixed states through the convex roof construction[82]:

$$E_F(\rho) = \min_{\{p_i,|\psi_i\rangle\}} p_i\, E_E\left(|\psi_i\rangle\right), \tag{2.25}$$

where the minimum is performed over all the possible pure state decompositions of ρ,

with positive probabilities p_i such that $\rho = \sum_i p_i \left|\psi_i\right\rangle \left\langle\psi_i\right|$ [5]. Although minimization in Eq. (2.25) is challenging to evaluate in general, Wootters [83, 84] presented a closed expression for E_F applicable to two-qubit mixed states:

$$E_F(\rho) = h\left(\frac{1}{2} + \frac{1}{2}\sqrt{1 - C^2(\rho)}\right), \tag{2.26}$$

where $h(x) = x\log_2 x - (1-x)\log_2(1-x)$ and the concurrence $C(\rho) = \max\{0, \lambda_1 - \lambda_2 - \lambda_3 - \lambda_4\}$, where λ_i are the square roots of the eigenvalues, sorted in descending order, of the operator $\rho(\sigma_y \otimes \sigma_y)\rho^*(\sigma_y \otimes \sigma_y)$

Similar to the entanglement of formation, other convex roof measures exist, such as the entanglement cost E_C and the entanglement of distillation E_D. These measures are also both monotonic and faithful, making them useful tools for entanglement quantification. For a more detailed discussion on them, Refs. [10, 65] are recommended.

The second class of entanglement measures originates from the concept of "distance" between quantum states. Measures from this class can be generally expressed as [72]

$$E(\rho) = \min_{\sigma\in\mathcal{S}} \mathcal{D}(\rho||\sigma), \tag{2.27}$$

where $\mathcal{D}$ represents a measure of the distance between ρ and σ, and the minimum is taken over the set $\mathcal{S}$ of separable states to find the separable state σ closest to ρ.

A distance measure $\mathcal{D}$ can be utilized in Eq. (2.27), if it does not increase under non-local quantum operations, meaning that $\mathcal{D}(\mathcal{O}(\rho)||\mathcal{O}(\sigma)) \leq \mathcal{D}(\rho||\sigma)$ for any non-local quantum operation such that $\mathcal{O} \neq \mathcal{O}_A \otimes \mathcal{O}_B$. Additionally, $\mathcal{D}$ must vanish on separable states since $\mathcal{D}(\rho||\sigma) = 0$ if and only if $\rho = \sigma \in \mathcal{H}_{AB}$.

Among the distance-based entanglement measures, the *relative entropy of entanglement* is the most popular one. It is defined as [85]

$$E_{RE}(\rho) = \min_{\sigma\in\mathcal{S}} S(\rho||\sigma). \tag{2.28}$$

Here, $\mathcal{S}(\rho||\sigma)$ is the quantum relative entropy between ρ and σ, defined in Eq. (2.16). One of the attractions of the relative entropy-based entanglement measure is that

[5] Unless otherwise stated, the remainder of this section will assume that all states represent a bipartite system, i.e., $\rho \equiv \rho_{AB}$.

relativistic entropy has an important place in quantum information theory [73]. Furthermore, it corresponds to the entanglement entropy E_E of the reduced states for pure states.

Another intriguing set of entanglement measures, which do not fit into the previously mentioned categories, is based on the Peres–Horodecki criterion. A key distinction of these measures from the others is their computational ease, despite their lack of faithfulness.

One such entanglement measure is the *negativity* $\mathcal{N}$, which was defined for any bipartite quantum system in Ref. [86] as a "computable measure of entanglement". It is given by

$$\mathcal{N}(\rho) = \frac{||\rho^{T_B}|| - 1}{2}. \tag{2.29}$$

Here, $||\cdot||$ denotes trace norm, given by $||\sigma|| = \mathrm{Tr}\left[\sqrt{\sigma\sigma^\dagger}\right]$ for any density operator σ. The subtraction of 1 and division by 2 ensure that the negativity is always zero for separable states. Importantly, negativity is an entanglement monotone, such that $\mathcal{N}\left(\mathcal{O}(\rho)\right) \leq \mathcal{N}(\rho)$ for any non-local quantum operation $\mathcal{O} \in \mathcal{H}_{AB}$.

The negativity measure can be also presented using the eigenvalues of $\sqrt{\rho^{T_B}(\rho^{T_B})^\dagger}$:

$$\mathcal{N}(\rho) = \left|\sum_{\lambda_i<0} \lambda_i\right| = \sum_i \frac{|\lambda_i| - \lambda_i}{2}, \tag{2.30}$$

where $\{\lambda_i\}$ is the set of eigenvalues.

Another entanglement measure associated with the same criteria is the *logarithmic negativity* E_N, defined in Ref. [87] as

$$E_N(\rho) = \log_2 ||\rho^{T_B}||. \tag{2.31}$$

Like negativity, the logarithmic negativity is an entanglement monotone but is not faithful. Its computational ease makes it especially appealing. Furthermore, its relation to the negativity can be expressed as

$$E_N(\rho) = \log_2 ||2\mathcal{N}(\rho) - 1||. \tag{2.32}$$

Although negativity and logarithmic negativity are valuable tools for quantifying entanglement and they become zero for separable states, there are instances where

a mixed state remains inseparable but all eigenvalues of its partial transpose are positive [88]. Such mixed states are known as *bound entangled states* [89].

2.2.3 Quantum discord

For a very long time, entanglement was believed to be responsible for all the correlations of quantum mechanical origin. However, the advent of quantum discord unveiled that quantum correlation could exist even in separable states. The term "quantum discord" refers to this first identified measure of quantum correlations beyond entanglement. To delve deeper into quantum discord and other quantum correlations beyond entanglement, you can look at Refs. [38, 66, 67].

The seminal work by Ollivier and Zurek [30] showed that the mixed separable states, as defined in Eq. (2.21), might possess inherent quantum properties. Such quantumness could be perturbed by local measurements because there is a loss of shared information caused by these local measurements.

To explore this phenomenon, let's introduce a subclass of bipartite mixed separable states, which remain unaffected by local projective measurements on one of their subsystems. Such a state is represented as

$$\rho_{cq} = \sum_i p_i \left|i\right\rangle \left\langle i\right| \otimes \rho_i^B, \tag{2.33}$$

where $\{|i\rangle\}$ are the orthonormal basis in $\mathcal{H}_A$ with nonnegative probabilities p_i, and $\{\rho_i^B\}$ are the quantum states in $\mathcal{H}_B$. The mixed separable states having the form of ρ_{cq} are called quantum-classical[6] because any local measurements on subsystem A do not disturb the global state. This can be shown as

$$\rho_{cq}^{\Pi^A} = \sum_i p_i \left(\Pi_i^A \otimes \mathbb{1}\right) \left(\left|i\right\rangle \left\langle i\right| \otimes \rho_i^B\right) \left(\Pi_i^A \otimes \mathbb{1}\right) = \rho_{cq} \tag{2.34}$$

where $\{\Pi_i^A = |i\rangle \langle i|\}$ are the measurement operators for a projective measurement on A in the basis $\{|i\rangle\}$.

A disruption of the quantum part via local measurements on the "classical" part reflects a quantum nature of correlations between two subsystems in this mixed

[6]Similarly, a *quantum-classical* state can be defined as in form $\rho_{qc} = \sum_i p_i \rho_i^A \otimes |i\rangle \langle i|$.

separable state. A primary and commonly used quantification of these quantum correlations is called *quantum discord*.

To quantify discord, Ollivier and Zurek [30] observed that while the two expressions of mutual information are consistently identical in classical information theory, their quantum counterparts can differ in some mixed separable states. This difference essentially characterizes the quantum discord.

As previously mentioned in Subsec. 2.2.1, the quantity H in Eq. (2.14) is a well-established expression of mutual information in classical information theory, and its quantum counterpart I, Eq. (2.15), has been recognized as a comprehensive measure of total correlations in a bipartite quantum state.

The secondary expression of classical mutual information, represented by $J(X:Y)$, involves the concept of conditional entropy and is introduced as [59, 62]

$$J(X:Y) = H(X) - H(X|Y). \tag{2.35}$$

Here, the conditional entropy $H(X|Y)$ quantifies the uncertainty of a random variable X conditional on knowing the value of another random variable Y. This can be mathematically defined as

$$H(X|Y) = \sum_y p_y H(X|y), \tag{2.36}$$

where p_y is the probability of Y being y, and $H(X|y)$ is the entropy of X based on knowing a specific realization y of Y.

Extending this idea to the quantum realm, the counterpart of $H(X|y)$ for a bipartite quantum system is the entropy of one subsystem conditional on a particular outcome of the local measurement on another subsystem. Thus, for a bipartite quantum state ρ_{AB}, we can express the entropy of ρ_A conditioned on a projective measurement on subsystem B as [30]

$$S\left(\rho_{AB}|\{\Pi_i^B\}\right) = \sum_i p_i S\left(\rho_{A|\Pi_i^B}\right), \tag{2.37}$$

where $\{\Pi_i^B\}$ denotes the measurement operators of a projective measurement Π^B, and the state $\rho_{A|\Pi_i^B} = \mathrm{Tr}_B[\Pi_i^B \rho_{AB}]/p_i$ is the post-measurement reduced state of subsystem A with corresponding probability $p_i = \mathrm{Tr}\left[\Pi_i^B \rho_{AB}\right]$.

Following this, the second expression J in Eq. (2.35) can be extended to a quantum system as follows:

$$J_{\Pi^B}(\rho_{AB}) = S(\rho_A) - S\left(\rho_{AB}|\{\Pi_i^B\}\right), \tag{2.38}$$

where the subscript Π^B in $J_{\Pi^B}(\rho_{AB})$ indicates the dependence of this on the choice of a local projective measurement on B. The expression J_{Π^B} then quantifies the amount of information obtained about A through a local measurement on B.

Building upon these definitions, Ollivier and Zurek identified the quantum discord as the difference between the aforementioned quantum counterparts of the two classical mutual information quantities [30]:

$$D_{\Pi^B}(\rho_{AB}) = I(\rho_{AB}) - J_{\Pi^B}(\rho_{AB}) \tag{2.39}$$

This means the quantum discord effectively quantifies the amount of shared information or correlation that is inaccessible via local measurements on B.

Notably, the quantum discord is not symmetric under swapping subsystems A and B, i.e., $D_{\Pi^B}(\rho_{AB}) \neq D_{\Pi^A}(\rho_{BA})$. While D_{Π^B} vanishes for classical-quantum states ρ_{qc} because such states can be disturbed by local measurements on B, it is not necessarily zero for classical-quantum states ρ_{cq}, highlighting its asymmetry.

One can easily define the *measurement-independent discord* by taking the minimum over all possible local projective measurements on B:

$$D_B(\rho_{AB}) = \min_{\Pi^B} D_{\Pi^B}(\rho_{AB}) \tag{2.40}$$

The above minimization allows us to determine the measurement that causes the least disturbance to A while maximizing the information extracted about A by measuring B.

Around the same time, Henderson and Vedral [29] introduced a measure of *classical correlation* C_B in bipartite quantum states. This is defined as determining the maximum disturbance of Eq. (2.39) over all possible POVM performed on subsystem B:

$$C_B(\rho_{AB}) = \max_{E^B} J_{E^B}(\rho_{AB}) = \max_{E^B} \left[S(\rho_A) - S\left(\rho_{AB}|\{E_i^B\}\right)\right]. \tag{2.41}$$

Given that all quantum correlations including entanglement are perturbed by local measurements, the maximum disturbance of subsystem A ensures that C_B only quantifies all classical correlations from any bipartite quantum state. Note that, as discussed in Subsec. 2.1.2, one can perform the above optimization via projection measurements instead of POVMs without loss of generality.

In summation, quantum discord can be defined as the difference between the quantum mutual information I and the classical correlation C_B [29]:

$$D_B(\rho_{AB}) = I(\rho_{AB}) - C_B(\rho_{AB}). \tag{2.42}$$

Similar to Eqs. (2.39) and (2.40), this quantity too is nonnegative and vanished in the case of quantum-classical states only. In the discussions of Chap. 3, we will utilize this definition as our measure of quantum correlations beyond entanglement.

2.3 Electronic structure theory

The study of electronic structure theory forms the foundational framework for understanding the behavior of electrons within atoms and molecules. This realm of quantum chemistry plays a vital role in explaining chemical bonding, reaction mechanisms, and various physicochemical properties of matter [90]. At the core of electronic structure theory is the molecular Hamiltonian, which describes all interactions among electrons, nuclei, and between electrons and nuclei. Since even the computational demands of solving its time-independent Schrödinger equation increase exponentially with the size of the system [91], approximate methods and corresponding numerical applications have been developed to solve this problem [4, 47].

The following section will delve into the fundamental parts of electronic structure theory. We will introduce the molecular Hamiltonian, discuss the concept of antisymmetric wave functions, describe the Hartree-Fock (HF) method, and some post-HF methods used in the subsequent research chapters.[7]

[7]The content here is mostly based on Refs. [4, 47, 90].

2.3.1 The molecular Hamiltonian

The non-relativistic Hamiltonian H_{mol} that represents the total energy for a molecular system consisting of n electrons and N nuclei is given by [90]:

$$H_{\text{mol}} = -\frac{1}{2}\sum_{i}^{n}\nabla_i^2 - \sum_{A}^{N}\frac{1}{2M_A}\nabla_A^2 - \sum_{A,i}\frac{Z_A}{r_{Ai}} + \sum_{A>B}\frac{Z_A Z_B}{R_{AB}} + \sum_{i>j}\frac{1}{r_{ij}}, \tag{2.43}$$

where i, j denote electrons and A, B denote nuclei, with $r_{ij} = |\mathbf{r}_i - \mathbf{r}_j|$, $R_{Ai} = |\mathbf{R}_A - \mathbf{r}_i|$, and $R_{AB} = |\mathbf{R}_A - \mathbf{R}_B|$. Each term within H_{mol} corresponds to a specific facet of the system. The initial term represents the kinetic energy attributed to the electrons, while the subsequent term accounts for the kinetic energy associated with the nuclei. While the third one embodies the attractive interactions between electrons and nuclei, the fourth term encapsulates the repulsive forces among distinct nuclei. Lastly, the fifth term characterizes the repulsion arising from electron-electron interactions.

The *Born-Oppenheimer approximation* assumes the nuclear motion to be considerably slower than the electron motion due to the substantial mass difference [92]. This approximation allows us to neglect the nuclear kinetic energy in comparison to the faster electron dynamics, leading to the derivation of the electronic Hamiltonian H_{el} from H_{mol}:

$$H_{\text{el}} = -\frac{1}{2}\sum_{i}^{n}\nabla_i^2 - \sum_{A,i}\frac{Z_A}{r_{Ai}} + \sum_{A>B}\frac{Z_A Z_B}{R_{AB}} + \sum_{i>j}\frac{1}{r_{ij}}. \tag{2.44}$$

The electronic part H_{el} omits the kinetic energy of the nuclei, which is the second term in H_{mol}. The rest of the terms remain identical to those in H_{mol}.

The electronic Hamiltonian in Eq. (2.44) can be deconstructed into its integral parts [90]:

$$H_{\text{el}} = \sum_{i}^{n}\hat{h}(i) + \sum_{i<j}^{n}\hat{g}(i,j) + V_N. \tag{2.45}$$

Here, $\hat{h}(i)$ encompasses the kinetic energy of the i-th electron and its interaction with all the nuclei:

$$\hat{h}(i) = -\frac{1}{2}\nabla_i^2 + \sum_{A}\frac{Z_A}{r_{iA}}, \tag{2.46}$$

In contrast, $\hat{g}(i,j)$ signifies the repulsion between the i-th and j-th electrons:

$$\hat{g}(i,j) = \frac{1}{r_{ij}}. \tag{2.47}$$

The term V_N is constant for a given set of fixed nuclear coordinates, reflecting the assumption of immobile nuclei by the Born-Oppenheimer approximation.

2.3.2 Antisymmetric wavefunction

In electronic structure theory, it is necessary to formulate a wave function for multi-electron systems that respects the indistinguishability of electrons and the Pauli exclusion principle. These conditions lead to the requirement of antisymmetry, meaning the wavefunction must change its sign when the coordinates of any two electrons are swapped.

Mathematically, for a system of n electrons, the multi-electron wavefunction can be represented as a product of single-electron wavefunctions (or orbitals). This is referred to as a *Hartree Product* [90]:

$$\Psi(\mathbf{x}_1, \mathbf{x}_2, \cdots, \mathbf{x}_n) = \varphi_1(\mathbf{x}_1)\varphi_2(\mathbf{x}_2)\cdots\varphi_n(\mathbf{x}_n). \tag{2.48}$$

The $\varphi_i(\mathbf{x}_i)$ are termed *spin-orbitals* since each one is simply constructed as the product of a spatial orbital $\phi(\mathbf{r}_i)$ and a spin state $|w\rangle$ with either spin-up (α) or spin-down (β)., i.e., $\varphi_i(\mathbf{x}_i) \equiv \phi(\mathbf{r}_i) \otimes |w\rangle$. Although the product allows a simple approach to describing a multi-electron system, it fails inherently to take into account the antisymmetry principle.

Considering a two-electron system, the antisymmetrized wave function appears as:

$$\Psi(\mathbf{x}_1, \mathbf{x}_2) = \frac{1}{\sqrt{2}}\left(\varphi_1(\mathbf{x}_1)\varphi_2(\mathbf{x}_2) - \varphi_1(\mathbf{x}_2)\varphi_2(\mathbf{x}_1)\right). \tag{2.49}$$

This antisymmetric principle can be represented more conveniently by determinant structure:

$$\Psi(\mathbf{x}_1, \mathbf{x}_2) = \frac{1}{\sqrt{2}}\begin{vmatrix} \varphi_1(\mathbf{x}_1) & \varphi_2(\mathbf{x}_1) \\ \varphi_1(\mathbf{x}_2) & \varphi_2(\mathbf{x}_2) \end{vmatrix}. \tag{2.50}$$

This matrix structure, by its very nature, changes sign when any two of its rows (or columns) are swapped.

For a general n-electron system, the antisymmetric multi-electron wavefunction can be written as [90]

$$\Psi(\mathbf{x}_1, \mathbf{x}_2, \cdots, \mathbf{x}_n) \equiv \frac{1}{\sqrt{n!}} \begin{vmatrix} \varphi_1(\mathbf{x}_1) & \varphi_1(\mathbf{x}_2) & \dots & \varphi_1(\mathbf{x}_n) \\ \varphi_2(\mathbf{x}_1) & \varphi_2(\mathbf{x}_2) & \dots & \varphi_2(\mathbf{x}_n) \\ \vdots & \vdots & \ddots & \vdots \\ \varphi_N(\mathbf{x}_1) & \varphi_n(\mathbf{x}_2) & \dots & \varphi_N(\mathbf{x}_n) \end{vmatrix}. \tag{2.51}$$

The above determinant of occupied spin-orbitals is known as a *Slater determinant*, which can be represented shorthand as $|\varphi_1\varphi_2\cdots\varphi_n|$. By expanding the determinant, we obtain $n!$ terms corresponding to the Hartree Products, each associated with a different sign. The n electrons are arranged in all possible $n!$ ways among the n spin-orbitals, maintaining their indistinguishability as required by the antisymmetry principle.

2.3.3 Hatree-Fock method

The *Hartree-Fock* (HF) method is a cornerstone of electronic structure theory. It offers a variation method to solve the *electronic Schrödinger equation* for an n-electron system:

$$H_{\text{el}}\Psi_{HF} = E_{\text{HF}}\Psi_{HF}. \tag{2.52}$$

This framework assumes the HF wavefunction Ψ_{HF} as a single Slater determinant. This determinant is constructed from the n occupied spin-orbitals such that $\Psi_{HF} = |\varphi_1\varphi_2\cdots\varphi_n|$.

Determining the wavefunction that corresponds to the lowest possible energy (or the ground state) for a system, the optimization process aims to minimize the HF energy E_{HF} [90]:

$$\begin{aligned} E_{HF} &= \frac{\langle\Psi_{HF}|\, H_{el}\, |\Psi_{HF}\rangle}{\langle\Psi_{HF}|\Psi_{HF}\rangle} \\ &= V_N + \sum_i^n \langle\varphi_i|\, \hat{h}\, |\varphi_i\rangle + \sum_{i,j}^n \left(\langle\varphi_i\varphi_i|\, \hat{g}\, |\varphi_j\varphi_j\rangle - \langle\varphi_i\varphi_j|\, \hat{g}\, |\varphi_i\varphi_j\rangle\right). \end{aligned} \tag{2.53}$$

Here, the term $\langle\varphi_i|\,\hat{h}\,|\varphi_i\rangle$ represents the one-electron integrals, and the terms in the last summation correspond to the two-electron integrals. As presented in the following part, this optimization can be obtained by finding the spin-orbitals that minimize E_{HF}.

The one-electron integrals are associated with the individual characteristics of electrons within the system. They represent the kinetic energy and the potential energy of an electron in the field of the atomic nuclei:

$$\langle\varphi_i|\,\hat{h}\,|\varphi_i\rangle = \int d\mathbf{x}\;\varphi_i^*(\mathbf{x})\hat{h}(\mathbf{x})\varphi_i(\mathbf{x}), \tag{2.54}$$

This integral physically signifies the electron's average kinetic energy and electron-nuclear potential energy in the ith orbital φ_i.

On the other hand, the two-electron integrals arise from interactions between electron pairs:

$$\langle\varphi_i\varphi_j|\,\hat{g}\,|\varphi_k\varphi_m\rangle = \int d\mathbf{x}_1 d\mathbf{x}_2\;\varphi_i^*(\mathbf{x}_1)\varphi_j^*(\mathbf{x}_2)\frac{1}{r_{12}}\varphi_k(\mathbf{x}_1)\varphi_m(\mathbf{x}_2), \tag{2.55}$$

i.e., the two-electron integral captures the expectation value of the electron-electron repulsion energy when the electrons are in the orbitals φ_i and φ_j.

Hartree-Fock Equations

In the quest to find the optimal set of spin-orbitals minimizing the HF energy, we consider small variations in the spin-orbitals, represented as $\{\varphi_i \to \varphi_i + \delta\varphi_i\}$. The only assumption made is that spin-orbitals remain orthogonal throughout the process.

To achieve this, Lagrange's method of undetermined multipliers is utilized. In this context, a functional or Lagrangian $\mathcal{L}$ for spin-orbitals is defined as [47]

$$\mathcal{L}\left[\{\varphi_i\}\right] = E_{HF}\left[\{\varphi_i\}\right] - \sum_{i,j}\epsilon_{ij}(S_{ij} - \delta_{ij}), \tag{2.56}$$

where ϵ_{ij} are the Lagrange multipliers and $S_{ij} = \langle\varphi_i|\varphi_j\rangle$ represents overlaps between spin orbitals. The overlap integral S_{ij} is given as $\int d\mathbf{x}\;\varphi_i^*(\mathbf{x})\varphi_j(\mathbf{x})$.

Following this, by setting the first variation of the functional to zero, $\delta\mathcal{L}\left[\{|\varphi_i\rangle\}\right] = 0$, and performing subsequent algebraic manipulations, we obtain a set of simultaneous eigenvalue equations known as the *Hartree-Fock equations* [90]:

$$F\,|\varphi_i(\mathbf{x})\rangle = \epsilon_i\,|\varphi_i(\mathbf{x})\rangle\,, \quad i = 1, 2, \ldots, n \tag{2.57}$$

Here, ϵ_i denotes the energy eigenvalue associated with the spin-orbital φ_i and F represents the *Fock operator*, which is written as

$$F = \hat{h} + \sum_{i}^{n}(J_i - K_i). \tag{2.58}$$

In this expression, J_i and K_i are known as the *Coulomb* and *exchange* operators, respectively. They are applied as follows:

$$J_i\;\varphi_j(\mathbf{x}_1) = \varphi_j(\mathbf{x}_1)\int d\mathbf{x}_2\;\varphi_i^*(\mathbf{x}_2)\frac{1}{r_{12}}\varphi_i(\mathbf{x}_2) \tag{2.59}$$

$$K_i\;\varphi_j(\mathbf{x}_1) = \varphi_i(\mathbf{x}_1)\int d\mathbf{x}_2\;\varphi_i^*(\mathbf{x}_2)\frac{1}{r_{12}}\varphi_j(\mathbf{x}_2) \tag{2.60}$$

The Coulomb operator J_i represents the average effect of the electron in orbital φ_i repelling the other electron in orbital φ_j. On the other hand, the exchange operator K_i arises due to the requirement of antisymmetry for the multi-electron wavefunction, representing the average effect of interchanging the two electrons.

From the HF equations, it becomes evident that the HF method simplifies the many-body problem by transforming it into a set of one-electron problems. This is done by assuming that each electron moves in the averaged field of all others.

Roothann-Hall Equations

The Hartree-Fock equations can either be solved numerically (exact Hartree-Fock) or as a set of eigenvalue problems by projecting the spin-orbitals onto a finite-sized set of basis functions, leading to Hartree-Fock-Roothan equations [3].

A $2N$-dimensional spin-orbital basis—constructed from the product space of N spatial basis functions $\{\eta_\mu(\mathbf{r})\}$ and the spin basis $\{\alpha, \beta\}$—is given by $\{\chi_\mu\} = \{\eta_\mu\}\otimes\{\alpha, \beta\}$. Each spin-orbital can then be written as a linear combination of the basis $\{\chi_\mu\}$ [90]:

$$\varphi_i = \sum_{\mu}^{2N} C_{\mu i}\;\chi_\mu. \tag{2.61}$$

The most physically intuitive basis is the set of atomic orbitals (AO) for each constituent atom, termed the *linear combination of atomic orbitals* (LCAO) approximation. Expanding atomic orbitals using Slater-type functions is physically accurate but computationally demanding [47]. Instead, Gaussian-type AOs (GTO) are computationally efficient but less accurate on their own, often requiring multiple GTOs to approximate the behavior of a single STO. In the following chapters, we worked with the minimal STO-6G basis set [93] and Dunning's correlation-consistent basis sets [94].

Upon choosing a suitable basis set and substituting its Eq. (2.61) into the Hartree-Fock equations in Eq. (2.57), we can project these equations onto the basis functions $\langle\chi_j|$, yielding $2N$ coupled equations [90]:

$$\sum_{\mu}^{2N} C_{\mu i} F_{ji} = \epsilon_i \sum_{\mu}^{2N} C_{\mu i} S_{ji}, \tag{2.62}$$

where $F_{ji} = \langle\chi_j| F |\chi_i\rangle$ and $S_{ji} = \langle\chi_j|\chi_i\rangle$. These algebraic equations are collectively known as the *Roothaan-Hall* equations.

The Roothaan-Hall equations can be represented in matrix form as

$$\mathbf{FC} = \epsilon\mathbf{SC}. \tag{2.63}$$

In this equation, $\mathbf{F} = \{F_{ji}\}$ denotes the Fock matrix, $\mathbf{S} = \{S_{ji}\}$ is the overlap matrix, and $\mathbf{C} = \{C_{ji}\}$ is the matrix of MO coefficients. ϵ is a diagonal matrix, with each element representing spin-orbital energy $\{\epsilon_i\}$.

While Eq. (2.63) appears similar to an ordinary eigenvalue equation, the appearance of the overlap matrix $\mathbf{S}$ makes it non-linear. Thus, the Fock matrix $\mathbf{F}$ cannot be diagonalized. Instead, the solution involves choosing an optimal basis set and then executing the following iterative process:

1. Specify the molecular structure, electronic state of interest (singlet, triplet, etc.), and more importantly, the basis set $\{\chi_\mu\}$. Then, compute $\mathbf{S} = \langle\chi_\nu|\chi_\mu\rangle$.
2. Make an initial guess for the MO coefficients matrix $\mathbf{C}$ to construct spin-orbitals in Eq. (2.61).
3. Construct $\mathbf{F}$ in Eq. (2.58) by calculating 1- and 2-electron integrals in Eqs. (2.59) and (2.60) .

4. Solve $\det(F_{ji} - \epsilon_i S_{ji}) = 0$ to obtain an initial estimate for the spin-orbital energies $\{\epsilon_i\}$.
5. Solve Eq. (2.63) with the calculated energies $\{\epsilon_i\}$ from Step 4.
6. With the newly obtained MO coefficients $\{C_{ji}\}$, reconstruct $\mathbf{F}$.
7. Repeat Steps 5 and 6 until $\mathbf{C}$ remains unchanged from one iteration to the next.

Due to this iterative process, the Hartree-Fock method is called the *self-consistent-field* procedure. In specific molecular systems where exchange interactions among spin-orbitals can be ignored, the spin coordinates of φ_i can be integrated independently without involving the HF method. In this scheme, for the n-electron system, the number of the HF equations in Eq. (2.57) reduces to $n/2$ [47]. This treatment is called a *restricted* Hartree-Fock (RHF) method. Conversely, in the unrestricted Hartree-Fock (UHF) method, the spin-up and spin-down MOs should be independently computed.

For molecular systems like noble gases, Slater determinants where all MOs are either doubly occupied or empty are referred to as *closed-shell* configurations. Other possible determinants are termed *open-shell* configurations. Notably, the closed-shell configurations can be efficiently solved using the RHF method without computational loss [47].

2.3.4 Some post-HF methods

Configuration interaction (CI)

Electron correlations can be integrated into the framework by supplementing the reference state $|\Psi_{HF}\rangle$ with Slater determinants of all possible excited electronic configurations. This method is called the *configuration interaction* (CI) and a generic CI-wavefunction can be mathematically formulated as [95]

$$\begin{aligned} |\Psi_{CI}\rangle &= c_0 |\Psi_{HF}\rangle + \sum_i \sum_a c_i^a |\Psi_i^a\rangle + \sum_{i<j} \sum_{a<b} c_{ij}^{ab} |\Psi_{ij}^{ab}\rangle + \sum_{i<j<k} \sum_{a<b<c} c_{ijk}^{abc} |\Psi_{ijk}^{abc}\rangle + \cdots \\ &= \sum_{i=0} c_i |\Psi_i\rangle , \end{aligned} \tag{2.64}$$

where $|\Psi_i\rangle$ indicates the Slater determinant of a specific electron arrangement.

Optimization in this context involves minimizing the energy defined by $E = \langle\Psi_{CI}| H |\Psi_{CI}/ \langle\Psi_{CI}|\Psi_{CI}\rangle\rangle$, with respect to the expansion coefficients $\{c_i\}$ of the CI-wavefunction, so-called CI coefficients. This is expressed in the Lagrangian functional $\mathcal{L}$ as [96]

$$\begin{aligned} \mathcal{L} &= \langle\Psi_{CI}| H |\Psi_{CI}\rangle - E(\langle\Psi_{CI}|\Psi_{CI}\rangle - 1) \\ &= \sum_{i,j} c_i^* c_j H_{ij} - E\left(\sum_{i,j} c_i^* c_j S_{ij} - \delta_{ij}\right), \end{aligned} \tag{2.65}$$

where $H_{ij} = \langle\Psi_i| H |\Psi_j\rangle$ and $S_{ij} = \langle\Psi_i|\Psi_j\rangle$.

Given the condition $\delta\mathcal{L} = 0$, each CI coefficient c_i of $|\Psi_i\rangle$ has an equation as follows [96]:

$$\sum_j H_{ij} c_j - E_{CI} S_{ij} c_j = 0. \tag{2.66}$$

This set of all equations constitutes the CI *secular equations*. They can be concisely represented as the matrix equation:

$$\mathbf{HC} = E\mathbf{SC}, \tag{2.67}$$

where $\mathbf{C}$ denotes the column-vector containing the CI coefficients $\{c_i\}$, thus called the *CI vector*. As Slater determinants are built from orthonormal spin orbitals, $\mathbf{S}$ equals the identity matrix, simplifying Eq. (2.66) to

$$\mathbf{HC} = E\mathbf{C}. \tag{2.68}$$

Solving the secular equations is synonymous with diagonalizing $\mathbf{C}$ and thus the CI energy E_{CI} is obtained as the lowest eigenvalue of $\mathbf{C}$, with the corresponding eigenvector which contains the optimal CI coefficients of $|\Psi_{CI}\rangle$.

Considering all excitations in $|\Psi_{CI}\rangle$ yields an exact solution to the electronic Schrödinger equation. This approach is known as *full*-CI method. Nonetheless, as the number of Slater determinants grows, the system size expands exponentially. For a set of N basis functions, with n_α spin-up and n_β spin-down electrons, the number of determinants N_{det} can be found by [97]

$$N_{\text{det}} = \binom{N}{n_\alpha}\binom{n}{N_\beta}. \tag{2.69}$$

Various strategies are available to truncate the number of determinants in the CI-wavefunction. One way is to limit the excitation level of determinants. For instance, limiting CI-wavefunction $|\Psi_{CI}\rangle$ with only single and double excitations results in the CISD method [47]. An alternative approach is based on the *complete active space* (CAS) method, where MOs are partitioned into sets of active and inactive orbitals. The corresponding *complete-active-space* CI (CASCI) wavefunction is constructed from all possible configurations of electrons within a specified active space of orbitals while keeping the inactive orbitals either fully occupied or unoccupied [98]. Such a selection procedure concentrates on the most energetically active MOs to make the computation more feasible while decreasing energy.

Multi-configurational self-consistent field

In certain molecular systems, when several dominant electronic configurations are present, the reference HF determinant may be an inadequate approximation of the ground state wavefunction. This situation is often encountered in systems with strong static correlation effects [47]. To address this inadequacy, a common strategy is to introduce a multireference wave function in the *multi-configurational self-consistent field* (MCSCF) framework [90].

Within the MCSCF method, its wavefunction is expressed similarly to the CI method, as detailed in Eq. (2.64):

$$|\Psi_{MCSCF}\rangle = \sum_{i=0} c_i \, |\Psi_i\rangle \, . \tag{2.70}$$

To determine its optimal form, the expectation value of the energy is minimized:

$$E_{MCSCF} = \sum_{i,j} c_i^* c_j \, \langle \Psi_i | \, H \, | \Psi_j \rangle \, . \tag{2.71}$$

Compared to the CI method, the distinctive feature of the MCSCF method lies in its optimization process. While the CI approach focuses solely on optimizing the CI coefficients $\{c_i\}$ of electronic configurations in Eq. (2.70), the MCSCF method additionally optimizes the atomic orbital coefficients of MOs at each iteration step.

As with the CI method, the MCSCF wavefunction, including all configurations, leads to the exact FCI energy and wavefunction. However, in practice, the MCSCF

wavefunction can be expanded using a chosen subset of configurations. The complete active space (CAS) approach is also the most common selection method for MCSCF, termed *complete-active-space self-consistent field* CASSCF [99].

Chapter 3

QUANTIFICATION OF FERMIONIC CORRELATIONS

Section 2.2 is devoted to understanding and measuring quantum correlations in distinguishable systems based on the unique subspace separability of Hilbert space for each subsystem. This separability enables us to precisely measure and use correlations when particles can be individually addressed and manipulated. However, when dealing with quantum systems composed of indistinguishable particles, such as fermions, even the basic task of defining a subsystem becomes challenging.

In Sec. 3.1, we introduce the fermionic mode picture—which is a way to genuinely describe correlations in a fermionic system—and offer a concrete introduction for fermionic-mode correlations, mostly based on Refs. [46, 100]. Subsequently, in Sec. 3.2, utilizing these tools of fermionic information theory, we proposed a method for a comprehensive and exactly additive decomposition of the total orbital correlations into their respective classical and quantum parts in the fermionic mode picture. Subsequently, we demonstrate this method's application to the electronic structure of some simple molecular structures[1].

3.1 Fermionic-mode correlations

The characteristics of indistinguishable systems in quantum mechanics are remarkably different from those in classical mechanics. Whereas in classical systems, indistinguishability arises due to experimental limitations, particles like electrons in a quantum system are fundamentally identical [102, 103]. This inherent indistinguishability of quantum particles presents a fundamental challenge in their study of quantum correlations.

To illustrate, consider a two-particle state where each subsystem has one par-

[1]The contents here were published in *New Journal of Physics* [101].

ticle. In the mode picture, the state is denoted as $|1,1\rangle_{AB}$, corresponding to its representation in the second quantization. Interestingly, this is not an entangled state. But due to the particles' indistinguishable nature, in the particle picture, this state is represented by a two-particle state as follows:

$$\frac{|0\rangle_A|1\rangle_B \pm |1\rangle_A|0\rangle_B}{\sqrt{2}}. \tag{3.1}$$

Here, the state is (anti-)symmetrized for bosons (fermions) and gives an impression of an entangled state in the particle picture. However, some works [104–107] argue that the entanglement in Eq. (3.1) is not physical because the indistinguishable nature of the particles makes it pointless to assign which particle has the label A or B.

In systems of indistinguishable particles, bipartite correlations between modes must be considered if one wants to extract physically usable entanglement or discord [46, 108–116]. This is because modes are orthogonal to each other, so using them, distinguishable systems can be defined in which subsystems consisting of modes can be individually addressed. However, ongoing studies investigate the usefulness of correlations in the particle picture for some systems of interest [107]. For instance, an interesting work explores the resource value of particle entanglement in processes encountered in optical and cold atomic systems [117].

This section is organized as follows. In Subsec. 3.1.1, we begin by exhibiting a mathematical structure of the fermionic state space consisting of fermionic modes. Considering the inherent antisymmetry principle, we define the wedge product fermionic Hilbert space. Subsequently, in Subsec. 3.1.2, we define the notion of the fermionic subsystem and redefine the fermionic partial tracing operation to get the physical fermionic state of a subsystem. In addition, the fermionic states physically accessible by local observers must satisfy local parity and particle number superselection rules (SSR). Therefore, in Subsec. 3.1.3, we introduce SSRs in general and discuss how to derive explicit forms of the physical fermionic states and observables that respect such rules. Finally, we characterize uncorrelated and correlated fermionic states and then discuss quantifying the correlations between fermionic modes.

3.1.1 Fermionic state space

The *fermionic modes*, characterized by creation and annihilation operators, satisfy certain anticommutation relations, which essentially encode the intrinsic behavior of fermions [118]. For instance, they indicate that the multi-mode fermionic state is antisymmetric with respect to the exchange of two modes, which captures the indistinguishable nature of fermions.

Let us consider a set of N fermionic modes with each one associated with a creation operator $f_i^\dagger$ and an annihilation operator f_i, that satisfy the canonical anticommutation relations [118]:

$$\{f_i, f_j^\dagger\} = \delta_{ij}\mathbb{1}, \quad \{f_i, f_j\} = \{f_i^\dagger, f_j^\dagger\} = 0, \tag{3.2}$$

where the anticommutator $\{A, B\} = AB + BA$ for any quantum operators A and B. The *vacuum state*, denoted by $|0\rangle$, is annihilated by any f_i, i.e., $f_i |0\rangle = 0 \ \forall\, i$. Building up from the vacuum state, we use the creation operators $f_i^\dagger$ to create single excitations in ith modes, mathematically $f_i^\dagger |0\rangle = |1_i\rangle$.

As can be seen from the first anticommutation relation, $|1_i\rangle$ are orthonormal, and further, they form a complete basis of a single-fermion Hilbert space $\mathcal{H}_{1-f}$, whereas $|0\rangle \in \mathcal{H}_{0-f}$. Thus, any one-fermion state in $\mathcal{H}_{1-f}$ can be expressed as [46]

$$|\psi_{1-f}\rangle = \sum_{i=1}^{n} c_i |1_i\rangle \,. \tag{3.3}$$

What about states with more than one fermion? In quantum mechanics for distinguishable particles, multiparticle states are often described as tensor products of single-particle states. Due to the antisymmetry of the fermionic states with respect to the change of the mode order, a two-fermion state can be represented as the antisymmetrized product of two single-fermion states, using the *wedge product* ($\wedge$). This product gives us the antisymmetric necessity inherently [46]:

$$\begin{aligned} |1_i\rangle \wedge |1_j\rangle &= f_i^\dagger |0\rangle \wedge f_j^\dagger |0\rangle = f_i^\dagger f_j^\dagger |0\rangle \\ &\equiv \frac{1}{\sqrt{2}} \left(|1_i\rangle \otimes |1_j\rangle - |1_j\rangle \otimes |1_i\rangle \right). \end{aligned} \tag{3.4}$$

Thus, any two-fermion state is just an element of the wedge product space of two single-fermion Hilbert spaces, i.e., $\mathcal{H}_{2-f} = \mathcal{H}_{1-f} \wedge \mathcal{H}_{1-f}$ [100].

Generalizing this, N-fermion states that live in $\mathcal{H}_{N-f} = \mathcal{H}_{1-f}^{\wedge N}$ can then be constructed by wedge product of N single-fermion states. Consequently, *N-mode fermionic Hilbert space* $\mathcal{F}_N$, also called *Fock space*, is given as the direct sum over all fermion numbers [118]:

$$\mathcal{F}_N = \bigoplus_{i=0}^{N} \mathcal{H}_{i-f}, \tag{3.5}$$

and $\mathcal{F}_N$ can be spanned by the orthonormal basis set $\mathcal{B}$ that has the dimension of 2^N:

$$\begin{aligned} \mathcal{B} &= \{|0\rangle, |1_1\rangle, |1_2\rangle, \|1_1 1_2\rangle\rangle, |1_3\rangle, \|1_1 1_3\rangle\rangle, \|1_2 1_3\rangle\rangle, \|1_1 1_2 1_3\rangle\rangle, \ldots, \|1_1 1_2 \cdots 1_N\rangle\rangle\} \\ &\equiv \{\|m_1 m_2 \cdots m_N\rangle\rangle \mid m = \{0, 1\}\}, \end{aligned} \tag{3.6}$$

where $\|1_i 1_j \cdots 1_k\rangle\rangle$ with $i < j < k$ and $k \leq N$ is a shorthand for $|1_i\rangle \wedge |1_j\rangle \wedge \cdots \wedge |1_k\rangle$ in which unoccuppied modes are not written. Here, the double ket $\|\cdot\rangle\rangle$ is used to indicate that a wedge product between modes occurs.

Given basis set $\mathcal{B}$, a general state in $\mathcal{F}_N$ can be expressed as [46]

$$|\psi\rangle = \mu_0 |0\rangle + \sum_i^N \mu_i |1_i\rangle + \sum_{j<k} \mu_{jk} \|1_j 1_k\rangle\rangle + \cdots + \mu_N \|1_1 1_2 \cdots 1_N\rangle\rangle, \tag{3.7}$$

where the complex coeffiencets $\mu_0, \mu_i, \mu_{jk}, \ldots, \mu_N$ satisfying the normalization condition such that $|\mu_0|^2 + \sum_i |\mu_i|^2 + \sum_{j,k} |\mu_{jk}|^2 + \cdots + |\mu_N|^2 = 1$.

The N-mode Hilbert space $\mathcal{F}_N$ in the most general case can be decomposed as the wedge product of the single-mode Hilbert spaces $\mathcal{H}_i$ [100]:

$$\mathcal{F}_N = \bigwedge_{i=1}^{N} \mathcal{H}_i = \mathcal{H}_1 \wedge \cdots \wedge \mathcal{H}_N, \tag{3.8}$$

Here, $\mathcal{H}_i$ is spanned by the orthonormal basis $E_i = \{|0\rangle, |1_i\rangle\}$. Thus, this decomposition allows us to define subsystems.

To define the dual space of $\mathcal{F}_N$, the action of the wedge product on the dual space elements must be consistent with the inner product definition. In the simplest case, the dual of a two-fermion state is given as

$$(|1_i\rangle \wedge |1_j\rangle)^\dagger = (f_i^\dagger f_j^\dagger |0\rangle)^\dagger = \langle 0| f_j f_i = \langle 1_i| \wedge \langle 1_j|. \tag{3.9}$$

Here, the dual of the two-fermion state is $\langle 0| f_j f_i$ but not $\langle 0| f_i f_j$ since $\langle 0| f_j f_i f_i^\dagger f_j^\dagger |0\rangle = 1$ whereas $\langle 0| f_i f_j f_i^\dagger f_j^\dagger |0\rangle = -1$ according to the anticommutation relations. These results can be obtained from the general definition of the inner product between two-fermion states:

$$\begin{aligned}(\langle 1_k| \wedge \langle 1_m|)(|1_i\rangle \wedge |1_j\rangle) &= \langle 0| f_k \underbrace{f_m f_i^\dagger}_{\delta_{mi} - f_i^\dagger f_m} f_j^\dagger |0\rangle \\ &= \delta_{mi} \langle 0| f_k f_j^\dagger |0\rangle - \langle 0| f_k f_i^\dagger f_m f_j^\dagger |0\rangle \\ &= \delta_{mi}\delta_{kj} - \delta_{ki} \langle 0| f_m f_j^\dagger |0\rangle + \underbrace{\langle 0| f_i^\dagger}_{0} f_k f_m f_j^\dagger |0\rangle \\ &= \delta_{mi}\delta_{kj} - \delta_{ki}\delta_{mj}. \end{aligned} \tag{3.10}$$

As one can see, this product can be represented as the determinant of a matrix with elements being delta functions. Therefore, the inner product between the arbitrary excitations $|\psi\rangle = f_{i_1}^\dagger \cdots f_{i_k}^\dagger |0\rangle$ and $|\phi\rangle = f_{j_1}^\dagger \cdots f_{j_m}^\dagger |0\rangle$ is given by [100]

$$\langle \psi|\phi\rangle = \langle 0| f_{i_k} \cdots f_{i_1} f_{j_1}^\dagger \cdots f_{j_m}^\dagger |0\rangle = \begin{cases} 0 & \text{for } k \neq m \\ \det(W_k) & \text{for } k = m \end{cases} \tag{3.11}$$

where

$$W_k = \begin{pmatrix} \delta_{i_1,j_1} & \cdots & \delta_{i_1,j_k} \\ \vdots & \ddots & \vdots \\ \delta_{i_k,j_1} & \cdots & \delta_{i_k,j_k} \end{pmatrix}. \tag{3.12}$$

Similar to the case of the distinguishable particles system, a generic pure density operator in N-mode Hilbert space $\mathcal{F}_N$ can be obtained by taking the projector on the fermionic state $|\psi\rangle$ from Eq. (3.7):

$$\begin{aligned}\rho = |\psi\rangle\langle\psi| &= |\mu_0|^2 |0\rangle\langle 0| + \sum_{i,i'} \mu_i \mu_{i'}^* |1_i\rangle\langle 1_{i'}| + \sum_{j,j',k,k'} \mu_{jk}\mu_{j'k'}^* \|1_j 1_k\rangle\rangle\langle\langle 1_{j'} 1_{k'}\| \\ &\quad + \cdots + \sum_i (\mu_i \mu_0^* |1_i\rangle\langle 0| + \text{H.c.}) + \cdots . \end{aligned} \tag{3.13}$$

Here, H.c. represents the Hermitian conjugate of $\mu_i \mu_0^* |1_i\rangle\langle 0|$. One can easily check that any density operator in $\mathcal{F}_N$ fulfills the three conditions for representing a physical density operator: the normalization $\text{Tr}[\rho] = 1$, the Hermiticity $\rho = \rho^\dagger$, and the positivity $\langle\phi| \rho |\phi\rangle \geq 0 \ \forall |\phi\rangle \in \mathcal{F}_N$.

A mixed state can be also formed from the incoherent mixtures of pure fermionic states:

$$\rho = \sum_i p_i \left|\psi_i\right\rangle \left\langle\psi_i\right| \tag{3.14}$$

where $\sum_i p_i = 1$. While the mixed states simply meet the conditions of normalization and Hermiticity, an additional requirement is needed to confirm positivity: this is the parity superselection rule, as discussed in Ref. [100].

3.1.2 Fermionic subsystem

The essential ingredients for investigating quantum correlations in a quantum state are reduced states concerning some partition of its Hilbert space to subsystems. Since the basis of a single mode consists of a vacuum state and its excitation, defining a reduced state by taking qubit partial trace gives rise to some ambiguity [46, 119]. Thus, as introduced in Ref. [119], one should redefine the partial trace operation for fermionic systems to eliminate these ambiguities.

With the help of the following *consistency conditions* for the physical definition of the reduced state formalism [46], we can define a genuine fermionic partial trace operation. These conditions state that the reduced density operator contains all the information about the subsystem obtained from the global state when local measurements are solely performed on that specific subsystem. Mathematically, for any bipartition to finite-mode fermionic subsystems A and B of global Hilbert space $\mathcal{H}_{AB} = \mathcal{H}_A \wedge \mathcal{H}_B$, a partial tracing procedure over $\mathcal{H}_B$ of any state $\rho_{AB} \in \mathcal{H}_{AB}$, i.e., $\mathrm{Tr}_B[\rho_{AB}] = \rho_A$, must satisfy [46]

$$\mathrm{Tr}[\mathcal{O}_A \rho_{AB}] = \mathrm{Tr}[\mathcal{O}_A \rho_A], \tag{3.15}$$

for all local operators $\mathcal{O}_A \equiv \mathcal{O}_A \wedge \mathbb{1}$ acting only on $\mathcal{H}_A$. This condition uniquely defines the reduced states of any global state and the partial trace operation without allowing ambiguity [119].

Given a global state ρ for a fermionic system composed of N modes, the reduced states concerning a particular subsystem composed of one or more modes can be

obtained by tracing over the set of modes $M = \{\mu_1, \ldots, \mu_M\}$ that do not belong to that subsystem:

$$\mathrm{Tr}_M[\rho] = \mathrm{Tr}_{\mu_1} \circ \mathrm{Tr}_{\mu_2} \circ \cdots \circ \mathrm{Tr}_{\mu_M}[\rho], \tag{3.16}$$

where each single-mode partial trace operation satisfies the physically imposed consistency conditions by ignoring the information of whether the respective mode in set M is occupied or not [100]. Then, the operation of partial tracing an arbitrary mode m is given by [119]

$$\begin{gathered}\mathrm{Tr}_\mu \left[(f_1^\dagger)^{s_1} \cdots (f_m^\dagger)^{s_m} \cdots (f_N^\dagger)^{s_N} |0\rangle \langle 0| f_N^{r_N} \cdots f_m^{r_m} \cdots f_1^{r_1} \right] \\ \shortparallel \\ \delta_{s_m r_m} (-1)^k (f_1^\dagger)^{s_1} \cdots (f_{m-1}^\dagger)^{s_{m-1}} (f_{m+1}^\dagger)^{s_{m+1}} \cdots (f_N^\dagger)^{s_N} |0\rangle\langle 0| f_N^{r_N} \cdots f_{m+1}^{r_{m+1}} f_{m-1}^{r_{m-1}} \cdots f_1^{r_1}.\end{gathered} \tag{3.17}$$

Here, the term $(-1)^k$ introduces a necessary phase factor due to the anticommutation relations of fermionic operators. This factor depends on the occupation numbers of modes higher than the m-th mode such that $k = s_m \sum_{j=m}^{N-1} s_{j+1} + r_m \sum_{k=m}^{N-1} r_{k+1}$ with $s_i, r_j \in \{0, 1\}$.

3.1.3 Superselection rules

Beyond the constraints in the Hilbert space of fermions due to the anticommutation relations inherent to fermionic statistics, an additional and equally important constraint arises due to the *parity superselection rule* (P-SSR). Superselection rules (SSRs) are essentially a set of constraints emerging from fundamental system symmetries, such as parity or charge conservation [120], or from practical limitations, for instance, particle number conservation due to energy conservation.

The P-SSR dictates that fermionic quantum states in a coherent superposition of states with even and odd parities are not physically allowed. Historically, this rule was introduced to describe elementary particles within quantum field theory due to the deep relationship between quantum mechanics and special relativity [120].

In the quest to develop a reasonable quantum information theory for fermions (QFT), different perspectives have arisen regarding the inherent justification for P-SSR. First, Ref. [119] showed that the P-SSR emerges naturally when considering the

demands of both Lorentz invariance and symmetry in a relativistic QFT framework. This emergence ensures that the reduced states of a pure fermionic state have the same spectra, which is crucial for the definition of bipartite correlations. Contrarily, Ref. [121] suggests that one might not need relativity as the basis for justifying the P-SSR in fermionic quantum information theory. Instead, the rule found its foundational basis in the no-signaling principle.

Considering a bipartite fermionic system represented as AB, the no-signaling principle implies that operations conducted by any local observer on A must commute with those performed by the local observer on B. This commutativity is only possible if the local states of A and B are superpositions of states with consistent parity, so the global state is also. That is why only states of an arbitrary fermionic system that satisfy the P-SSR correspond to *physical states* for local observers.

Aside from the P-SSR, another superselection rule relevant to our ongoing work is the *number superselection rule* (N-SSR) [122]. This rule becomes indispensable when dealing with fermionic systems in the low-energy regime where pairs of fermions cannot spontaneously be annihilated or created. Within quantum chemistry and condensed matter physics, it is clear that physical fermionic states must also be subject to the N-SSR.

In essence, SSRs pertain to the local conservation of specific physical quantities in fermionic systems, denoted as Q. For a system subjected to Q-SSR, its associated density matrix ρ must respect the conservation of Q, both globally on ρ and locally on all defined subsystems. The relationship formally can be expressed as:

$$\rho^Q = \sum_{i_1,\cdots,i_n} \Pi_{i_n} \wedge \cdots \wedge \Pi_{i_1} \rho \, \Pi_{i_1} \wedge \cdots \wedge \Pi_{i_n}. \tag{3.18}$$

Here, every projector operation Π_{i_m} in i-th subsystem corresponds to a projection onto a possible allowed value of Q. A Q-SSR essentially transforms ρ into ρ^Q such that it satisfies the equation $\left[\rho^Q, Q\right] = 0$. This modified density matrix ρ^Q must be block diagonal in the eigenbasis of Q, implying that some off-diagonal elements of the original ρ have been eliminated to comply with the conservation rule.

It is crucial to note that SSRs can lead to new applications for quantum information processing both in general perspective [123–126] and in specific tasks, such

as quantum teleportation [127–129].

3.1.4 Fermionic-mode entanglement

For a system composed of distinguishable particles, the entirely uncorrelated bipartite pure states are the product states of the form $\rho_A \otimes \rho_B$. As mentioned in 2.2, this description implicates the lack of entanglement between the subsystems for pure states.

However, when considering fermionic systems, there exist states $\rho_{AB} \neq \rho_A \wedge \rho_B$ that exhibit the same expectation values as $\rho_A \wedge \rho_B$ for local observables. This intriguing phenomenon is a result of the fact that some fermionic states cannot be fully constructed only by performing local measurements on A and B, i.e., fermionic systems do not satisfy the local tomography principle [130].

Because of this deviation from distinguishable particles, a new characterization of uncorrelated states for fermionic systems should be proposed. That is why Refs. [100, 131] suggest that the fermionic uncorrelated states ρ_{AB} across any partition of A and B must satisfy the following more general relation:

$$\mathrm{Tr}[\rho_{AB}(\mathcal{O}_A \wedge \mathcal{O}_B)] = \mathrm{Tr}[\rho_A \mathcal{O}_A]\,\mathrm{Tr}[\rho_B \mathcal{O}_B], \tag{3.19}$$

for all local observables $\mathcal{O}_A \equiv \mathcal{O}_A \wedge \mathbb{1}$ and $\mathcal{O}_B \equiv \mathbb{1} \wedge \mathcal{O}_B$ on the subspace spanned by the modes on A and B respectively. This equation offers a mathematical representation of the concept that the measurements of observables on A do not interfere with those on B and vice versa.

With the above definition of fermionic uncorrelated states, we can define the fermionic separable states shared by parties A and B as follows [131]:

$$\rho_{AB} = \sum_i p_i \rho_{AB}^i, \tag{3.20}$$

where $0 \leq p_i \leq 1$, $\sum_i p_i = 1$, and the states ρ_{AB}^i are uncorrelated states that satisfy Eq. (3.19). An entangled fermionic state ρ_{AB} shared by two parties A and B is a state that cannot be decomposed into such a sum of uncorrelated states.

For pure bipartite fermionic states, the Schmidt decomposition also provides a useful analytical tool like distinguishable systems [100]. Given any pure fermionic

physical states $|\psi_{AB}\rangle$, we have:

$$|\psi_{AB}\rangle = \sum_i p_i \, |i_A\rangle \wedge |i_B\rangle \,, \tag{3.21}$$

where $\{|i_A\rangle\} \in \mathcal{H}_\mathcal{A}$ and $|i_B\rangle \in \mathcal{H}_\mathcal{B}$ are orthonormal bases, and $\{p_i\}$ are Schmidt coefficients. In a way that parallels the situation with distinguishable particles, we see that a pure fermionic state $|\psi_{AB}\rangle$ is a separable (hence an uncorrelated) state if and only if it possesses a Schmidt number 1.

Fermionic entanglement measures

For a fermionic pure state $|\psi_{AB}\rangle \in \mathcal{H}_A \wedge \mathcal{H}_B$, the entropy of entanglement can be computed similarly to distinguishable systems since it is a function of the eigenvalues of the reduced states ρ_A or ρ_B [46]. Thus it is defined as follows:

$$E_E(|\psi_{AB}\rangle) = S(\rho_{A/B}) = -\operatorname{Tr}\left[\rho_{A/B} \log_2 \rho_{A/B}\right] \tag{3.22}$$

Here, the states of subsystems $\rho_{A/B}$ are constructed by tracing out all modes not included in the corresponding subsystem. The only difference from the distinguishable systems is that the tracing operation is performed from the fermionic partial trace operation, defined in Eq. (3.17).

As discussed in Sec. 2.2, for mixed states, the entanglement of formation is defined through the convex roof extension of the entanglement entropy:

$$E_F(\rho_{AB}) = \min_{\{p_i, |\psi_i\rangle\}} p_i \, E_E\left(|\psi_i\rangle\right). \tag{3.23}$$

where the mixed fermionic state is decomposed into a set of pure fermionic states as $\rho = \sum_i p_i \, |\psi_i\rangle \langle\psi_i|$. This is fully analogous to the distinguishable systems definition in Eq. (2.25). For two fermionic modes, the minimization over all states that respect the superselection rules can be computed effectively [132]. However, executing this minimization step becomes difficult or even impossible for systems with more than two modes, even while respecting the SSRs.

Another entanglement measure for fermionic mixed states is the entanglement negativity which can be relatively easily computed for fermionic mixed states as well as distinguishable systems. The fermionic negativity, proposed in Ref. [133]

and investigated in Refs. [134–136] , is given as like Eq. (2.29) by just inserting fermionic form of partial transpose. Similar to the fermionic partial trace defined in Eq. (3.17), the fermionic partial transpose also involves a phase factor ϕ. The fermionic partial transpose operation between any element of bipartite fermionic state ρ_{AB} with $N(M)$ modes in subsystem $A(B)$ is given by [136]

$$\begin{aligned}&\left[(f^{\dagger}_{A_1})^{s_{A_1}}\cdots(f^{\dagger}_{A_N})^{s_{A_N}}(f^{\dagger}_{B_1})^{s_{B_1}}\cdots(f^{\dagger}_{B_M})^{s_{B_M}}\left|0\right\rangle\left\langle 0\right| f^{r_{B_M}}_{B_M}\cdots f^{r_{B_1}}_{B_1} f^{r_{A_N}}_{A_N}\cdots f^{r_{A_1}}_{A_1}\right]^{\mathrm{T}_A}\\ &\cong \\ &(-1)^{\phi}\hat{\mathrm{U}}_A\Big[(f^{\dagger}_{A_1})^{r_{A_1}}\cdots(f^{\dagger}_{A_N})^{r_{A_N}}(f^{\dagger}_{B_1})^{s_{B_1}}\cdots(f^{\dagger}_{B_M})^{s_{B_M}}\left|0\right\rangle \\ &\qquad\left\langle 0\right| f^{r_{B_M}}_{B_M}\cdots f^{r_{B_1}}_{B_1} f^{s_{A_N}}_{A_N}\cdots f^{s_{A_1}}_{A_1}\Big]^{\mathrm{T}_A}\hat{\mathrm{U}}^{\dagger}_A.\end{aligned} \tag{3.24}$$

The phase factor is defined as

$$\phi = [(\tau_A + \bar{\tau}_A) \bmod 2]/2 + (\tau_A + \bar{\tau}_A)(\tau_B + \bar{\tau}_B). \tag{3.25}$$

where $\tau_{A(B)} = \sum_{j=A_1(B_1)}^{A_N(B_M} s_j$ and $\bar{\tau}_{A(B)} = \sum_{j=A_1(B_1)}^{A_N(B_M)} r_j$ are the number of occupied modes in each subsystem. $\mathrm{U}_A = \prod_{j=A_1}^{A_N}(f_j + f_j^{\dagger})$ is a unitary transformation acting on $\mathcal{H}_A$. Regarding the eigenvalues of $U_A^{\dagger}\rho^{T_A}U_A$ and ρ^{T_A} having identical eigenvalues, they give equivalent values for the entanglement negativity [136].

The logarithmic fermionic negativity, similar to Eq. (2.31), can be defined by replacing the fermionic partial transpose. The fermionic entanglement negativity provides a computationally efficient tool for classifying entangled states in subsystems comprising two or three fermionic modes [136]. Among the various properties of an entanglement measure that should satisfy, the fermionic entanglement negativity is nonincreasing (monotone) under LOCC that regards P-SSR. As distinct from the entanglement negativity for distinguishable systems, the fermionic counterpart is faithful since any fermionic entangled state that remains positive under partial transposition operation (known as the positive partial transpose entangled state) has not been countered [136].

3.1.5 Fermionic-mode discord

The total correlation between any two subsystems consisting of fermionic modes can be defined in a manner similar to distinguishable systems through the quantum

mutual information, as stated in Eq. (2.15). This is feasible since the von Neumann entropy is also a well-defined quantity in fermionic systems when subsystems are constructed by the fermionic partial operation [46].

Furthermore, the classical correlation measure, as mentioned in Eq. (2.41), as well as the measurement-independent quantum discord defined in Eq. (2.42), can be directly applied to any partition of any fermionic quantum states. This applicability holds under fermionic partial trace operation and well-defined local projective operations regarding P-SSR. As with distinguishable systems, in order to properly quantify bipartite correlations, accurate optimization in Eq. (2.41) is crucial.

The need for optimization poses a numeric challenge, even in qubit systems. This is primarily due to the requirement to include all possible local projective measurements. Interestingly, in fermionic systems, SSRs considerably limit the number of permissible measurements, thereby simplifying the optimization.

Utilizing the N-SSR, Ref. [137] proposed an analytic expression to compute the quantum discord between two modes in a general fermionic state, either pure or mixed, without an optimization procedure. Moreover, the optimization procedure in studying correlations between subsystems involving more than two modes can be made numerically effective under the constraints of SSRs. In a subsequent Subsec. 3.2.2, we will discuss the optimization process in correlations between two orbitals, where each orbital consists of two modes.

3.2 Orbital correlations in molecular electronic ground states

In what follows, after introducing how to describe electronic ground states in the mode picture and discussing the computational details of quantifying orbital discord, we present the results of the proper dissection of classical and quantum correlations shared between the Hartree–Fock (HF) molecular orbitals (MOs) of the water molecule H_2O, 2-propenyl C_3H_5, and dicarbon anion C_2^-.

3.2.1 Molecular electronic ground states in mode picture

Each MO consists of two modes, one representing α spin-orbital and the other β spin-orbital. Thus, the ith MO can be written on the 2-mode Hilbert space using the basis of $\{|0\rangle, f^\dagger_{\varphi_{2i-1}}|0\rangle, f^\dagger_{\varphi_{2i}}|0\rangle, f^\dagger_{\varphi_{2i-1}} f^\dagger_{\varphi_{2i}}|0\rangle\}$ where $f^\dagger_{\varphi_{2i-1}}$ and $f^\dagger_{\varphi_{2i}}$ are respectively creation operators of spin-up and spin-down orbitals of i-th MO.

Any electronic configuration represented by a Slater determinant in Eq. (2.51) can be expressed in the mode picture by defining the wedge product to preserve its antisymmetric characteristic. Thus, any configuration—represented by a Slater determinant consisting of occupied spin-orbitals $|\varphi_k \varphi_m \dots \varphi_n|$ where $k < m < n$—can be rewritten in mode picture as $|\varphi_k\rangle \wedge |\varphi_m\rangle \wedge \dots \wedge |\varphi_n\rangle$.

Therefore, for a molecular system consisting of n_e electrons and n MOs, the HF configuration can be given in $2n$-mode Hilbert space as

$$\begin{aligned} |\Psi_{HF}\rangle &= |\varphi_1\rangle \wedge |\varphi_2\rangle \wedge \dots \wedge |\varphi_{n_e}\rangle \\ &= f_1^\dagger f_2^\dagger \dots f_{n_e}^\dagger |0\rangle, \end{aligned} \tag{3.26}$$

where $f^\dagger_{2i-1}$ and $f^\dagger_{2i}$ are respectively creation operators of spin-up and spin-down orbitals of i-th HF-MO.

Therefore, in the mode picture, the CI-wavefunction, as defined in Eq. (2.64), can be represented as

$$|\Psi_{CI}\rangle = \frac{1}{N}\left(c_0 + \sum_{i,a} c_i^a f_a^\dagger f_i + \sum_{i<j}\sum_{a<b} c_{ij}^{ab} f_a^\dagger f_b^\dagger f_i f_j + \dots\right)|\Psi_{HF}\rangle. \tag{3.27}$$

Here, each pair of $f_a^\dagger f_i$ corresponds to an excitation operator such that an electron in the mode i of $|\Psi_{HF}\rangle$ is excited to mode a.

For simplicity, an occupation number vector can be defined for each electronic configuration. Thus, a generic electronic state $|\Psi\rangle$ of a molecular system consisting of n_e electrons and n-MOs can be written as occupation number vector representation as

$$\begin{aligned} |\Psi\rangle &= \sum_{\vec{s}} c_{\vec{s}} (f_1^\dagger)^{s_1} (f_2^\dagger)^{s_2} \dots (f_{2n}^\dagger)^{s_{2n}} |0\rangle \\ &= \sum_{\vec{s}} c_{\vec{s}} \, \|s_1 s_2 \dots s_{2n}\rangle\!\rangle_{\varphi_1 \varphi_2 \dots \varphi_{2n}}, \end{aligned} \tag{3.28}$$

where $s_\mu \in \{0,1\}$, $\sum_{\mu=1}^{2n} s_\mu = n_e$, and each $\vec{s} = \{s_1, s_2, ..., s_{2n}\}$ corresponds to a possible electronic configuration. The second line shows the occupation number vector representation of the state, and because of its simplicity from now on, we continue with this representation.

We then construct the following $2^{2n} \times 2^{2n}$ density matrix:

$$\rho = |\Psi\rangle\langle\Psi| = \sum_{\vec{s},\vec{r}} \lambda_{\vec{s}}\, \lambda_{\vec{r}}\, \|s_1 \dots s_{2n}\rangle\rangle\langle\langle r_1 \dots r_{2n}\|, \tag{3.29}$$

When the number of orbitals n is greater than 10, the dimension of this matrix exceeds the computational power of classical computers. Therefore, for further calculations, we stored the nonzero elements of the density matrices of molecules in memory using the *sparse matrix representation*. Furthermore, the single and two-orbital reduced states can be calculated by taking the partial trace of the fermionic state defined in Eq. (3.17) over the modes of the remaining orbitals.

To investigate the impact of local SSRs on orbital correlations, we projected the ground state density matrix into the different sectors of the Fock space, as we introduced in Eq. (3.18). For local P-SSR, the Fock space of an orbital is divided into even and odd sectors. Regarding local N-SSRs, the projection operators divide the same two-mode Fock spaces into three sectors: where no excitation exists, where there is one excitation, and where there are two excitations.

We can concretize this using the following two-orbital ground state example:

$$\lambda_1\|11,00\rangle\rangle + \lambda_2\|10,01\rangle\rangle + \lambda_3\|01,10\rangle\rangle + \lambda_4\|00,11\rangle\rangle, \tag{3.30}$$

where a comma separates the modes of the two MOs. Local P-SSR eliminates the density matrix terms $\rho_{\mu,\nu} = \rho_{\nu,\mu} = \lambda_\mu\lambda_\nu$ with $\mu = \{1,4\}$ and $\nu = \{2,3\}$. The term $\rho_{1,4} = \rho_{4,1}$ further vanishes after the application of local N-SSR.

3.2.2 Orbital discord

The amount of the total correlations defined in Eq. (2.15) shared between any two MOs was measured by inserting two-orbital reduced state ρ_{LR} where $L(R)$ denoted the left (right) orbital. And "right-orbital-classical" correlation $C(R)$ can be identified amount of the maximum information about the left orbital that can be extracted

after the measurements $\{\Pi_{i_R}\}$ performed on the right orbital and given by Eq. (2.41). Similarly, as we discussed before, when the shared correlations between the orbitals are extracted by performing local measurements on the left orbital, one can end up with a "left-orbital-classical" correlation $C(R)$.

In N-mode fermionic systems, SSRs considerably limit the number of permissible measurements, thereby simplifying the optimization process in classical correlation calculation in Eq. (2.41) and so quantum discord calculation in Eq. (2.42). For the orbital-orbital case, the number of parameters required in this optimization is significantly reduced in the presence of SSRs. P-SSR only allows the following projection operations:

$$\{\|\varphi\rangle\rangle_{\psi_{R_1}\psi_{R_2}}^{\mathrm{P-SSR}}\} \supset \begin{cases} \alpha_1\|00\rangle\rangle + \alpha_2\|11\rangle\rangle, \\ \alpha_3\|01\rangle\rangle + \alpha_4\|10\rangle\rangle, \\ \alpha_4^*\|01\rangle\rangle - \alpha_3^*\|10\rangle\rangle, \\ \alpha_2^*\|00\rangle\rangle - \alpha_1^*\|11\rangle\rangle, \end{cases} \tag{3.31}$$

which means that the optimization can be done with eight real parameters: For $k = 1, 2, 3, 4$, since $\alpha_k = x_k + iy_k$ and $\alpha_k^* = x_k \times iy_k$, four different $\{x_k, y_k\}$ real pairs are sufficient to describe all the permissible measurements.

On the other hand, in the case of N-SSR preservation, the permitted measurements $\{\Pi_{i_R}\}$ to be described with only two complexes, i.e., four real parameters, as follows:

$$\{\|\varphi\rangle\rangle_{\psi_{R_1}\psi_{R_2}}^{\mathrm{N-SSR}}\} \supset \begin{cases} \|00\rangle\rangle, \\ \beta_1\|01\rangle\rangle + \beta_2\|10\rangle\rangle, \\ \beta_2^*\|01\rangle\rangle - \beta_1^*\|10\rangle\rangle, \\ \|11\rangle\rangle, \end{cases} \tag{3.32}$$

In summary, with the inclusion of SSRs, the number of real parameters required for optimization in orbital correlation decomposition is significantly reduced. Thus, all calculations can be performed with four real parameters under P-SSR and two real parameters under N-SSR in spherical coordinates.

Algorithm 1 Quantum discord for two-orbital reduced states under P-SSR

Require: ρ_{LR}, ρ_L, ρ_R, N_θ, N_ϕ

1: $\|\Pi_1\rangle\rangle \leftarrow \cos(\theta/2)\|00\rangle\rangle + e^{i\phi}\sin(\theta/2)\|11\rangle\rangle$ **then** $\Pi_1 \leftarrow \|\Pi_1\rangle\rangle\langle\langle\Pi_1\|$;
2: $\|\Pi_2\rangle\rangle \leftarrow \cos(\theta/2)\|01\rangle\rangle + e^{i\phi}\sin(\theta/2)\|10\rangle\rangle$ **then** $\Pi_2 \leftarrow \|\Pi_2\rangle\rangle\langle\langle\Pi_2\|$;
3: $\|\Pi_3\rangle\rangle \leftarrow e^{-i\phi}\sin(\theta/2)\|01\rangle\rangle - \cos(\theta/2)\|10\rangle\rangle$ **then** $\Pi_3 \leftarrow \|\Pi_3\rangle\rangle\langle\langle\Pi_3\|$;
4: $\|\Pi_4\rangle\rangle \leftarrow e^{-i\phi}\sin(\theta/2)\|00\rangle\rangle - \cos(\theta/2)\|11\rangle\rangle$ **then** $\Pi_4 \leftarrow \|\Pi_4\rangle\rangle\langle\langle\Pi_4\|$;
5: MutInfo$I \leftarrow \rho_{LR} - \rho_L - \rho_R$;
6: Initialize MutInfoMat$J$ as $N_\theta \times N_\phi$ matrix
7: **for** $\theta_k = 0$ to N_θ **do**
8: $\quad\theta \leftarrow \pi\,\theta_k/N_\theta$;
9: $\quad$**for** $\phi_m = 0$ to N_ϕ **do**
10: $\quad\quad\phi \leftarrow \pi\,\phi_m/N_\phi$;
11: $\quad\quad$Replace θ and ϕ in Π_1, Π_2, Π_3 and Π_4;
12: $\quad\quad$**for** $i = 1$ to 4 **do**
13: $\quad\quad\quad\rho_{\Pi_i} = \Pi_i\rho_{LR}\Pi_i/\operatorname{Tr}[\Pi_i\rho_{LR}\Pi_i]$
14: $\quad\quad$**end for**
15: $\quad\quad$MutInfo$J[N_\theta, N_\phi] \leftarrow S(\rho_{L/R}) - \sum_i p_i\,S(\rho_{\Pi_i})$
16: $\quad$**end for**
17: **end for**
18: QD$(\rho_{LR}) \leftarrow$ MutInfo$I$ − MaxValue[MutInfoMat$J$]

Algorithm 1 illustrates the calculation of quantum discord for a two-orbital state under P-SSR. The inputs, N_θ and N_ϕ, represent the resolutions for the polar angle θ and azimuthal angle ϕ used in the optimization process. The projectors specified in steps 1-4 are allowed under P-SSR, as listed in Table 3.31. In step 5, the mutual information MutInfo$I$, corresponding to the total correlation, is calculated using the formula defined in Eq. (2.15). From steps 7 to 11, a double loop is conducted over all possible combinations of the angles θ and ϕ within the resolution set by N_θ and N_ϕ to calculate the second expression of mutual information, defined in Eq. (2.38). After completion of the double loop (in step 17), quantum discord, as given in Eq. (2.42),

is calculated as the difference between the mutual information MutInfo$I$ and the maximum value in the matrix MutInfo$J$.

A vital flexibility of this algorithm lies in steps 13 and 15. For calculating the left (right) quantum discord, one needs to apply the projective operators to the left (right) in step 13, and substitute the entropy of the right (left) orbital in step 15. Also, the algorithm can be easily adapted to N-SSR by replacing the P-SSR projection operators with those listed in Table 3.32.

3.2.3 Water

The water molecule (H_2O) is among the primary molecules necessary for the sustenance of various life forms. The water molecule, composed of 10 electrons, has two lone pairs of electrons localized around the oxygen atom. These pairs share a tetrahedral geometry with the delocalized electron pairs in the H-O bonds, whereby the H-O-H angle is approximately 104.5 degrees. For the molecule to achieve this geometry, prior to forming the covalent bonds, a hybridization of the oxygen atom's orbitals is required, implying a state of quantum superposition [1]. Upon establishing H-O bonds, this quantumness could permeate the entire molecule as orbital entanglement. In this context, it would be expected to find a high degree of quantum correlation amongst the MOs, which is why we have decided to investigate the water molecule.

At the HF/STO-6G level using the Gaussian09 program [138], the optimal geometry of the water molecule exhibits bond lengths of 1.02 $\mathring{A}$ and bond angles of 96.8°. CISD calculations are based on 10 electrons and 7 HF-MOs, corresponding to a dimension of $2^{14} = 16,384$ in its density matrix representation. However, the CISD ground state only involves 31 different electronic configurations. The CI energy converges at $-75.737545702\ E_{\mathrm{h}}$.

In Table 3.1, we present the numerical results for the pairwise correlations in the water molecule's CISD/STO-6G ground state. These results are based on the arrangement of the HF orbitals—$1a_1$, $2a_1$, $1b_2$, $3a_1$, $1b_1$, $4a_1$, and $2b_2$—in an energetically ascending order from 1 to 7. The total correlation I and fermionic logarithmic

entanglement negativity E_N are also provided both in their exact values and in the fractions remaining in the presence of SSRs. Further, Table 3.1 details what percentage of the total correlation decomposes into classical correlation and quantum discord in the presence of the local parity SSR (P-SSR) and particle number SSR (N-SSR).

Table 3.1: The correlations shared among HF orbital pairs in the CISD/STO-6G ground state of H_2O. The total correlation I and logarithmic entanglement negativity E_N survived under the SSRs are given as percentages, with N and P subscripts indicating the respective SSR.

H_2O CISD/STO-6G										
(L,R)	I	$I_{(P)}$ =	$C_{(P)}(L,R)$ +	$D_{(P)}(L,R)$	$I_{(N)}$ =	$C_{(N)}$ +	$D_{(N)}$	E	$E_{(P)}$	$E_{(N)}$
(2, 3)	0.021	100%	73.8%, 73.8%	26.2%, 26.2%	84.1%	73.7%	10.4%	0.0035	100%	99.3%
(2, 4)	0.032	56.9%	35.7%, 35.7%	21.2%, 21.2%	42.6%	35.6%	7.0%	0.0092	34.8%	34.6%
(2, 5)	0.0019	100%	0.8%, 0.5%	**99.2%**, **99.5%**	0.37%	0.37%	0%	0.28×10^{-5}	100%	0%
(2, 6)	0.048	99.4%	76.3%, 74.3%	23.1%, 25.1%	75.4%	74.3%	1.0%	0.081	98.2%	0.4%
(2, 7)	0.019	100%	82.9%, 87.5%	17.1%, 12.5%	80.3%	77.8%	**2.5%**	0.033	100%	**0%**
(3, 4)	0.094	100%	79.4%, 79.3%	20.6%, 20.7%	88.1%	79.1%	9.0%	0.013	100%	98.9%
(3, 5)	0.0020	100%	3.1%, 1.5%	**96.9%**, **98.5%**	1.3%	1.3%	0%	0.13×10^{-4}	100%	0%
(3, 6)	0.13	100%	87.8%, 87.6%	12.2%, 12.4%	83.9%	82.4%	**1.5%**	0.10	100%	**0%**
(3, 7)	0.23	99.9%	72.8%, 73.3%	27.1%, 26.6%	70.7%	69.8%	0.9%	0.24	93.9%	0.4%
(4, 5)	0.0029	100%	1.9%, 1.0%	**98.1%**, **99.0%**	0.7%	0.7%	0%	0.12×10^{-4}	100%	0%
(4, 6)	0.14	98.1%	78.0%, 74.3%	20.1%, 23.8%	75.5%	74.3%	1.2%	0.21	69.3%	0.5%
(4, 7)	0.10	100%	81.2%, 83.5%	18.8%, 16.5%	77.3%	75.8%	**1.5%**	0.11	100%	**0%**
(5, 6)	0.011	100%	37.7%, 62.0%	**62.3%**, 38.0%	33.9%	33.9%	0%	0.058	100%	0%
(5, 7)	0.0020	100%	38.3%, 61.2%	**61.7%**, 38.8%	16.0%	16.0%	0%	0.017	100%	0%
(6, 7)	0.13	100%	85.1%, 85.1%	14.9%, 14.9%	93.1%	85.0%	8.1%	0.017	100%	99.0%

Two noteworthy outcomes raise questions about the main conclusions drawn in Ref. [28]. Firstly, we observe the existence of certain orbitals that predominantly share quantum discord as a correlation in the presence of local P-SSR (refer to correlations highlighted with bold lines in Table 3.1). Since classical correlations were considered with inappropriate measure in Ref. [28], quantum correlations never emerged as dominant. Consequently, they inferred that quantum correlations are insignificant in chemical bonding. However, our results based on appropriate measurement indicate insufficient evidence for such inferences and that further study of this issue is warranted.

Significantly, in all pairs involving the 5th orbital, $1b_1$, quantum correlations are the dominant type of correlation under P-SSR. This one is the highest-energetic

occupied molecular orbital (HOMO) in the HF ground state, and it does not possess any component other than the $2p_x$ atomic orbital of its oxygen atom, with a lone pair of electrons. Notably, while HOMO is paired with either of the $4a_1$ or $2b_2$ orbitals—numbered 6 and 7 respectively and both exhibiting antibonding characteristics—quantum discord is stronger than classical correlations, but only if local measurements performed over the $1b_1$. In contrast, when measurements are performed over the other orbital in the pair, quantum discord appears weaker.

Our second significant finding concerns that there exist pairwise orbital correlations in which quantum discord survives even in the absence of orbital entanglement after applying local N-SSR (refer to values underlined in Table 3.1). In Ref. [28], the authors concluded that the possibility of using molecular systems in quantum technologies is relatively low, reasoning from the predominant loss of orbital entanglement under N-SSR. However, as discussed in Section 2.2.3, not only entanglement but also discord is used as a resource in quantum information tasks.

The orbital pairs $(2,7)$, $(3,6)$, and $(4,7)$ share quantum correlations beyond entanglement. While the 2nd and 3rd orbitals are bonding orbitals $2a_1$ and $1b_2$, the 4th orbital $3a_1$ displays more of a lone pair character than that of bonding. This indicates that the pairs having quantum discord in the absence of entanglement do not necessarily consist of orbitals with opposite bonding/antibonding characters. Upon closer examination, it is seen that these pairs are composed of one filled and one empty orbital with opposite a_1/b_2 symmetries. Therefore, there is a possibility that the presence of quantum correlations under SSRs may be related to orbital symmetries.

We additionally perform CASSCF/cc-pVXZ calculations in the Molpro [139, 140], Psi4 [141, 142], and PySCF [143, 144] programs in the active space consisting of 8 electrons in $2a_1$, $1b_2$, $3a_1$, $1b_1$, $4a_1$, and $2b_2$ HF orbitals. Since this active space is constructed from orbitals investigated in the CISD/STO-6G ground state, it allows us to investigate the impact of the used basis set on orbital correlations.

Since the CI coefficients—from which we construct the electronic ground state—almost perfectly matched in all program outputs, in Table 3.2, we only summarize the results of PySCF/CASSCF using the cc-pVTZ basis. When comparing with Ta-

Table 3.2: The pairwise total correlations in the CASSCF(8,6)/cc-pVTZ ground state of H_2O and their exact additive decomposition into classical correlations and quantum discord in the presence of SSRs.

H_2O CASSCF(8,6)/cc-pVTZ

(L,R)	I	$I_{(P)} = C_{(P)}(L,R) + D_{(P)}(L,R)$			$I_{(N)} = C_{(N)} + D_{(N)}$			E	$E_{(P)}$	$E_{(N)}$
(2, 3)	0.017	100%	78.07%, 78.00%	21.93%, 22.00%	87.19%	77.99%	9.20%	0.002	100%	100%
(2, 4)	0.026	57.83%	39.13%, 39.15%	18.70%, 18.68%	45.91%	39.04%	6.87%	0.008	31.31%	31.28%
(2, 5)	0.001	100%	0.42%, 0.27%	**99.58%, 99.73%**	0.10%	0.10%	0%	0	0%	0%
(2, 6)	0.038	99.97%	80.62%, 78.53%	19.35%, 21.45%	79.89%	78.53%	1.36%	0.065	99.89%	0.96%
(2, 7)	0.017	100%	80.21%, 84.93%	19.79%, 15.07%	78.76%	75.98%	**2.78%**	0.038	100%	**0%**
(3, 4)	0.058	100%	88.80%, 88.80%	11.20%, 11.20%	93.91%	88.80%	5.11%	0.005	100%	100%
(3, 5)	0.001	100%	1.53%, 0.90%	**98.47%, 99.10%**	0.08%	0.08%	0%	0	0%	0%
(3, 6)	0.092	100%	91.23%, 91.18%	8.77%, 8.82%	91.50%	88.50%	**3.01%**	0.059	100%	**0%**
(3, 7)	0.180	100%	71.22%, 71.62%	28.78%, 28.38%	71.95%	69.73%	2.22%	0.207	99.56%	3.14%
(4, 5)	0.001	100%	0.99%, 0.56%	**99.01%, 99.44%**	0.18%	0.18%	0%	0	0%	0%
(4, 6)	0.120	99.99%	74.85%, 73.14%	25.14%, 26.85%	76.13%	73.14%	2.99%	0.152	98.48%	3.86%
(4, 7)	0.061	100%	87.77%, 88.63%	12.23%, 11.37%	88.57%	84.67%	**3.90%**	0.057	100%	**0%**
(5, 6)	0.004	100%	36.64%, 63.13%	**63.36%**, 36.87%	31.39%	31.39%	0%	0.030	100%	0%
(5, 7)	0.001	100%	37.30%, 62.53%	**62.70%**, 37.47%	21.50%	21.50%	0%	0.014	100%	0%
(6, 7)	0.090	100%	91.19%, 91.19%	8.81%, 8.81%	96.10%	91.19%	4.91%	0.007	100%	100%

ble 3.1, it is observed that the total amounts of orbital correlations slightly decrease as the accuracy and precision of the basis increase. However, there is no change in the decomposition of these correlations into classical and quantum components. Specifically, there are no noticeable differences between Table 3.1 and Table 3.2. We confirmed the same similarities in the calculations made with other cc-pVXZ bases. In this context, we can conclude that our three crucial findings about the pairwise orbital correlations in the CISD/STO-6G ground state are also fully valid in the CASSCF/cc-pVXZ ground states.

Another noteworthy result arises when considering the following scenario: What if the density matrix of an orbital pair described a qubit system? To address this question, we recalculate the entanglement in two-orbital density matrices using the multipartite entanglement measure proposed in Ref. [145]. This measure gives the entanglement negativity in Eq. (2.29) for two-qubit states and it can be easily computable using the code provided in Ref. [146], together with the parser YALMIP [147] and the solver SDPT3 [148, 149]. The results show that some two-orbital density matrices are separable for qubit systems, whereas they are entangled in the fermionic mode picture, as shown in the underlined instances in Table 3.3. This suggests that

Table 3.3: The amounts of quantum entanglement shared between the HF orbital pairs in the water molecule's CISD/STO-6G basis state. The values given with the letter "q" in parentheses are calculated using the multi-qubit entanglement criterion instead of the fermionic logarithmic entanglement negativity.

(L, R)	E	E_P	E_N	$E(q)$	$E_P(q)$	$E_N(q)$
$(2, 3)$	0.0035	0.0035	0.0035	0.0000	0.0000	0.0000
$(2, 4)$	0.0092	0.0032	0.0032	0.0002	0.0000	0.0000
$(2, 5)$	0.0000	0.0000	0.0000	0.0000	0.0000	0.0000
$(2, 6)$	0.0825	0.0800	0.0004	0.0216	0.0215	0.0000
$(2, 7)$	0.0329	0.0329	0.0000	0.0066	0.0066	0.0000
$(3, 4)$	0.0134	0.0134	0.0133	0.0000	0.0000	0.0000
$(3, 5)$	0.0000	0.0000	0.0000	0.0000	0.0000	0.0000
$(3, 6)$	0.1045	0.1045	0.0000	0.0304	0.0304	0.0000
$(3, 7)$	0.2439	0.2291	0.0010	0.0788	0.0788	0.0000
$(4, 5)$	0.0000	0.0000	0.0000	0.0000	0.0000	0.0000
$(4, 6)$	0.2166	0.1502	0.0012	0.0468	0.0463	0.0000
$(4, 7)$	0.1141	0.1141	0.0000	0.0332	0.0332	0.0000
$(5, 6)$	0.0584	0.0584	0.0000	0.0157	0.0157	0.0000
$(5, 7)$	0.0174	0.0174	0.0000	0.0034	0.0034	0.0000
$(6, 7)$	0.0169	0.0169	0.0167	0.0000	0.0000	0.0000

orbital entanglement is underestimated when standard quantum information theory is used instead of the fermionic one. This observation also contradicts an expectation mentioned in Ref [28].

3.2.4 2-Propenyl

The other molecular system we have examined is 2-propenyl (C_3H_5), one of the smallest linear molecules containing a π bond. The valence bond theory suggests that there is resonance in the electronic ground state of this molecule between the C–C=C and C=C–C valence bond structures, meaning the molecule exists in a

superposition of these two configurations. As a reflection of this, we expect high quantum correlations, especially between the π orbitals of this molecule.

In C_3H_5, the optimized geometry using the STO-6G minimal basis set reveals bond lengths of 1.41 $\mathring{A}$ and bond angles of 124.4°between neighboring carbon atoms. The electronic structure of the molecule encompasses 23 electrons and 20 HF-MOs, resulting in a CISD energy of -116.35450180 E_h. As the 20 HF-MOs in 2-propenyl formed 136 different orbital pairs, we preferred to visualize our results in Figure 3.1 rather than summarizing them in a table.

Figure 3.1: The pairwise total correlations in the doublet ground state of C_3H_5 and their proper decomposition into classical correlations and quantum discord in the presence of superselection rules (SSRs). The quantum discord is simply quantum entanglement for the pairs that share nonzero logarithmic negativity on the left panel.

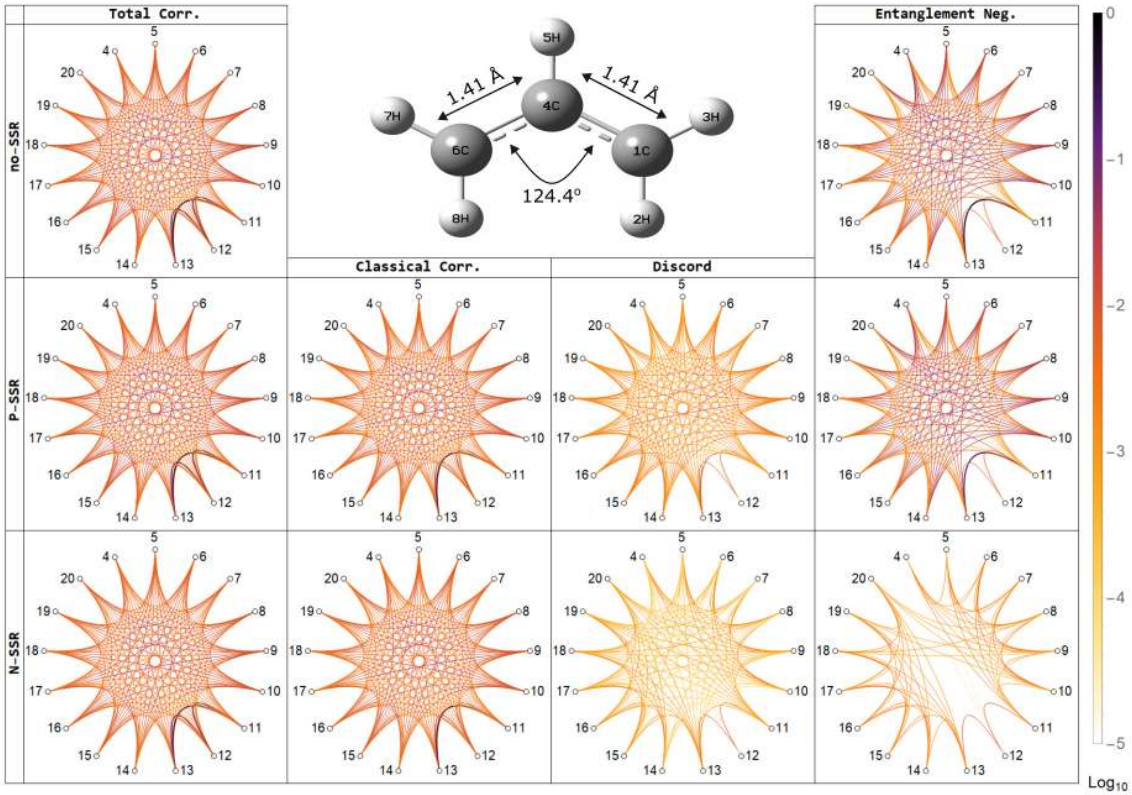

In our results, the orbital pair $(11, 13)$ exhibits the highest total correlation at 0.49, while the pair $(11, 17)$ has the least, without SSRs. In this molecule, we did

not encounter a situation where orbital discord is stronger than classical orbital correlations in this molecule.

Remarkably, entanglement and quantum discord values of pairs $(11, 12)$ and $(12, 13)$ remain unaltered by local SSRs. Also, the 12th orbital does not have a negligible amount of logarithmic entanglement negativity with orbitals other than 11 and 13. On the other hand, despite the $(11, 13)$ orbital pair being separable, it contains quantum discord in the presence of local N-SSR. These three aforementioned orbitals share a unique symmetry distinct from others and it may hint at a connection between orbital symmetries and their correlations. Each of the 11th, 12th, and 13th orbitals—corresponding respectively to HOMO, half-occupied orbital, and the lowest unoccupied orbital (LUMO) in the HF ground state—is a superposition of only the three $2p_z$ atomic orbitals of the carbon atoms, and therefore they display a π-orbital character.

We also observe that the orbital pairs $(7, 13)$, $(8, 13)$, $(9, 13)$, $(10, 13)$, $(11, 14)$, and $(11, 17)$ share quantum correlations beyond entanglement, regardless of which SSR is applied. Moreover, 51 orbital pairs have quantum discord under local N-SSR, even without any entanglement. Such findings support that orbital entanglement cannot be regarded as a comprehensive measure of quantum orbital correlations, as assumed earlier in Ref. [28].

3.2.5 Dicarbon anion

Another prototypical molecule we investigated is the dicarbon anion (C_2^-). The literature presents ongoing debates about the bond order between carbon atoms in C_2^-: hybridization theory predicts 3, MO theory predicts 2, and valence bond theory predicts the presence of 4 bonds between carbons [150]. Our decision to study this molecule arises from anticipation that the low bond order predicted by MO theory might manifest in our results as a lack of correlations between MOs.

In C_2^-, the optimized molecular geometry at the HF/STO-6G level using Gaussian09 exhibits an interatomic distance of 1.25 $\mathring{A}$. The CISD ground state, built from an electronic structure of 13 electrons and 10 HF-MOs, has 53 different electronic

Figure 3.2: The pairwise total correlations in the doublet ground state of C_2^- and their exact additive decomposition into classical correlations and quantum discord in SSRs. Quantum discord includes entanglement for the pairs that share nonzero logarithmic negativity on the left panel. Otherwise, it quantifies quantum correlations beyond entanglement.

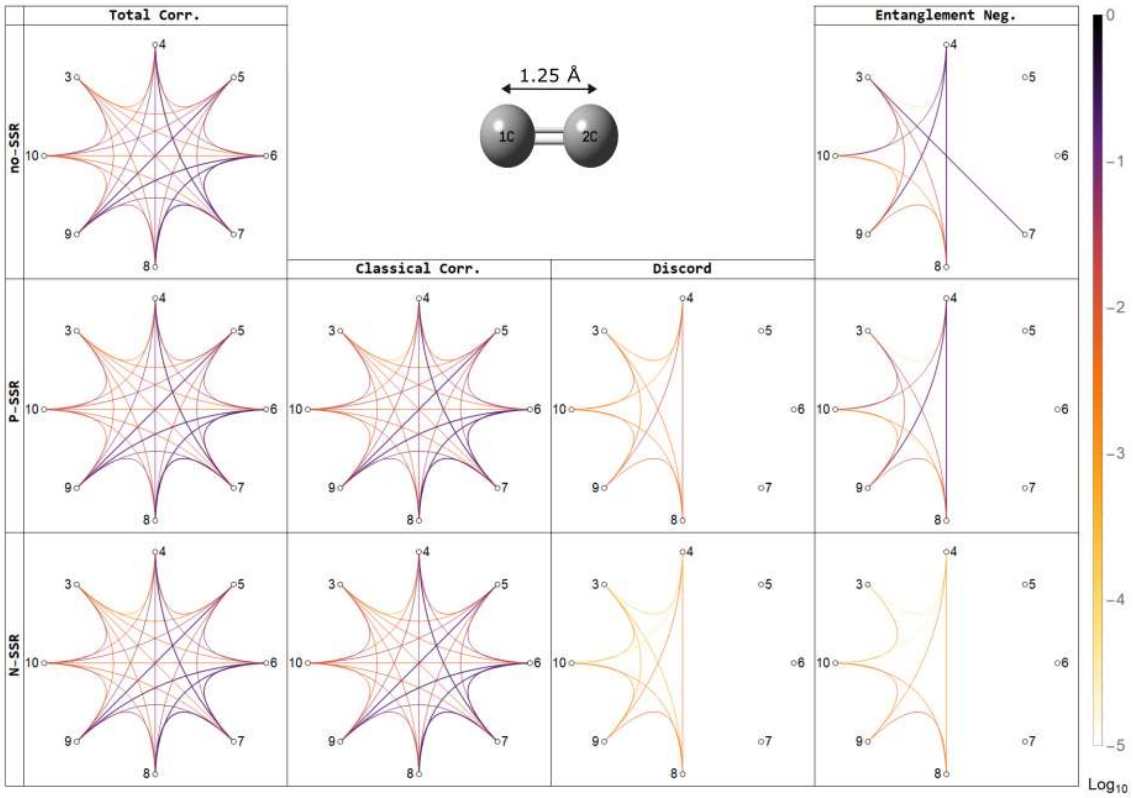

configurations. The computed CISD energy for this molecule is $-75.293354472\ E_\mathrm{h}$.

As shown in Fig. 3.2, in the absence of SSRs, the total correlations range from 0.00025 for the orbital pair $(3,4)$ to 0.2 for the $(7,8)$ pair. The former is the only pair whose dominant pairwise correlation is quantum discord under the local P-SSR. However, its quantum discord does not vanish under the local N-SSR, while its logarithmic entanglement negativity is always small enough to be neglected. These 3rd and 4th orbitals correspond to the HF MOs $2\sigma_g$ and $2\sigma_u^*$. The simultaneous occupancy of these two orbitals, which has a probability of 0.91 in the ground state, implies the absence of a σ bond between the C atoms and reduces the bond order of the molecule.

Quantum discord in the pairs of orbitals $(3, 8)$ and $(3, 9)$ exists despite the lack of entanglement in the presence of the local N-SSR. The 3rd orbital is the bonding σ orbital ($2\sigma_g$), while the 8th and 9th ones are degenerate antibonding π-orbitals ($1\pi_g^*$). Furthermore, the pairwise quantum correlations distributed among the antibonding orbitals 8, 9, and 10 seem not to be affected significantly by the local SSRs. The last orbital, $3\sigma_\mu^*$, distinctly displays a σ character, unlike the orbitals 8 and 9.

3.2.6 Outlook

In this section, we have investigated orbital-orbital correlations in specific molecular electronic states, properly decomposing these correlations into their classical and quantum components through the novel introduction of orbital discord. We have also considered the additional constraints imposed by local superselection rules on these reduced states. Notably, the computational complexity of orbital discord is lower when compared to the four-qubit quantum discord. This efficiency lets us comprehensively address both classical and quantum parts of the pairwise orbital correlations under SSRs.

Our analysis primarily reveals that quantum orbital correlations can surpass their classical counterparts. Intriguingly, quantum orbital discord can survive without orbital entanglement. Contrary to the previous claims in Ref. [28], our findings indicate that the lack of orbital entanglement doesn't diminish the resourcefulness of molecular systems in quantum technologies. This is because the quantum correlations beyond entanglement can be used as a resource in certain quantum information tasks, including remote state preparation and optimal state discrimination protocols.

Orbital correlation measures employed in our study and in Ref. [28] are computationally expensive due to the involved optimization process. Contrarily, previous works—that incorrectly defined the total orbital correlations as entanglement—had lesser computational demands as they only focused on entropy calculations. Thus, the primary obstacle to investigating chemical bonds by genuinely decomposing total correlations arises from computational limitations. This challenge might be solved in the near future by developing methods that originate from machine learning-based

calculations of fermionic correlation [151] or that extract these correlations from tensor network states more efficiently [152].

The above calculations are limited to the HF-MOs that allow electrons to be delocalized. Subsequent to our study, Ref. [153] proposed an orbital optimization scheme in which each MO in the π-structure of planar molecules can be distinctly localized to a single atomic center. This is achieved by maximizing the resourcefulness of these MOs. MOs that are completely localized to specific atoms, called atomic-like orbitals, are the best method to examine chemical bonding phenomena. Its success was demonstrated in Ref. [153], as these atomic-like orbitals allow us to determine the bond order of certain chemical bonds with great accuracy by looking at orbital-orbital correlations.

Chapter 4

AROMATICITY AS A SUPERPOSITION PHENOMENA

Aromaticity is considered one of the unicorns in the framework of chemical bonding since it can't be directly observed and lacks a clear quantum physical foundation. A widely accepted definition describes aromaticity as electron delocalization through overlapping atomic orbitals within a set of atoms that form a closed loop. To analyze this phenomenon, orbital-orbital correlations are not sufficient as examined covalent bonds in the previous chapter. However, the framework of multi-orbital correlations is required because such a multi-orbital bonding phenomenon is more than the sum of the two-orbital bonds.

We approach the problem from a different perspective. Instead of working from molecular orbital or valence bond theory, we measure directly the superposition of overlapping atomic orbitals. This measure describes multi-orbital superposition as a measure of closed-loop electron delocalization because atomic orbitals are localized.

The structure of this chapter is as follows. In Sec. 4.1, we begin with a historical introduction of aromaticity and then detail aromaticity descriptors based on the physicochemical properties resulting from the aromaticity of molecules. In Subsec. 4.2.1, we delve into the quantification of superposition in nonorthogonal quantum states and its limitations, while in the following Subsec. 4.2.2, we introduce the biorthogonal framework that addresses these limitations. Subsequently, in Sec. 4.3 (see the preprint of the containing content in Ref.[154]), we present results for applying these concepts to analyze electron delocalization in the π-electronic structures of ground states for some aromatic molecules.

4.1 Aromaticity

4.1.1 Historical introduction to aromaticity

Aromaticity is a fundamental concept in chemistry, essential for understanding a wide range of molecules' stability, reactivity, and properties. Defining aromaticity has proven challenging due to its diverse manifestations and the continuous discovery of new aromatic compounds. This subsection will explore the historical development of the aromaticity concept, advances in understanding chemical bonding, the expansion of aromaticity types, and the modern definitions and challenges faced in this field.

Early discoveries and the concept of aromaticity

Three decades after Faraday isolated benzene (C_6H_6) from gas light oil and determined its empirical formula as well as its physical properties [155], Hofmann coined the term "aromatic" in his research on benzene and its monocarboxylic derivatives [156]. This term—inspired by the Greek word *aroma* for pleasant odor—was used due to the unexpectedly stable nature of these compounds, which necessitated separate classification. For almost half a century, benzene's peculiar properties and structure puzzled chemists. It was Kekulé who identified compounds structurally similar to benzene as aromatic and proposed the first reasonable structure for benzene, a cyclic hexagonal arrangement of carbon atoms with alternating single and double bonds [157]. Although not entirely accurate, this model began a more systematic understanding of aromatic compounds and laid the groundwork for developing the concept of aromaticity.

Shortly after the isolation of benzene, naphthalene was identified as a result of cool tar distillation [158], and Erlenmeyer proposed its structure as two fused benzenes in 1866. Subsequently, the discovery of other polycyclic rings like anthracene and phenanthrene that exhibited aromatic properties led to expanding the definition of aromaticity to include polycyclic hydrocarbons. By the late 19th century, the realm of aromatic compounds grew with the discovery of significant compounds containing heteroatoms, such as pyridine, furan, pyrrole, and thiophene. Bamberger

proposed a monocyclic structure for these compounds, similar to Kekulé's benzene structures [159].

Advances in chemical bonding and aromaticity

The next step in understanding aromaticity came from the development of quantum mechanics and its applications in explaining chemical bonding. Our understanding of chemical bonding began with the Lewis structure, which represents a bond as a sharing of two electrons between two atoms to form an octet [160]. The valence bond (VB) theory was subsequently developed based on this idea. Heitler and London provided a quantum mechanical insight into Lewis's electron-pair bonding by applying the Schrödinger wave equation to the bonding in dihydrogen (H_2) [161]. Their findings highlighted that such bonding arises from quantum mechanical resonance interactions, where two atoms share spin-paired electrons via their local orbitals. In modern terms, the Heitler-London (HL) wavefunction represents the bonding in H_2 as a superposition of two spin configurations corresponding to two possible covalent VB structures. This superposition of covalent terms explains the lower total energy in the molecular form of H_2 compared to the total energy of two separate hydrogen atoms. Today, their work is known as the Heitler-London valence bond (HLVB) theory, which solely considers covalent VB structures [2].

Building on this, Pauling improved the Heitler-London framework of chemical bonding by incorporating ionic VB structures into the superposition of the electron pair bond wavefunction [162, 163]. This addition not only further lowered the total energy but also presented a generalized picture of bonding, where covalent and ionic bonds are viewed as the extreme forms of a continuously defined bond. In the case of benzene, Pauling demonstrated that the resonance of two predominant covalent VB structures indicates the delocalization of electrons in the double bonds between carbon atoms [1]. Thus, Pauling's model supported Kekule's idea and explained the aromaticity of benzene as the resonance of its covalent VB structures.

Hückel's rule and the expansion of aromatic types

At the same time that Pauling was developing modern VB theory, Hückel intro-

duced a rule based on his primitive version of the molecular orbital theory, nowadays known as the Hückel molecular orbital (HMO) theory, which provided a quantitative criterion for aromaticity [164]. According to *Hückel's rule*, molecules that are planar, cyclic, and fully conjugated molecules are called aromatic if they contain $4n + 2$ π-electrons, while those with $4n$ π-electrons are less stable and are termed *antiaromatic*. The HMO theory predicts the electronic properties in conjugated molecules, like benzene, by focusing on the delocalization of π-electrons. The theory suggests that the molecular orbitals in conjugated systems can be approximated as linear combinations of atomic orbitals on the involved atoms. By solving an effective Hamiltonian which describes the π framework, one can determine which linear combinations form bonding and anti-bonding π molecular orbitals [165].

While Hückel's $4n+2$ rule successfully characterized the aromaticity of archetypical organic molecules, the discovery of new types of aromatic molecules added complexity. The first known metalloaromatic compound—referring to aromaticity in a cyclic molecule containing a metal atom or ion as part of its structure—expanded the scope of aromaticity beyond organic chemistry [166]. Furthermore, the emergence of three-dimensional aromatics, including fullerenes and nanotubes, redefined the traditional view of planar conjugated systems [167, 168]. In addition, Möbius aromaticity occurring in molecules with a twisted or non-planar structure—in which the delocalized π-electrons follow a Möbius strip topology—displays behavior precisely opposite to the $4n+2$ rule [169, 170]. Another significant breakthrough occurred with the discovery of the first all-metal aromatic cluster, Al_4^{2-} [171]. These compounds can exhibit σ-, π-, and even δ-electron delocalization (involving d orbitals) [172]. By 2017, the reported number of aromaticity types had reached forty-five [173], reflecting the continuous evolution of aromaticity and more importantly lack of a universally accepted definition of aromaticity.

Modern definition and challenges

Aromaticity is regarded as one of the unicorns in chemistry, an ancient intuitive concept that lacks a directly observable nature and a well-defined quantum physical basis [174]. This elusive nature leads to the perplexing manifestation of a vast

array of aromaticity types and the challenge of formulating an unambiguous definition [175, 176]. The definition and boundaries of aromaticity have been continually reevaluated to encompass the full spectrum of new aromatic compounds [177]. In modern literature, a widely accepted definition states that aromaticity is primarily manifested by electron delocalization within a set of atoms forming a closed loop, either two- or three-dimensionally [48].

4.1.2 Descriptors of aromaticity

Since aromaticity is a directly observable concept, unlike energy, the descriptors of a molecule's aromatic character are built upon quantifying physicochemical properties that exhibit some aspect of aromaticity. Consequently, numerous existing aromaticity descriptors are based on the energetic [178, 179], structural [180, 181], magnetic [48, 182], and electronic [183, 184] properties of molecules.

Energetic Descriptors

The energetic stabilization resulting from aromaticity represents one of the most significant characteristics of aromatic compounds. Energy-based aromaticity indices evaluate energetic stabilization differences compared to a reference system. For instance, the *resonance energy* (RE), the oldest energetic index, quantifies the energy differential between a given actual molecule and its theoretical resonance counterpart with localized π-electrons. In benzene's context, this resonance refers to one of its Kekulé structures [185]. These methods often take advantage of the fact that cyclic compounds with conjugated π-electrons often exhibit greater stability than their linear counterparts.

As its name indicates, the RE index has been introduced regarding VB theory for aromatic molecules with cyclic π-electron delocalization [1]. Even if the VB theory is the most suitable framework for calculating RE, it can be obtained using the block-localized wavefunction (BLW) method within the MO theory. This computational quantum chemistry method involves partitioning the molecular system into distinct "blocks" [186]. By doing so, the wavefunction of the molecule is modified to constrain electron delocalization within the specified blocks, leading to localized MOs. The

energy difference between the wholly delocalized wavefunction and its block-localized counterpart provides the RE [187].

Alongside the RE, the *aromatic stabilization energy* (ASE) is among the most commonly utilized energy-based indices. ASE is a measure that quantifies the energetic stabilization of aromatic compounds compared to a conjugated but nonaromatic reference system. One popula way to calculate ASE is to determine reaction energies in isodesmic or homodesmotic reactions [188].

Structural Descriptors

The structural, also known as geometric, aromaticity descriptors are founded on the principle that the tendency towards bond length equalization and the symmetry of the ring are essential aspects of aromaticity [180]. The two most commonly utilized descriptors derived from molecular structures are the *Julg index* and the *harmonic oscillator model of aromaticity* (HOMA) index [181].

The Julg index [189] is the first quantitative structural-based aromaticity index that relies on a normalized variance function for carbon-carbon (C-C) bond lengths within a carbocyclic ring:

$$A_j = 1 - \frac{255}{n} \sum_{i=1}^{n} \left(1 - \frac{R_i}{R_{av}}\right)^2 , \tag{4.1}$$

where n represents the number of bonds in the ring, R_i is the bond length of the ith bond, and R_{av} denotes the mean value of all bond lengths. The constant 255 is chosen as the normalization condition to yield unity for benzene.

The HOMA index advances the approach of the Julg index by substituting the mean bond length in Eq. (4.1) with the optimal bond length R_{opt}. This optimal value represents a conceptual quantity for an idealized aromatic system in question [190]. The HOMA model's fundamental idea suggests that a molecule's aromaticity is associated with the deviation of its bond lengths from the idealized structure: the larger the discrepancy between the bond lengths in the actual molecule and the idealized form, the lower the aromaticity, and vice versa.

The HOMA index is then calculated as follows:

$$\mathrm{HOMA} = 1 - \frac{1}{n} \sum_{i=1}^{n} \alpha_i \left(R_{opt} - R_i\right)^2 , \tag{4.2}$$

where α is an empirical constant adjusted to give HOMA = 0 for a model nonaromatic system and HOMA = 1 for a system with all bonds equal to an optimal value. For C–C, carbon-nitrogen (C–N), and nitrogen-nitrogen (N–N) bonds, α_i = 257.7, 93.5, and 130.3, while R_{opt} = 1.388, 1.334, and 1.309 Å, respectively [191].

Magnetic Descriptors

Magnetic descriptors of aromaticity are based on the quantification of net electric current generated by delocalized π-electrons in the ring when a magnetic field is applied perpendicularly to the plane of the aromatic system [179].

This induced current is referred to as the *ring current*. In aromatic compounds, the ring current is *diatropic*, flowing in the clockwise direction when observed from the negative direction of the external magnetic field. In contrast, antiaromatic molecules exhibit a *paratropic* ring current, which flows in the counter-clockwise direction. The induced ring current can weaken or strengthen the applied field, resulting in shielding or deshielding effects. In aromatic compounds, the diatropic ring current generates a magnetic field that shields the inner part of the ring and deshields the outer part. In contrast, the paratropic currents in antiaromatic molecules produce the opposite effect [49].

The *nucleus independent chemical shift* (NICS)—probably the most widely used computational aromaticity descriptor—proposed by Schleyer et al. [192] as a quantitative aromaticity measure applicable to a broad range of molecules, from micro to macrocyclic aromatic compounds. It evaluates molecules' shielding or deshielding effects by calculating the magnetic shielding tensor $\vec{\sigma}$ at a specific point in space, often at the center or above the ring center. Since NICS values computed at the molecular plane level include substantial contributions from σ-electrons, the calculations are commonly performed 1 $\mathring{A}$ above the molecular plane to minimize this impact [193]. Rings with large negative NICS values indicate an aromatic diatropic ring current, while large positive values indicate an antiaromatic paratropic ring current.

NICS offers several advantages over other aromaticity descriptors: (i) it is an experimentally measurable quantity, (ii) it is highly accessible and easy to compute,

and (iii) it does not require reference values, making it universally applicable to any molecule.

The *anisotropy of the induced current density* (ACID) [194] is another robust magnetic descriptor for analyzing aromaticity. It provides a visualization of the induced ring current in a molecule, allowing for the direct assessment of aromatic and antiaromatic properties. ACID has been successfully applied to various molecular systems, including transition-metal complexes and heterocycles.

Electronic Descriptors

The majority of electronic-based aromaticity descriptors focus on evaluating electron delocalization, the primary cause of aromaticity. Electron delocalization is central to several fundamental chemical phenomena, including conjugation, hyperconjugation, and aromaticity [195]. However, since electron delocalization, like aromaticity, is not directly observable, there is no unique theoretical or experimental measurement method.

There are multiple methods to determine electron delocalization. One category of electron delocalization measures is predicated upon the electronic wavefunction. Some utilize the BLW approach, while others localize MOs, thereby providing information to identify regions where electron pairs are located within a molecule [196]. Moreover, regarding the VB theory, resonance structure weights, and energies can offer insight into electron delocalization [197]. In another category, electron delocalization is measured directly from the electron density and its derivatives. Notable examples include the Laplacian of the electron density [198], the ellipticity along the bond path [199], the noncovalent interaction index [200].

The last category of electron delocalization measures is derived from first-order (1-RDM) and higher-order density matrices (n-RDM), also referred to as 1- and n-electron density matrices. These are computationally more efficient than the above methods because 1-RDM, which describes the electron distributions in a molecule, is sufficient to analyze all electron delocalization in a ring.

Following this, a spinless two-electron density matrix, $\gamma(\mathbf{r}_1, \mathbf{r}_2)$, serves as the most common example of a higher-order density matrix. Its significance in electron

delocalization-based aromaticity descriptors relies on its relationship with *electron-sharing indices* (ESI) [184]. These indices are constructed on the part of $\gamma(\mathbf{r}_1, \mathbf{r}2)$ that captures all exchange and correlation effects, denoted as $\gamma_{XC}(\mathbf{r}_1, \mathbf{r}_2)$. The two-electron density matrix $\gamma(\mathbf{r}_1, \mathbf{r}_2)$ signifies the probability of finding two electrons at specific positions $\mathbf{r}_1$ and $\mathbf{r}_2$ in space simultaneously, regardless of the position of the other $N-2$ electrons. Similarly, the exchange-correlation density matrix $\gamma_{XC}(\mathbf{r}_1, \mathbf{r}_2)$ measures the extent to which an electron at $\mathbf{r}_2$ is influenced by the presence of another electron at $\mathbf{r}_1$. This can be defined as the difference between the total pair density and its uncorrelated part:

$$\gamma_{XC}(\mathbf{r}_1, \mathbf{r}_2) = \gamma(\mathbf{r}_1, \mathbf{r}_2) - \rho(\mathbf{r}_1)\rho(\mathbf{r}_2). \tag{4.3}$$

The uncorrelated part, $\rho(\mathbf{r}_1)\rho(\mathbf{r}_2)$, represents the probability of simultaneously finding two independent electrons at $\mathbf{r}_1$ and $\mathbf{r}_2$, irrespective of the positions of the remaining $N-2$ electrons.

Based on the exchange-correlation density, Bader et al. [201] introduced the *delocalization index* (DI), $\delta(A, B)$, also known as the two-center electron sharing index (2c-ESI). This index quantifies the number of electrons delocalized or shared between atoms A and B. The DI is calculated as an integral of $\gamma_{XC}(\mathbf{r}_1, \mathbf{r}_2)$ over atomic domains of A and B [202]:

$$\delta(A, B) = -2 \int_A \int_B \gamma_{XC}(\mathbf{r}_1, \mathbf{r}_2)\, d\mathbf{r}_1 d\mathbf{r}_2. \tag{4.4}$$

The above equation can be employed at any theoretical level as long as the first- and second-order density functions are available. When a molecule is represented by a single determinant closed-shell wavefunction at the Hartree-Fock or density functional theory (DFT) level [203], the expression for DI becomes

$$\delta(A, B) = 2 \sum_{i,j} S_{ij}(A) S_{ij}(B), \tag{4.5}$$

where the summation runs over all doubly occupied MOs in the molecule, and $S_{ij}(A)$ denotes the overlap between MOs i and j within the atomic domain of A.

To compute the integrations in Eq. (4.4) or overlaps in Eq. (4.5), various atomic partitions can be employed. These methods perform either coordinate-space or

Hilbert-space partitioning of electron density from ab initio calculations. The most utilized atomic partition is based on the *quantum theory of atoms in molecules* (QTAIM) [198, 204, 205], where atomic domains are called "atomic basins". These basins are regions in real space bounded by zero-flux surfaces in one-electron density matrix $\rho(\mathbf{r})$ or by infinity. Alternative atomic partitions, such as Mulliken-like partitioning in the Hilbert space spanned by basis functions, the fuzzy-atom approach [206], or the topological fuzzy Voronoi cell [207], can also be utilized for these calculations.

The concept of ESI can be extended to analyze electron delocalization across more than just two atomic domains. A *multicenter DI*, or Mc-ESI, considers M atoms ranging from A_1 to A_M, represented as a string $\mathcal{A} = [A_1, A_2, \ldots, A_M]$. For closed-shell single determinant wavefunctions, this multicenter DI, represented as $I_\mathcal{A}$, is described as [208]

$$I_\mathcal{A} = 2^M \sum_{i_1, i_2, \ldots, i_M} S_{i_1 i_2}(A_1) S_{i_2 i_3}(A_2) \ldots S_{i_M i_1}(A_M). \tag{4.6}$$

This formula assumes electron sharing exclusively occurs between neighboring atoms.

Furthermore, Bultinck et al. [209] introduced an alternative definition, known as the *multicenter electron delocalization index* (MCI), that takes into account all possible permutations of the M atoms:

$$\mathrm{MCI}(\mathcal{A}) = \frac{1}{2M} \sum_{P(\mathcal{A})} I_\mathcal{A}, \tag{4.7}$$

where P denotes all possible permutations within $\mathcal{A}$.

If the atomic domain set $\mathcal{A}$ represents a ring structure consisting of M atoms with the atoms ordered based on their connectivity in the ring, multicenter DIs in Eq. (4.6) and Eq. (4.7) serve as aromaticity descriptors for a molecular ring containing M atoms.

It is important to note the dependence of multicenter DIs on the number of ring atoms when using them as aromaticity descriptors. To effectively compare rings with varying sizes, normalization is required. The normalized versions of $I_\mathcal{A}$ and MCI, denoted as I_{NG} and I_{NB}, are respectively given as [210]

$$I_{NG}(\mathcal{A}) = \frac{\pi^2}{4} \frac{G(N_\pi)}{M N_\pi} I_\mathcal{A}^{1/M}, \tag{4.8}$$

$$I_{NB}(\mathcal{A}) = C\frac{G(N_\pi)}{MN_\pi}\,\mathrm{MCI}(\mathcal{A})^{1/M}, \tag{4.9}$$

where N_π is the number of π-electrons of the atoms in the ring, $G(N_\pi)$ is equal to 1 and -3 for aromatic and antiaromatic systems respectively, and $C = 1.5155$ is a proportionality constant.

Two additional notable DI-based aromaticity descriptors are the *fluctuation index* (FLU) and the *para-delocalization index* (PDI). FLU considers the uniformity of electron delocalization within the molecular ring and the bonding differences relative to a specific aromatic reference [211]. A system with a low FLU value exhibits a more evenly distributed electron density, indicative of aromaticity. On the other hand, PDI evaluates the electron sharing between the para positions of a given 6-MR, as follows [212]:

$$\mathrm{PDI}(\mathcal{A}) = \frac{\delta(A_1, A_4) + \delta(A_2, A_5) + \delta(A_3, A_6)}{3}. \tag{4.10}$$

A high PDI value indicates a higher degree of electron delocalization. A low PDI value implies a lesser degree of electron delocalization associated with nonaromatic or even antiaromatic systems. The primary limitation of PDI is that it is restricted to 6-MRs.

In addition to ESI-based aromaticity descriptors discussed above, there are popular alternative electron delocalization-based descriptors. The π component of the electron localization function (ELF) has been suggested as a descriptor for π aromatic systems [213–215]. ELF is a scalar real-space function characterized by high values in areas where electron pairs are localized. Another descriptor is the electron density of delocalized bonds (EDDB) [216] that is based on thedecomposition of the one-electron density matrix into densities localized at individual atoms, atom pairs, and groups of multiple atoms.

Progress and challenges in aromaticity descriptor development

A major challenge in the study of aromaticity quantification is the absence of a quantum physical basis for this property, which complicates its quantification. Despite significant advances in the field over the past decades, the applicability of many descriptors remains limited to basic cyclic compounds. Furthermore, different

aromaticity descriptors may yield inconsistent aromaticity ordering for certain series of compounds, and some may even fail to accurately correctly capture changes in aromaticity for particular cases [217]. For this reason, it is widely accepted that aromaticity analysis should be performed using a set of aromaticity descriptors [48, 218, 219].

Several studies have shown that descriptors based on electron delocalization serve as comprehensive aromaticity descriptors, outperforming many traditional structural, energetic, and magnetic-based ones [184]. However, there is still room for improvement. Introducing I_{NB} and I_{NG} marked considerable progress, but further efforts are required to broaden their applicability. The primary obstacle lies in extending their applicability toward larger and more complex systems, such as three-dimensional compounds.

4.2 Quantifying superposition

One of the counterintuitive concepts that make quantum mechanics an intriguing theory is the superposition principle, which allows quantum systems to exist in multiple states simultaneously [55]. This unique phenomenon has significant implications as a resource for tasks that cannot be accomplished through classical means. Therefore, the quantification and manipulation of various forms of quantum superposition, such as quantum coherence and quantum entanglement, have become subjects of great interest [220–224].

Accordingly, the quantum superposition of distinguishable (orthogonal) states, known as quantum coherence, has a well-grounded resource theory [221, 222]. When this unique form of superposition is shared between systems separated in space, it is referred to as quantum correlation specified in Section 2.2, which is better understood through its quantification and manipulation [223, 224]. The basis-independent nature of quantum correlations makes them a crucial resource for many emerging quantum technologies.

For nonorthogonal states, quantification and manipulation of superposition require generalizing the framework used in coherence theory. This generalization,

called the resource theory of superposition (RTS), is based on relaxing the orthogonality condition of basis states to linear independence [225–227]. Here, quantum superposition can exist in two different forms: not only as the linear combination of basis states but also with overlaps [228]. From this perspective, quantum coherence is viewed as a subset of superposition when nonclassicality is formed entirely in the form of a linear combination of basis states, and all the overlaps between these states vanish.

In this section, we start by exploring how superposition is quantified in nonorthogonal quantum states and its associated limitations. Following this, we present the biorthogonal framework, which offers solutions to these limitations, as originally highlighted in Ref. [228].

4.2.1 Superposition in nonorthogonal bases

Consider a d-dimensional Hilbert space denoted by $\mathcal{H}_d$, which possesses a normalized, linearly independent but not necessarily orthogonal finite basis $\{|c_i\rangle = 1, 2, \ldots, d\}$ such that $\langle c_i|c_j\rangle = S_{ij} \in \mathbb{C}$. Any density operator $\hat{\rho}$ living in $\mathcal{H}_d$ can be expressed in the basis $\{|c_i\rangle\}$ as follows:

$$\hat{\rho} = \sum_{i,j=1}^{d} \rho_{ij} |c_i\rangle\langle c_j|, \tag{4.11}$$

where the complex coefficients ρ_{ij} are equal to $\langle c_i^{\perp}|\hat{\rho}|c_j^{\perp}\rangle$, where $\{|c_i^{\perp}\rangle\}$ is the dual of the basis $\{|c_i\rangle\}$ and another nonorthogonal basis with relation $\langle c_i^{\perp}|c_j\rangle = \delta_{ij}$.

In the context of RTS [225–227], quantum states described by $\hat{\rho}_f = \sum_i p_i |c_i\rangle\langle c_i|$ are called *superposition-free* states, implying that their matrix representations ρ formed by ρ_{ij} contain only non-zero diagonal elements. Conversely, states that are not superposition-free are termed superposition states, including those with non-zero off-diagonal elements in ρ. Suppose a quantum system exists in a superposition state. It means that the resource value of this state can be used for certain quantum operations that cannot create or increase superposition in the basis of $\{|c_i\rangle\}$.

Quantifying the degree of superposition in a nonorthogonal quantum state is a functionally important way to understand its nonclassical properties and resource

value. The l_1-norm of quantum superposition provides a quantitative measure of the superposition present in a nonorthogonal state like Eq.(4.11):

$$l_1[\rho] = \sum_{i \neq j} |\rho_{ij}|, \tag{4.12}$$

which vanishes for superposition-free states. The definition of Eq. (4.12) is motivated by the fact that the diagonal and off-diagonal elements of ρ respectively encode the probability and nonclassicality information of density operator $\hat{\rho}$, in any fixed nonorthogonal or orthogonal basis [221]. However, as demonstrated in Ref. [101], when we regard $\hat{\rho}_f$ as the state of a composite system, it becomes evident that it should encompass superposition according to Eq. (4.12). This superposition arises not from a mere linear combination of nonorthogonal states but rather from their mutual overlaps. Consequently, the off-diagonal elements of ρ do not fully encode the complete information regarding the quantum superposition carried by the state $\hat{\rho}$.

4.2.2 Superposition in biorthogonal bases

The inconsistency of the nonorthogonal matrix representation ρ becomes apparent in its inability to satisfy the unit-trace requirement, which is one of three necessities for a physical density matrix (see Subsection 2.1.1 for discussion). This failure is because ρ fails to consider the overlaps that arise due to the superposition contained locally within the overlaps of the nonorthogonal basis states. It does not adequately distinguish between matrix elements to accurately represent the probability- and nonclassicality-related information encoded by its density operator $\hat{\rho}$.

We should introduce the Gram or overlap matrix S to address this inconsistency, which contains the necessary overlap information. Given a nonorthogonal basis $\{|c_i\rangle\}_{i=1}^{d}$, its overlap matrix S is composed of the inner products of basis states with elements $S_{ij} = \langle c_i|c_j\rangle$[1]. Then, the unit-trace requirement can be fulfilled by

[1]The overlap matrix is a valuable tool for determining whether a given set is linearly independent: if the determinant of S is positive, the corresponding basis is linearly independent.

considering the following expressions:

$$\mathrm{tr}\left[\hat{\rho}\right] = \sum_i \langle c_i^{\perp}|\hat{\rho}|c_i\rangle = 1 = \mathrm{tr}\left[\rho S\right]. \tag{4.13}$$

On the other hand, an extension of the nonorthogonal basis $\{|c_i\rangle\}$ to the biorthogonal basis $\left\{|c_i\rangle, |c_i^{\perp}\rangle\right\}$ inherently incorporates the overlap information through the structure of the dual basis [229], as defined by

$$|c_i^{\perp}\rangle = \sum_j S_{ji}^{-1}|c_j\rangle. \tag{4.14}$$

Therefore, we can say that the representation of a nonorthogonal basis with a biorthogonal counterpart resolves inconsistencies such as the unit-trace requirement by naturally contributing overlap information in the overlap matrix S.

By employing the biorthogonal basis $\left\{|c_i\rangle, |c_i^{\perp}\rangle\right\}$, we can represent the state described in Eq. (4.11) as follows:

$$\hat{\rho} = \sum_{i,j=1}^{d} \bar{\rho}_{ij}|c_i^{\perp}\rangle\langle c_j|, \tag{4.15}$$

which allows us to construct an alternative matrix form for $\hat{\rho}$, known as the *biorthogonal* matrix representation ρ_{BO} with the elements $\{\bar{\rho}_{ij}\} = \left\{\langle c_i^{\perp}|\hat{\rho}|c_j\rangle\right\}$. This matrix is a non-Hermitian one that retains the trace-one property. In other words, since $\rho_{BO} = \rho S$, the trace of ρ_{BO} should be equal to one, as shown in Eq. (4.13). Therefore, ρ_{BO} encapsulates all the (non-)probabilistic information in its (off-)diagonal elements. Consequently, this representation enables us to quantify the total superposition in a state $\hat{\rho}$ using the following expression:

$$l_1\left[\rho_{BO}\right] = \sum_{i\neq j} |\bar{\rho}_{ij}|. \tag{4.16}$$

Hence, Eq. (4.16) serves as a measure for *genuine* quantum superposition since it quantifies all types of superposition. On the other hand, Eq. (4.12) only quantifies *inter-basis* superposition.

It is worth noting that the biorthogonality framework presented here also facilitates consistent generalizations of conventional quantum mechanics for finite-dimensional systems [229–231]. These generalizations incorporate non-Hermitian observables with complete but nonorthogonal eigenbasis.

4.3 Superposition in aromaticity

In the realm of molecular electronic states, the importance of overlaps between nonorthogonal states is most evident. Chemical bonding and other related quantum chemical phenomena can be originated from the overlaps between nonorthogonal atomic orbitals [232–234]. From this perspective, aromaticity can be defined as the overlaps between atomic orbitals in which delocalized electrons reside. By following this idea, in the following subsections, we will focus on examining some archetypical aromatic and antiaromatic molecules presented in Tables 4.1, 4.3, and 4.4 by quantifying the superposition shared between atomic orbitals with delocalized electrons.

4.3.1 Construction of electronic states

The molecules we study here exhibit planar and cyclic structures, wherein the electrons involved in the formation of π-bonds become delocalized across the atoms within the ring. We can then conceptualize their aromaticity as a superposition within the cyclic π-subspace of the molecular electronic system in its atomic orbital basis.

Therefore, for each examined molecule, our specific focus lies on the π-electronic substructure, characterized solely by the π-MOs and the π-electrons occupying them. The state representing π-structure can be obtained by exciting the π-electrons over the reference state $|\Psi_{HF}\rangle$ within the π-MOs. The complete active space (CAS) method [4] can be exploited to obtain such a state by selecting the π-MOs and π–electrons as the active space. Thus, the electronic ground state of the π-structure, denoted by $|\Psi_\pi\rangle$, for a molecular system with N_π π-MOs and n_e^π π-electrons can be expressed as a linear combination of all electronic configurations in the basis of π-MOs:

$$|\Psi_\pi\rangle = \sum_{\vec{s}} \lambda_{\vec{s}} \, |s_1 s_2 \dots s_{2N_\pi}\rangle_{\psi_1^\pi \psi_2^\pi \dots \psi_{2N_\pi}^\pi}, \tag{4.17}$$

where $s_\mu \in \{0, 1\}$, $\sum_{\mu=1}^{2N_\pi} s_\mu = n_e^\pi$, and each $\vec{s} = \{s_1, s_2, ..., s_{2N_\pi}\}$ corresponds to a possible electronic configuration. The coefficients of the different configurations, $\lambda_{\vec{s}}$ is determined by optimizing the π-MOs in the active space using the CASSCF

method.

The subsequent step involves rewriting $|\Psi_\pi\rangle$ in the nonorthogonal AO basis. To accomplish this, we leverage the fact that for the planar cyclic molecules we consider, each π-molecular spin-orbital ψ_μ^π can be expressed as a linear combination of the p-atomic orbitals $\{p_\nu^\pi\}$ involved in the π-bonds, as shown below:

$$\psi_\mu \;=\; \sum_\nu \; C_{\nu\mu} p_\nu^\pi. \tag{4.18}$$

Here, $C_{\nu\mu}$ represents the contribution of the νth atom's p-AO, p_ν^π, to the μth π-MO. The AO coefficients of each MO are also obtained from the CASSCF calculation.

Once we have obtained the coefficients for all π-MOs in Eq. (4.18), we can construct the coefficient matrix C. This matrix contains the coefficients of each p-AO in each π-MO. By utilizing this matrix, we can represent each configuration in Eq. (4.17) as a linear combination of configurations in the p-AO basis (see Refs. [2, 5] for detailed calculation process). Consequently, we can expand the π-electronic structure state in (4.17) using the π-AO basis $\{p_\nu^\pi\}$ in the following form:

$$|\Psi_\pi^{AO}\rangle = \sum_{\vec{s}} \lambda_{\vec{s}}^{AO} |s_1 s_2 \dots s_{2N_\pi}\rangle_{p_1^\pi p_2^\pi \dots p_{2N_\pi}^\pi}, \tag{4.19}$$

where $\chi_{2\nu-1}$ and $\chi_{2\nu}$ denote the up and down atomic spin-orbitals of the νth atomic orbital p_ν^π, respectively. $\lambda_{\vec{s}}^{AO}$ represents the expansion coefficient of the electronic state in the p-AO basis.

To quantify the inter-basis superposition, we utilize Eq. (4.12), specifically $l_1[|\Psi_\pi^{AO}\rangle\langle\Psi_\pi^{AO}|]$. In order to represent the π-electronic structure state in the biorthogonal p-AO basis, we begin by obtaining the overlap matrix S. The elements of S indicate the overlaps of electron configurations in the AO basis, determined through the inner product of configurations:

$$S_{km} = \langle k_1 k_2 \dots k_{2N_\pi} | m_1 m_2 \dots m_{2N_\pi}\rangle_{p_1^\pi p_2^\pi \dots p_{2N_\pi}^\pi}. \tag{4.20}$$

Once the overlap matrix is obtained, it becomes straightforward to derive the biorthogonal density matrix representation ρ_{BO} for $|\Psi_\pi^{AO}\rangle$, using the relationship $\rho_{BO} = |\Psi_\pi^{AO}\rangle\langle\Psi_\pi^{AO}|\, S$.

Now that we have constructed the electronic state of π-structure in nonorthogonal p atomic orbitals and its biorthogonal form, we are ready to show the superposition results in both bases for the examined molecules and discuss them.

Before going into the results, let me briefly clarify how the numerical calculations were performed. Except for hexazine (N_6), borole (C_4H_5B), and cyclopentadienyl cation ($C_5H_5^+$), all the molecules' optimized geometries were obtained at the B3LYP/aug-cc-pVTZ from the CCCBDB database [235]. The other geometries were optimized in the Gaussian 09 [138] at the same level of theory. All HF and CASSCF calculations have been performed using the PySCF program package [143, 144] with STO-6G minimal basis set.

4.3.2 Three-membered rings

As discussed in 4.1, Hückel's $4n + 2$ rule states that a planar, cyclic, conjugated molecule is aromatic if it contains $4n+2$ π-electrons and has antiaromatic character if it carries $4n$ π-electrons. The three-membered rings (3-MRs) in Table 4.1 are among the most miniature molecular systems that follow this rule. Therefore, the cyclopropenyl cation $C_3H_3^+$, with its 2π electrons, precisely aligns with the rule for $n = 0$, so it is classified as the simplest Hückel aromatic [236]. In contrast, the cyclopropenyl anion $C_3H_3^-$, with 4π electrons, is called antiaromatic[2]. The cyclopropenyl radical C_3H_3, bearing 3π electrons, does not conform to the $4n$ or $4n + 2$ conditions and is thus categorized as nonaromatic.

According to our results, when the cyclopropenyl radical C_3H_3 transforms into its ionic forms, distinct changes in the amount of superposition are observed. In the antiaromatic $C_3H_3^-$ form, there's a significant increase in the inter-basis superposition shared between nonorthogonal electronic configurations, which increased from 3.66 to 4.43. Conversely, in the aromatic $C_3H_3^+$ form, the genuine superposition shared between biorthogonal electronic configurations is more evident, even if the genuine superposition in $C_3H_3^-$ also increases.

[2]A current study presents computational results that strongly indicate $C_3H_3^-$ does not possess antiaromatic character, at least energetically [237].

Table 4.1: Quantifying the quantum delocalization in the ground state of nonaromatic cyclopropene and its ions with the same triangular structure. According to both measures $l_1[\rho]$ and $l_1[\rho_{BO}]$, the nonaromatic molecule exhibits the minimum superposition. The antiaromatic cyclopropenyl anion demonstrates the maximum inter-base superposition, while the aromatic cyclopropenyl cation displays the maximum genuine superposition.

	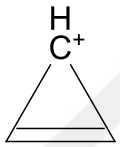 Cyclopropenyl Cation	 Cyclopropenyl Radical	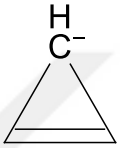 Cyclopropenyl Anion
$l_1[\rho]$	3.60	3.66	4.43
$l_1[\rho_{BO}]$	7.74	6.34	6.71

Consequently, we demonstrate the power of the biorthogonal framework even in such a simple molecular system. While the cation form has the lowest superposition in the nonorthogonal AOs, it possesses the highest value in the biorthogonal AOs. This shows us that in aromaticity, the superposition arising from the overlap between electronic configurations, rather than the superposition from the linear combination of nonorthogonal electronic configurations, represents the nature of delocalized electrons.

4.3.3 Five-membered rings

The molecules under consideration here are pentagonal structures denoted by C_4H_4X (see Table 4.3). In both MO and AO bases, the π-electronic structures of the cyclopentadienyl anion ($C_5H_5^-$), pyrrole (C_4H_5N), and furan (C_4H_4O) are composed of 5 π-MOs (p-AOs) and 6 π-electrons, whereas those of borole (C_4H_5B) and cyclopentadienyl cation ($C_5H_5^+$) comprise 5 π-MOs (p-AOs) and 4 π-electrons. For

pyrrole (furan), each carbon atom contributes one p-AO and an electron to the π-electronic structure. Meanwhile, the nitrogen (oxygen) in pyrrole (furan), undergoing sp^2 hybridization, contributes a lone electron pair in a p-AO to π-structure. In borole, however, the contributed p-AO of the boron atom to the π-electronic system is empty.

The cyclopentadienyl anion is deemed aromatic based on Hückel's rule. Moreover, pyrrole and furan are known as hetero-aromatic molecules [238]. The expected order of aromaticity among these three compounds is cyclopentadienyl anion > pyrrole > furan [49]. Likewise, according to Hückel's rule, the cyclopentadienyl cation is antiaromatic. Nevertheless, borole exhibits less antiaromaticity than the cyclopentadienyl cation [49].

As shown in the last two rows of Table 4.3, you can also see that these orders are confirmed by two multicenter delocalization indices I_R[3] and MCI, which are defined in Eq. (4.6) and Eq. (4.7) respectively. The higher the aromaticity, the larger the I_R and MCI. Although I_R yields only small values for antiaromatic molecules, MCI and I_R give negative values, allowing us to distinguish antiaromatic molecules from nonaromatic ones.

Apart from the 3-MRs mentioned above, the superposition results at the HF level[4] for 5-MRs are presented in Table 4.3, as well as the results at the CASSCF level. The comparison of results at two different levels sheds light on the role of electron-electron correlations in aromaticity since these correlations are only involved at the post-HF level. Table 4.3 shows that superpositions at the HF level are higher than those computed at the CASSCF level in both bases. This can be interpreted as electron-electron interactionsat reducing the total electron delocalization in this context. However, further research is inevitably needed to explain these outcomes.

Beyond this comparative analysis, our findings indicate that both $l_1[\rho]$ and $l_1[\rho_{BO}]$, at both HF and CASSCF levels, effectively quantify the extent of elec-

[3]Substituting R for $\mathcal{A}$ in the subindex is to indicate that atoms forming a ring are taken into account.

[4]For that, we considered the superposition in the π-structure of $|\psi_{HF}\rangle$ on both nonorthogonal and biorthogonal forms of AOs instead of $|\psi_\pi\rangle$.

Table 4.2: The ground state delocalization of electrons within the π structure of five-membered heterocyclic molecules, represented as C_4H_4X, is quantified by superposition measures in the levels of HF and CASSCF. Both measures $l_1[\rho]$ and $l_1[\rho_{BO}]$ reliably provide the expected distinction between aromatic (X = {CH^-, NH, O}) or antiaromatic (X = {BH, CH^+}) molecules at both levels.

		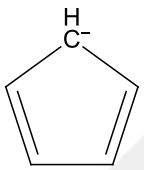	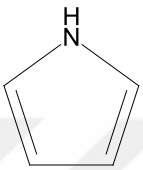	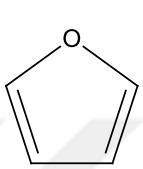	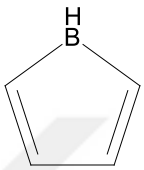	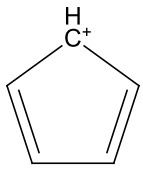
HF	$l_1[\rho]$	30.40	26.66	25.70	14.72	18.77
	$l_1[\rho_{BO}]$	88.72	77.73	72.20	43.94	53.10
CASSCF	$l_1[\rho]$	26.48	23.70	22.93	13.30	17.79
	$l_1[\rho_{BO}]$	78.02	68.93	64.24	39.53	49.14
	$I_R^{(a)}$	0.048	0.031	0.022	0.004	0.000
	MCI$^{(a)}$	0.068	0.043	0.028	-0.003	-0.038

(a) MCI and I_R values were taken from Refs. [49, 217].

tron delocalization in the π-electronic structures of these 5-MRs, aligning with the expected order of aromaticity among them. Conversely, these measures indicate a higher superposition in the π-electronic structure of the antiaromatic cyclopentadienyl cation than in borole, even though the superposition is lesser than in aromatic compounds.

In conclusion, the quantity of superposition in both bases is substantial enough to distinguish between aromatic and antiaromatic molecules, but the inconsistency in ordering among the antiaromatics warrants further attention. It is also intriguing that the expected aromaticity order is obtained in both bases. This suggests that, contrary to the results in 3-MRs, the superposition arising from overlaps between electronic configurations plays no significant role in the aromaticity of these molecules.

Table 4.3: The ground state delocalization of electrons within the π structure of five-membered heterocyclic molecules, represented as C_4H_4X, is quantified by superposition measures in the levels of HF and CASSCF. Both measures $l_1[\rho]$ and $l_1[\rho_{BO}]$ reliably provide the expected distinction between aromatic (X = {CH^-, NH, O}) or antiaromatic (X = {BH, CH^+}) molecules at both levels.

		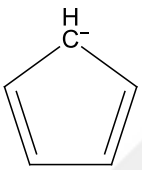	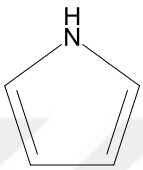	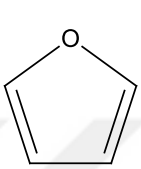	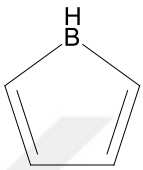	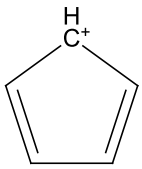
HF	$l_1[\rho]$	30.40	26.66	25.70	14.72	18.77
	$l_1[\rho_{BO}]$	88.72	77.73	72.20	43.94	53.10
CASSCF	$l_1[\rho]$	26.48	23.70	22.93	13.30	17.79
	$l_1[\rho_{BO}]$	78.02	68.93	64.24	39.53	49.14
	I_R	0.048	0.031	0.022	0.004	0.000
	MCI	0.068	0.043	0.028	-0.003	-0.038

(a) MCI and I_R values were taken from Refs. [49, 217].

4.3.4 Six-membered rings

Let us move on to a collection of molecules presented in Figure 4.1, characterized by a hexagonal π-electronic structure comprising 6 orbitals and 6 electrons. These molecules are widely recognized as aromatic in the literature, with their expected order of aromaticity as follows: benzene (C_6H_6) > pyridine (C_5H_5N) > pyridazine ($C_4H_4N_2$) ≈ pyrazine ($C_4H_4N_2$) ≈ pyrimidine ($C_4H_4N_2$) > triazine ($C_3H_3N_3$) > hexazine (N_6) > borazine ($B_3N_3H_6$) [178].

Evaluating the order above is one of the tests used to assess the effectiveness of aromaticity descriptors [217]. Nonetheless, even the most successful descriptors fail to predict the expected trend accurately. For instance, as presented in Table 4.4, the PDI considers pyrazine, pyridazine, and hexazine more aromatic than benzene. This contradicts the conventional belief that if carbon atoms in benzene are replaced

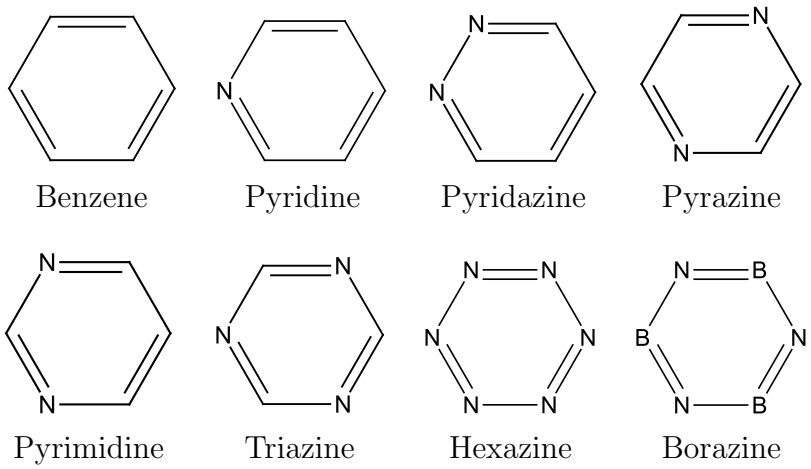

Figure 4.1: The 2D structures of examined 6-MR aromatic molecules.

with nitrogen, the aromaticity should gradually decrease. Similarly, the multicenter indices I_R and MCI infer that pyridazine is more aromatic than pyridine. Beyond the electronic-based aromaticity descriptors, both the structural-based descriptor HOMA, defined in Eq. (4.2), and the magnetic-based descriptor NICS, introduced in 4.1.2, fail to establish a reasonable order for the series, as shown in Table 4.4 and discussed in Refs. [49, 217].

Table 4.4 demonstrates that the inter-basis superposition measured by $l_1[\rho]$ fails to replicate the expected aromaticity order. However, the genuine quantum superposition quantified by $l_1[\rho_{BO}]$ achieves a high degree of accuracy in reproducing this order, except for the ordering between triazine and hexazine. These observations suggest that the density matrix representation in the biorthogonal AO basis, ρ_{BO}, encompasses comprehensive information about the extent of electron delocalization in the π-structure of an aromatic molecular system.

Moreover, the deviation in our results from the conventional order—particularly the expectation that the triazine's π-electronic structure should be more delocalized than hexazine's— warrants further investigation. We previously mentioned that hexazine appears more aromatic than triazine, according to certain aromaticity measures like PDI. Our calculations may yield a similar finding because hexazine possesses a more symmetric structure despite having more nitrogen atoms than tri-

Table 4.4: Quantifying ground state quantum delocalization in six-membered ring molecules: Comparative analysis of quantum superposition measures $l_1[\rho]$ and $l_1[\rho_{BO}]$ for assessing aromaticity order. Our results highlight the superior efficacy of $l_1[\rho_{BO}]$ in evaluating electron delocalization within the π-structure of the visualized molecular systems compared to $l_1[\rho]$.

	$l_1[\rho]$	$l_1[\rho_{BO}]$	PDI	I_R	MCI	HOMA	NICS(0)
Benzene	65.42	267.04	0.103	0.0478	0.072	0.989	-8.05
Pyridine	66.51	265.96	0.103	0.0456	0.068	0.995	-6.82
Pyridazine	68.45	263.67	0.105	0.0469	0.069	0.981	-5.35
Pyrazine	68.20	265.11	0.108	0.0435	0.065	0.996	-5.36
Pyrimidine	67.59	264.32	0.101	0.0440	0.065	0.999	-5.53
Triazine	82.72	250.94	0.096	0.0427	0.063	1.000	-4.07
Hexazine	78.48	255.47	0.131	—	—	0.984	-7.29
Borazine	32.19	133.32	—	—	—	—	—

(a) The values of all aromaticity descriptors were taken from Ref. [49].

azine. When we examine the overlaps between electronic configurations, we may measure not only the amount of electron delocalization but also the uniformity of its distribution. This observation is supported by the ordering of pyrazine > pyrimidine > pyridazine, as indicated in Table 4.4. Although these three molecules have an equal number of nitrogen atoms, the hydrocarbon pathways connecting the two nitrogen atoms exhibit symmetry in pyrazine, while they display complete antisymmetry in pyridazine.

4.3.5 Outlook

Throughout this section, we have explored the concept of aromaticity as an application of the RTS. Our primary aim was to quantify the electron delocalization in the ground state π-electronic structures of representative monocyclic molecules re-

garding the quantum superposition present among localized AOs. For this purpose, we performed electronic state calculations using the HF and CASSCF methods and adopted the mode picture. Then, we utilized the l_1 norm to measure the amount of quantum superposition in the electronic density matrices expressed in nonorthogonal and biorthogonal AO bases.

Our above results provide compelling evidence for accurately reproducing the expected order of aromaticity in most molecules studied. This achievement is made possible through the genuine quantum superposition displayed by the biorthogonal density matrices. In contrast, nonorthogonal density matrices containing inter-base quantum superposition prove inadequate in accurately ordering these molecules. Our results highlight the exceptional success of the biorthogonal framework in capturing all nonclassicality in nonorthogonal systems, as demonstrated by the electron delocalization in molecular systems.

Beyond planar molecules

The method we are proposing here is not restricted to planar molecules characterized by an electronic structure featuring a separation of σ and π orbitals. Our approach is applicable to any molecular system where there's noticeable electron delocalization within specific molecular orbitals. Thus, by targeting these relevant orbitals, our method can effectively be employed. However, a challenge arises when moving beyond planar molecules due to the increased computational complexity because the number of atomic orbitals in which electrons are delocalized grows. If we can ensure that quantifying aromaticity at the HF level works as well, we can make the superposition calculations in larger molecules at this level with good computational efficiency.

Superposition in valence bond structures

Our objective is to replicate these calculations using valence bond structures as the nonorthogonal basis. Within VB theory, electron delocalization is elegantly described as a linear combination of resonance structures. This representation indicated that electrons may not be localized to one specific region but instead can be

spread over multiple atomic centers. Thus, the superposition in this basis can give us chemically more intuitive results. In particular, the Kekulé basis [239] holds excellent potential for investigating significantly larger molecules without compromising accuracy.

Technological possibilities

Our findings uncover the potential applications of chemical systems within the RTS, particularly in technological domains. A series of experiments have previously explored the phenomenon of delocalization in such systems [240–242], providing a foundation for employing similar experimental setups to harness the power of superposition in various areas. These foundational works open up exciting possibilities for leveraging molecular systems in cutting-edge fields such as quantum information, quantum metrology, and quantum cryptology.

Superposition-based aromaticity descriptor

While the biorthogonal extension of RTS provides a holistic framework for electron delocalization in molecular π-structures, the current superposition measures fail to distinguish between electron delocalization in aromatic and antiaromatic molecules. Previous research suggests that the distinction between aromatic and antiaromatic molecules lies not in the overall extent of electron delocalization but in the distribution of contributions from different bipartite delocalization terms [243]. Additionally, different types of superpositions can be transformed into different forms of energy, as observed in the field of quantum thermodynamics [45, 244]. We conjecture that the relationship between energy and superpositions in aromatic, nonaromatic, and antiaromatic molecules differs in this context, resulting in distinct kinetic and thermodynamic consequences. Discovering a method to uncover this connection could lead us to a superposition-based measure of aromaticity and facilitate the development of a quantum resource theory for this phenomenon.

Moreover, we present a novel method that offers significant advancements in anatomically investigating electron delocalization within aromatic and antiaromatic systems. In addition to examining the bipartite terms analyzed in a previous

study [243], our delocalization calculations also encompass multipartite terms. For instance, we consider delocalization involving three atoms, which cannot be solely expressed in terms of delocalization between two atoms. Furthermore, our method allows us to decompose the overall electron delocalization into contributions based on electron number. This enables us to compare different types of contributions, such as one-electron delocalization, two-electron delocalization, three-electron delocalization. By incorporating these additional aspects, our method may pave the way for a more comprehensive analysis of electron delocalization, shedding light on the intricate details of aromatic and antiaromatic molecules.

Chapter 5

CONCLUSION

In this thesis, we first investigated orbital-orbital correlations in molecular electronic states. We introduced a novel method to decompose total pairwise orbital correlations into classical and quantum correlations. Our analysis of archetypical molecular systems revealed that quantum orbital correlations can exceed their classical counterparts and intriguingly, even in some instances, orbital discord can survive in the absence of entanglement. These observations deviated from prior assumptions and paved the way for further investigation of orbital discord as a resource for certain tasks in the fermionic quantum information theory

Transitioning our focus to the puzzling nature of aromaticity, we proposed a new perspective on understanding and quantifying this concept. By quantifying the quantum superposition existing amongst localized but nonorthogonal atomic orbitals in the ground state of representative monocyclic molecules, we obtained a new measure of electron delocalization. Notably, we highlight that the biorthogonal framework is more successful than the conventional nonorthogonal representation in achieving and quantifying quantumness in a nonorthogonal basis.

In summary, our research underscores the pivotal role of second quantum revolution tools in advancing quantum chemistry. These tools might not only enhance our understanding of chemical bonding but also exploit the potential of molecular systems in quantum technologies. As we challenge previous paradigms and explore these molecular systems with these new tools, our findings point out that new insights in molecular quantum chemistry are inevitable.

BIBLIOGRAPHY

[1] Linus Pauling. *The Nature of the Chemical Bond*. 3rd. Ithaca, NY: Cornell University Press, 1989 (cit. on pp. 1, 48, 60, 62).

[2] Sason S Shaik and Philippe C Hiberty. *A chemist's guide to valence bond theory*. John Wiley & Sons, 2007 (cit. on pp. 1, 60, 74).

[3] Clemens Carel Johannes Roothaan. "New developments in molecular orbital theory". In: *Reviews of modern physics* 23.2 (1951), p. 69. DOI: https://doi.org/10.1103/RevModPhys.23.69 (cit. on pp. 1, 26).

[4] Trygve Helgaker, Poul Jorgensen, and Jeppe Olsen. *Molecular electronic-structure theory*. John Wiley & Sons, 2013 (cit. on pp. 1, 21, 73).

[5] PC Hiberty and C Leforestier. "Expansion of molecular orbital wave functions into valence bond wave functions. A simplified procedure". In: *Journal of the American Chemical Society* 100.7 (1978), pp. 2012–2017. DOI: https://doi.org/10.1021/ja00475a007 (cit. on pp. 1, 74).

[6] Sason Shaik, David Danovich, and Philippe C Hiberty. "Valence bond theory—Its birth, struggles with molecular orbital theory, its present state and future prospects". In: *Molecules* 26.6 (2021), p. 1624. DOI: https://doi.org/10.3390/molecules26061624 (cit. on p. 1).

[7] John Morrison Galbraith et al. "Valence bond and molecular orbital: two powerful theories that nicely complement one another". In: *Journal of Chemical Education* 98.12 (2021), pp. 3617–3620. DOI: https://doi.org/10.1021/acs.jchemed.1c00919 (cit. on p. 1).

[8] Jonathan P Dowling and Gerard J Milburn. "Quantum technology: the second quantum revolution". In: *Philosophical Transactions of the Royal Society of London. Series A: Mathematical, Physical and Engineering Sciences*

361.1809 (2003), pp. 1655–1674. DOI: https://doi.org/10.1098/rsta.2003.1227 (cit. on p. 1).

[9] Lars Jaeger. *The second quantum revolution: From Entanglement to Quantum Computing and Other Super-Technologies*. Springer, 2018 (cit. on p. 1).

[10] Ryszard Horodecki et al. "Quantum entanglement". In: *Reviews of modern physics* 81.2 (2009), p. 865. DOI: https://doi.org/10.1103/RevModPhys.81.865 (cit. on pp. 1, 10, 14–16).

[11] Charles H Bennett et al. "Teleporting an unknown quantum state via dual classical and Einstein-Podolsky-Rosen channels". In: *Physical review letters* 70.13 (1993), p. 1895. DOI: https://doi.org/10.1103/PhysRevLett.70.1895 (cit. on p. 1).

[12] Dik Bouwmeester et al. "Experimental quantum teleportation". In: *Nature* 390.6660 (1997), pp. 575–579. DOI: https://doi.org/10.1038/37539 (cit. on p. 1).

[13] Stefano Pirandola et al. "Advances in quantum teleportation". In: *Nature photonics* 9.10 (2015), pp. 641–652. DOI: https://doi.org/10.1038/nphoton.2015.154 (cit. on p. 1).

[14] Artur K Ekert. "Quantum cryptography based on Bell's theorem". In: *Physical review letters* 67.6 (1991), p. 661. DOI: https://doi.org/10.1103/PhysRevLett.67.661 (cit. on p. 1).

[15] Nicolas Gisin et al. "Quantum cryptography". In: *Reviews of modern physics* 74.1 (2002), p. 145. DOI: https://doi.org/10.1103/RevModPhys.74.145 (cit. on p. 1).

[16] Stefano Pirandola et al. "Advances in quantum cryptography". In: *Advances in optics and photonics* 12.4 (2020), pp. 1012–1236. DOI: https://doi.org/10.1364/AOP.361502 (cit. on p. 1).

[17] Katharina Boguslawski et al. "Entanglement measures for single-and multireference correlation effects". In: *The journal of physical chemistry letters* 3.21 (2012), pp. 3129–3135. DOI: https://doi.org/10.1021/jz301319v (cit. on p. 2).

[18] Katharina Boguslawski et al. "Orbital entanglement in bond-formation processes". In: *Journal of Chemical Theory and Computation* 9.7 (2013), pp. 2959–2973. DOI: https://doi.org/10.1021/ct400247p (cit. on p. 2).

[19] Matthieu Mottet et al. "Quantum entanglement in carbon–carbon, carbon–phosphorus and silicon–silicon bonds". In: *Physical Chemistry Chemical Physics* 16.19 (2014), pp. 8872–8880. DOI: https://doi.org/10.1039/C4CP00277F (cit. on p. 2).

[20] Leon Freitag et al. "Orbital entanglement and CASSCF analysis of the Ru–NO bond in a ruthenium nitrosyl complex". In: *Physical Chemistry Chemical Physics* 17.22 (2015), pp. 14383–14392. DOI: https://doi.org/10.1039/C4CP05278A (cit. on p. 2).

[21] Corinne Duperrouzel et al. "A quantum informational approach for dissecting chemical reactions". In: *Chemical Physics Letters* 621 (2015), pp. 160–164. DOI: https://doi.org/10.1016/j.cplett.2015.01.005 (cit. on p. 2).

[22] Yilin Zhao et al. "Dissecting the bond-formation process of d 10-metal–ethene complexes with multireference approaches". In: *Theoretical Chemistry Accounts* 134 (2015), pp. 1–10. DOI: https://doi.org/10.1007/s00214-015-1726-3 (cit. on p. 2).

[23] Katharina Boguslawski and Paweł Tecmer. "Orbital entanglement in quantum chemistry". In: *International Journal of Quantum Chemistry* 115.19 (2015), pp. 1289–1295. DOI: https://doi.org/10.1002/qua.24832 (cit. on p. 2).

[24] Szilárd Szalay et al. "The correlation theory of the chemical bond". In: *Scientific Reports* 7.1 (2017), p. 2237. DOI: https://doi.org/10.1038/s41598-017-02447-z (cit. on pp. 2, 3).

[25] Christopher J Stein and Markus Reiher. "Measuring multi-configurational character by orbital entanglement". In: *Molecular Physics* 115.17-18 (2017), pp. 2110–2119. DOI: https://doi.org/10.1080/00268976.2017.1288934 (cit. on p. 2).

[26] Christian Stemmle, Beate Paulus, and Örs Legeza. "Analysis of electron-correlation effects in strongly correlated systems (N 2 and N 2+) by applying the density-matrix renormalization-group method and quantum information theory". In: *Physical Review A* 97.2 (2018), p. 022505. DOI: https://doi.org/10.1103/PhysRevA.97.022505 (cit. on p. 2).

[27] Jan Brandejs et al. "Quantum information-based analysis of electron-deficient bonds". In: *The Journal of Chemical Physics* 150.20 (2019). DOI: https://doi.org/10.1063/1.5093497 (cit. on p. 2).

[28] L. Ding et al. "Concept of orbital entanglement and correlation in quantum chemistry". In: *J. Chem. Theory Comput.* 17.1 (2021), pp. 79–95. DOI: 10.1021/acs.jctc.0c00559 (cit. on pp. 2, 49, 50, 52, 54, 56).

[29] Leah Henderson and Vlatko Vedral. "Classical, quantum and total correlations". In: *J. Phys. A Math.* 34.35 (2001), p. 6899. DOI: https://doi.org/10.1088/0305-4470/34/35/315 (cit. on pp. 2, 11, 20, 21).

[30] Harold Ollivier and Wojciech H Zurek. "Quantum discord: a measure of the quantumness of correlations". In: *Physical review letters* 88.1 (2001), p. 017901. DOI: https://doi.org/10.1103/PhysRevLett.88.017901 (cit. on pp. 2, 11, 18–20).

[31] Steven R White and Richard L Martin. "Ab initio quantum chemistry using the density matrix renormalization group". In: *The Journal of chemical physics* 110.9 (1999), pp. 4127–4130. DOI: https://doi.org/10.1063/1.478295 (cit. on p. 2).

[32] Sebastian Wouters and Dimitri Van Neck. "The density matrix renormalization group for ab initio quantum chemistry". In: *The European Physical Jour-*

nal D 68 (2014), pp. 1–20. DOI: https://doi.org/10.1140/epjd/e2014-50500-1 (cit. on p. 2).

[33] Örs Legeza and Jeno Sólyom. "Optimizing the density-matrix renormalization group method using quantum information entropy". In: *Physical Review B* 68.19 (2003), p. 195116. DOI: https://doi.org/10.1103/PhysRevB.68.195116 (cit. on p. 2).

[34] Szilárd Szalay et al. "Tensor product methods and entanglement optimization for ab initio quantum chemistry". In: *International Journal of Quantum Chemistry* 115.19 (2015), pp. 1342–1391. DOI: https://doi.org/10.1002/qua.24898 (cit. on p. 2).

[35] Christian Krumnow et al. "Fermionic orbital optimization in tensor network states". In: *Physical review letters* 117.21 (2016), p. 210402. DOI: https://doi.org/10.1103/PhysRevLett.117.210402 (cit. on p. 2).

[36] Christopher J Stein and Markus Reiher. "Automated selection of active orbital spaces". In: *Journal of chemical theory and computation* 12.4 (2016), pp. 1760–1771. DOI: https://doi.org/10.1021/acs.jctc.6b00156 (cit. on p. 2).

[37] Kavan Modi et al. "Unified view of quantum and classical correlations". In: *Phys. Rev. Lett.* 104.8 (2010), p. 080501. DOI: https://doi.org/10.1103/PhysRevLett.104.080501 (cit. on pp. 2, 12).

[38] Anindita Bera et al. "Quantum discord and its allies: a review of recent progress". In: *Reports on Progress in Physics* 81.2 (2017), p. 024001. DOI: 10.1088/1361-6633/aa872f (cit. on pp. 2, 10, 18).

[39] Raoul Dillenschneider. "Quantum discord and quantum phase transition in spin chains". In: *Physical Review B* 78.22 (2008), p. 224413. DOI: https://doi.org/10.1103/PhysRevB.78.224413 (cit. on p. 2).

[40] Borivoje Dakić et al. "Quantum discord as resource for remote state preparation". In: *Nature Physics* 8.9 (2012), pp. 666–670. DOI: https://doi.org/10.1038/nphys2377 (cit. on p. 2).

[41] Stefano Pirandola. "Quantum discord as a resource for quantum cryptography". In: *Scientific reports* 4.1 (2014), p. 6956. DOI: https://doi.org/10.1038/srep06956 (cit. on p. 2).

[42] Davide Girolami, Tommaso Tufarelli, and Gerardo Adesso. "Characterizing nonclassical correlations via local quantum uncertainty". In: *Physical review letters* 110.24 (2013), p. 240402. DOI: https://doi.org/10.1103/PhysRevLett.110.240402 (cit. on p. 2).

[43] Davide Girolami et al. "Quantum discord determines the interferometric power of quantum states". In: *Physical Review Letters* 112.21 (2014), p. 210401. DOI: https://doi.org/10.1103/PhysRevLett.112.210401 (cit. on p. 2).

[44] Kaonan Micadei et al. "Reversing the direction of heat flow using quantum correlations". In: *Nature communications* 10.1 (2019), p. 2456. DOI: https://doi.org/10.1038/s41467-019-10333-7 (cit. on p. 2).

[45] Onur Pusuluk and Özgür E Müstecaplıoğlu. "Quantum Rayleigh problem and thermocoherent Onsager relations". In: *Physical Review Research* 3.2 (2021), p. 023235. DOI: https://doi.org/10.1103/PhysRevResearch.3.023235 (cit. on pp. 2, 83).

[46] Nicolai Friis, Antony R Lee, and David Edward Bruschi. "Fermionic-mode entanglement in quantum information". In: *Physical Review A* 87.2 (2013), p. 022338. DOI: https://doi.org/10.1103/PhysRevA.87.022338 (cit. on pp. 3, 32–35, 37, 41, 43).

[47] Frank Jensen. *Introduction to computational chemistry*. John wiley & sons, 2017 (cit. on pp. 3, 21, 25, 27, 28, 30).

[48] Zhongfang Chen et al. "Nucleus-independent chemical shifts (NICS) as an aromaticity criterion". In: *Chemical reviews* 105.10 (2005), pp. 3842–3888. DOI: https://doi.org/10.1021/cr030088+ (cit. on pp. 3, 62, 69).

[49] Miquel Solà et al. *Aromaticity and Antiaromaticity: Concepts and Applications*. John Wiley & Sons, 2022 (cit. on pp. 3, 64, 77–81).

[50] Luigi Amico et al. "Entanglement in many-body systems". In: *Reviews of modern physics* 80.2 (2008), p. 517. DOI: https://doi.org/10.1103/RevModPhys.80.517 (cit. on p. 3).

[51] Szilárd Szalay. "Multipartite entanglement measures". In: *Physical Review A* 92.4 (2015), p. 042329. DOI: https://doi.org/10.1103/PhysRevA.92.042329 (cit. on p. 3).

[52] Michael Walter, David Gross, and Jens Eisert. "Multipartite entanglement". In: *Quantum Information: From Foundations to Quantum Technology Applications*. Wiley Online Library, 2016. Chap. 14, pp. 293–330. DOI: https://doi.org/10.1002/9783527805785.ch14 (cit. on p. 3).

[53] CC Rulli and MS Sarandy. "Global quantum discord in multipartite systems". In: *Physical Review A* 84.4 (2011), p. 042109. DOI: https://doi.org/10.1103/PhysRevA.84.042109 (cit. on p. 3).

[54] Chandrashekar Radhakrishnan, Mathieu Laurière, and Tim Byrnes. "Multipartite generalization of quantum discord". In: *Physical Review Letters* 124.11 (2020), p. 110401. DOI: https://doi.org/10.1103/PhysRevLett.124.110401 (cit. on p. 3).

[55] Paul Adrien Maurice Dirac. *The principles of quantum mechanics*. 4th ed. The International series of monographs on physics 27. Oxford university press, 1981 (cit. on pp. 4, 69).

[56] Max Born. "Quantum mechanics of collision processes". In: *Uspekhi Fizich* (1926). Translated by D. H. Delphenich. URL: http://www.neo-classical-physics.info/uploads/3/4/3/6/34363841/born_-_qm_for_collisions_ii.pdf (cit. on p. 5).

[57] John Von Neumann. *Mathematical foundations of quantum mechanics: New edition*. Vol. 53. Princeton university press, 2018 (cit. on pp. 6, 8, 10).

[58] Ugo Fano. "Description of states in quantum mechanics by density matrix and operator techniques". In: *Reviews of modern physics* 29.1 (1957), p. 74. DOI: https://doi.org/10.1103/RevModPhys.29.74 (cit. on p. 6).

[59] Michael A Nielsen and Isaac L Chuang. *Quantum computation and quantum information*. Cambridge university press, 2010 (cit. on pp. 6–9, 11, 19).

[60] John Archibald Wheeler and Wojciech Hubert Zurek. *Quantum theory and measurement*. Vol. 40. Princeton University Press, 2014 (cit. on p. 8).

[61] Franck Laloë. *Do we really understand quantum mechanics?* Cambridge University Press, 2019 (cit. on p. 8).

[62] Mark M Wilde. *Quantum information theory*. Cambridge university press, 2013 (cit. on pp. 8, 19).

[63] Igor D Ivanovic. "How to differentiate between non-orthogonal states". In: *Physics Letters A* 123.6 (1987), pp. 257–259. DOI: https://doi.org/10.1016/0375-9601(88)91034-1 (cit. on p. 10).

[64] Joonwoo Bae and Leong-Chuan Kwek. "Quantum state discrimination and its applications". In: *Journal of Physics A: Mathematical and Theoretical* 48.8 (2015), p. 083001. DOI: https://doi.org/10.1088/1751-8113/48/8/083001 (cit. on p. 10).

[65] Martin B Plenio and Shashank Virmani. "An introduction to entanglement measures". In: *Quantum Inf. Comput.* 7.1 (2007), pp. 1–51. DOI: https://doi.org/10.48550/arXiv.quant-ph/0504163 (cit. on pp. 10, 14–16).

[66] Felipe Fernandes Fanchini, Diogo de Oliveira Soares Pinto, and Gerardo Adesso. *Lectures on general quantum correlations and their applications*. Springer, 2017 (cit. on pp. 10, 18).

[67] Alexander Streltsov and Alexander Streltsov. *Quantum correlations beyond entanglement*. Springer, 2015 (cit. on pp. 10, 18).

[68] Claude Elwood Shannon. "A mathematical theory of communication". In: *The Bell system technical journal* 27.3 (1948), pp. 379–423 (cit. on p. 10).

[69] Alfred Wehrl. "General properties of entropy". In: *Reviews of Modern Physics* 50.2 (1978), p. 221. DOI: https://doi.org/10.1103/RevModPhys.50.22 (cit. on p. 10).

[70] Benjamin Schumacher. "Quantum coding". In: *Physical Review A* 51.4 (1995), p. 2738. DOI: https://doi.org/10.1103/PhysRevA.51.2738 (cit. on p. 11).

[71] Thomas M Cover. *Elements of information theory*. John Wiley & Sons, 1999 (cit. on pp. 11, 12).

[72] Vlatko Vedral et al. "Quantifying entanglement". In: *Physical Review Letters* 78.12 (1997), p. 2275. DOI: https://doi.org/10.1103/PhysRevLett.78.2275 (cit. on pp. 12, 15, 16).

[73] Vlatko Vedral. "The role of relative entropy in quantum information theory". In: *Reviews of Modern Physics* 74.1 (2002), p. 197. DOI: https://doi.org/10.1103/RevModPhys.74.197 (cit. on pp. 12, 17).

[74] John D Trimmer. "The present situation in quantum mechanics: A translation of Schrödinger's" Cat Paradox" paper". In: *Proceedings of the American Philosophical Society* (1980), pp. 323–338. DOI: http://www.jstor.org/stable/986572 (cit. on p. 12).

[75] Reinhard F Werner. "Quantum states with Einstein-Podolsky-Rosen correlations admitting a hidden-variable model". In: *Physical Review A* 40.8 (1989), p. 4277. DOI: https://doi.org/10.1103/PhysRevA.40.4277 (cit. on p. 13).

[76] Eric Chitambar et al. "Everything you always wanted to know about LOCC (but were afraid to ask)". In: *Communications in Mathematical Physics* 328 (2014), pp. 303–326. DOI: https://doi.org/10.1007/s00220-014-1953-9 (cit. on p. 13).

[77] Michał Horodecki, Paweł Horodecki, and Ryszard Horodecki. "Separability of mixed states: necessary and sufficient conditions". In: *Physics Letters A* 223.1-2 (1996), pp. 1–8. DOI: https://doi.org/10.1016/S0375-9601(96)00706-2 (cit. on p. 14).

[78] Asher Peres. "Separability criterion for density matrices". In: *Physical Review Letters* 77.8 (1996), p. 1413. DOI: https://doi.org/10.1103/PhysRevLett.77.1413 (cit. on p. 14).

[79] Eric Chitambar and Gilad Gour. "Quantum resource theories". In: *Reviews of modern physics* 91.2 (2019), p. 025001. DOI: https://doi.org/10.1103/RevModPhys.91.025001 (cit. on p. 15).

[80] Charles H Bennett et al. "Concentrating partial entanglement by local operations". In: *Physical Review A* 53.4 (1996), p. 2046. DOI: https://doi.org/10.1103/PhysRevA.53.2046 (cit. on p. 15).

[81] Sandu Popescu and Daniel Rohrlich. "Thermodynamics and the measure of entanglement". In: *Physical Review A* 56.5 (1997), R3319. DOI: https://doi.org/10.1103/PhysRevA.56.R3319 (cit. on p. 15).

[82] Charles H Bennett et al. "Mixed-state entanglement and quantum error correction". In: *Physical Review A* 54.5 (1996), p. 3824. DOI: https://doi.org/10.1103/PhysRevA.54.3824 (cit. on p. 15).

[83] William K Wootters. "Entanglement of formation of an arbitrary state of two qubits". In: *Physical Review Letters* 80.10 (1998), p. 2245. DOI: https://doi.org/10.1103/PhysRevLett.80.2245 (cit. on p. 16).

[84] William K Wootters. "Entanglement of formation and concurrence". In: *Quantum Inf. Comput.* 1.1 (2001), pp. 27–44. DOI: https://www.rintonpress.com/journals/qic-1-1/eof2.pdf (cit. on p. 16).

[85] Vlatko Vedral and Martin B Plenio. "Entanglement measures and purification procedures". In: *Physical Review A* 57.3 (1998), p. 1619. DOI: https://doi.org/10.1103/PhysRevA.57.1619 (cit. on p. 16).

[86] Guifré Vidal and Reinhard F Werner. "Computable measure of entanglement". In: *Physical Review A* 65.3 (2002), p. 032314. DOI: https://doi.org/10.1103/PhysRevA.65.032314 (cit. on p. 17).

[87] Martin B Plenio. "Logarithmic negativity: a full entanglement monotone that is not convex". In: *Physical review letters* 95.9 (2005), p. 090503. DOI: https://doi.org/10.1103/PhysRevLett.95.090503 (cit. on p. 17).

[88] Pawel Horodecki. "Separability criterion and inseparable mixed states with positive partial transposition". In: *Physics Letters A* 232.5 (1997), pp. 333–339. DOI: https://doi.org/10.1016/S0375-9601(97)00416-7 (cit. on p. 18).

[89] Michał Horodecki, Paweł Horodecki, and Ryszard Horodecki. "Mixed-state entanglement and distillation: Is there a "bound" entanglement in nature?" In: *Physical Review Letters* 80.24 (1998), p. 5239. DOI: https://doi.org/10.1103/PhysRevLett.80.5239 (cit. on p. 18).

[90] Attila Szabo and Neil S Ostlund. *Modern quantum chemistry: introduction to advanced electronic structure theory*. Courier Corporation, 2012 (cit. on pp. 21–24, 26, 27, 30).

[91] Scott Aaronson. "Why quantum chemistry is hard". In: *Nature Physics* 5.10 (2009), pp. 707–708. DOI: https://doi.org/10.1038/nphys1415 (cit. on p. 21).

[92] Max Born and Robert Oppenheimer. "On the quantum theory of molecules". In: *Quantum Chemistry: Classic Scientific Papers*. World Scientific, 2000, pp. 1–24 (cit. on p. 22).

[93] Warren J Hehre, Robert F Stewart, and John A Pople. "Self-consistent molecular-orbital methods. I. Use of Gaussian expansions of Slater-type atomic orbitals". In: *The Journal of Chemical Physics* 51.6 (1969), pp. 2657–2664. DOI: https://doi.org/10.1063/1.1672392 (cit. on p. 27).

[94] Thom H Dunning Jr. "Gaussian basis sets for use in correlated molecular calculations. I. The atoms boron through neon and hydrogen". In: *The Journal of chemical physics* 90.2 (1989), pp. 1007–1023. DOI: https://doi.org/10.1063/1.456153 (cit. on p. 27).

[95] RK Nesbet. "Configuration interaction in orbital theories". In: *Proceedings of the Royal Society of London. Series A. Mathematical and Physical Sciences* 230.1182 (1955), pp. 312–321. DOI: https://doi.org/10.1098/rspa.1955.0134 (cit. on p. 28).

[96] C David Sherrill. "An introduction to configuration interaction theory". In: *School of Chemistry and Biochemistry, Georgia Institute of Technology* (1995) (cit. on p. 29).

[97] Hugh Graham Alexander Burton. "Holomorphic Hartree-Fock Theory: Moving Beyond the Coulson–Fischer Point". PhD thesis. University of Cambridge, 2020 (cit. on p. 29).

[98] Björn O Roos, Peter R Taylor, and Per EM Sigbahn. "A complete active space SCF method (CASSCF) using a density matrix formulated super-CI approach". In: *Chemical Physics* 48.2 (1980), pp. 157–173. DOI: https://doi.org/10.1016/0301-0104(80)80045-0 (cit. on p. 30).

[99] Björn O Roos. "The complete active space self-consistent field method and its applications in electronic structure calculations". In: *Advances in Chemical Physics: Ab Initio Methods in Quantum Chemistry Part 2* 69 (1987), pp. 399–445. DOI: https://doi.org/10.1002/9780470142943.ch7 (cit. on p. 31).

[100] Nicetu Tibau Vidal et al. "Quantum operations in an information theory for fermions". In: *Physical Review A* 104.3 (2021), p. 032411. DOI: https://doi.org/10.1103/PhysRevA.104.032411 (cit. on pp. 32, 34–38, 40).

[101] Onur Pusuluk et al. "Classical and quantum orbital correlations in molecular electronic states". In: *New Journal of Physics* 24.10 (2022), p. 102001. DOI: https://doi.org/10.1088/1367-2630/ac932b (cit. on pp. 32, 71).

[102] Simon Saunders. "The concept 'indistinguishable'". In: *Studies in History and Philosophy of Science Part B: Studies in History and Philosophy of Modern Physics* 71 (2020), pp. 37–59 (cit. on p. 32).

[103] Claude Cohen-Tannoudji, Bernard Diu, and Franck Laloë. "Systems of identical particles". In: *Quantum mechanics, volume 2: angular momentum, spin, and approximation methods*. John Wiley & Sons, 2019. Chap. 14, pp. 1419–1455 (cit. on p. 32).

[104] K Eckert et al. "Quantum correlations in systems of indistinguishable particles". In: *Annals of physics* 299.1 (2002), pp. 88–127. DOI: https://doi.org/10.1006/aphy.2002.6268 (cit. on p. 33).

[105] GianCarlo Ghirardi and Luca Marinatto. "General criterion for the entanglement of two indistinguishable particles". In: *Physical Review A* 70.1 (2004), p. 012109. DOI: https://doi.org/10.1103/PhysRevA.70.012109 (cit. on p. 33).

[106] Malte C Tichy, Florian Mintert, and Andreas Buchleitner. "Essential entanglement for atomic and molecular physics". In: *Journal of Physics B: Atomic, Molecular and Optical Physics* 44.19 (2011), p. 192001. DOI: 10.1088/0953-4075/44/19/192001 (cit. on p. 33).

[107] Fabio Benatti et al. "Entanglement in indistinguishable particle systems". In: *Physics Reports* 878 (2020), pp. 1–27. DOI: https://doi.org/10.1016/j.physrep.2020.07.003 (cit. on p. 33).

[108] Howard Mark Wiseman and John A Vaccaro. "Entanglement of indistinguishable particles shared between two parties". In: *Physical review letters* 91.9 (2003), p. 097902. DOI: https://doi.org/10.1103/PhysRevLett.91.097902 (cit. on p. 33).

[109] Yu Shi. "Quantum entanglement of identical particles". In: *Physical Review A* 67.2 (2003), p. 024301. DOI: https://doi.org/10.1103/PhysRevA.67.024301 (cit. on p. 33).

[110] N Killoran, M Cramer, and Martin B Plenio. "Extracting entanglement from identical particles". In: *Physical review letters* 112.15 (2014), p. 150501. DOI: https://doi.org/10.1103/PhysRevLett.112.150501 (cit. on p. 33).

[111] BJ Dalton et al. "New spin squeezing and other entanglement tests for two mode systems of identical bosons". In: *New Journal of Physics* 16.1 (2014), p. 013026. DOI: 10.1088/1367-2630/16/1/013026 (cit. on p. 33).

[112] Fabio Benatti, Roberto Floreanini, and Ugo Marzolino. "Entanglement in fermion systems and quantum metrology". In: *Physical Review A* 89.3 (2014), p. 032326. DOI: https://doi.org/10.1103/PhysRevA.89.032326 (cit. on p. 33).

[113] Rosario Lo Franco and Giuseppe Compagno. "Quantum entanglement of identical particles by standard information-theoretic notions". In: *Scientific reports* 6.1 (2016), pp. 1–10. DOI: https://doi.org/10.1038/srep20603 (cit. on p. 33).

[114] Rosario Lo Franco and Giuseppe Compagno. "Indistinguishability of elementary systems as a resource for quantum information processing". In: *Physical review letters* 120.24 (2018), p. 240403. DOI: https://doi.org/10.1103/PhysRevLett.120.240403 (cit. on p. 33).

[115] Giuseppe Compagno, Alessia Castellini, and Rosario Lo Franco. "Dealing with indistinguishable particles and their entanglement". In: *Philosophical Transactions of the Royal Society A: Mathematical, Physical and Engineering Sciences* 376.2123 (2018), p. 20170317. DOI: https://doi.org/10.1098/rsta.2017.0317 (cit. on p. 33).

[116] Szilárd Szalay et al. "Fermionic systems for quantum information people". In: *Journal of Physics A: Mathematical and Theoretical* 54.39 (2021), p. 393001. DOI: 10.1088/1751-8121/ac0646 (cit. on p. 33).

[117] Benjamin Morris et al. "Entanglement between identical particles is a useful and consistent resource". In: *Physical Review X* 10.4 (2020), p. 041012. DOI: https://doi.org/10.1103/PhysRevX.10.041012 (cit. on p. 33).

[118] Claude Cohen-Tannoudji, Bernard Diu, and Franck Laloë. "Creation and annihilation operators for identical particles". In: *Quantum mechanics, volume 3: fermions, bosons, photons, correlations, and entanglement*. John Wiley & Sons, 2019. Chap. 15, pp. 1591–1616 (cit. on pp. 34, 35).

[119] Nicolai Friis. "Reasonable fermionic quantum information theories require relativity". In: *New Journal of Physics* 18.3 (2016), p. 033014. DOI: 10.1088/1367-2630/18/3/033014 (cit. on pp. 37, 38).

[120] G. C. Wick, A. S. Wightman, and E. P. Wigner. "The intrinsic parity of elementary particles". In: *Physical Review* 88.1 (1952). DOI: https://doi.org/10.1103/PhysRev.88.101 (cit. on p. 38).

[121] Markus Johansson. "Comment on Reasonable fermionic quantum information theories require relativity'". In: *arXiv preprint arXiv:1610.00539* (2016). DOI: https://doi.org/10.48550/arXiv.1610.00539 (cit. on p. 39).

[122] G-C Wick, Arthur Strong Wightman, and Eugene P Wigner. "Superselection rule for charge". In: *Physical Review D* 1.12 (1970), p. 3267. DOI: https://doi.org/10.1103/PhysRevD.1.3267 (cit. on p. 39).

[123] Frank Verstraete and J Ignacio Cirac. "Quantum nonlocality in the presence of superselection rules and data hiding protocols". In: *Physical review letters* 91.1 (2003), p. 010404. DOI: https://doi.org/10.1103/PhysRevLett.91.010404 (cit. on p. 39).

[124] Stephen D Bartlett and Howard M Wiseman. "Entanglement constrained by superselection rules". In: *Physical review letters* 91.9 (2003), p. 097903. DOI: https://doi.org/10.1103/PhysRevLett.91.097903 (cit. on p. 39).

[125] Alexei Kitaev, Dominic Mayers, and John Preskill. "Superselection rules and quantum protocols". In: *Physical Review A* 69.5 (2004), p. 052326. DOI: https://doi.org/10.1103/PhysRevA.69.052326 (cit. on p. 39).

[126] Ömer Tırınk, Onur Pusuluk, and Gökhan Torun. "Manipulating fermionic mode entanglement in the presence of superselection rules". In: *arXiv preprint arXiv:2303.04559* (2023). DOI: https://doi.org/10.48550/arXiv.2303.04559 (cit. on p. 39).

[127] Edvin Olofsson et al. "Quantum teleportation of single-electron states". In: *Physical Review B* 101.19 (2020), p. 195403. DOI: https://doi.org/10.1103/PhysRevB.101.195403 (cit. on p. 40).

[128] Tiago Debarba et al. "Teleporting quantum information encoded in fermionic modes". In: *Physical Review A* 101.5 (2020), p. 052326. DOI: https://doi.org/10.1103/PhysRevA.101.052326 (cit. on p. 40).

[129] Anna Galler and Patrik Thunström. "Orbital and electronic entanglement in quantum teleportation schemes". In: *Physical Review Research* 3.3 (2021), p. 033120. DOI: https://doi.org/10.1103/PhysRevResearch.3.033120 (cit. on p. 40).

[130] Giacomo Mauro D'Ariano et al. "Fermionic computation is non-local tomographic and violates monogamy of entanglement". In: *Europhysics Letters* 107.2 (2014), p. 20009. DOI: 10.1209/0295-5075/107/20009 (cit. on p. 40).

[131] Mari-Carmen Bañuls, J Ignacio Cirac, and Michael M Wolf. "Entanglement in systems of indistinguishable fermions". In: *Journal of Physics: Conference Series*. Vol. 171. 1. IOP Publishing. 2009, p. 012032. DOI: 10.1088/1742-6596/171/1/012032 (cit. on p. 40).

[132] Pawel Caban et al. "Entanglement and tensor product decomposition for two fermions". In: *Journal of Physics A: Mathematical and General* 38.6 (2005), p. L79. DOI: 10.1088/0305-4470/38/6/L02 (cit. on p. 41).

[133] Hassan Shapourian, Ken Shiozaki, and Shinsei Ryu. "Partial time-reversal transformation and entanglement negativity in fermionic systems". In: *Phys. Rev. B* 95 (16 2017), p. 165101. DOI: 10.1103/PhysRevB.95.165101 (cit. on p. 41).

[134] Hassan Shapourian, Ken Shiozaki, and Shinsei Ryu. "Many-Body Topological Invariants for Fermionic Symmetry-Protected Topological Phases". In: *Phys. Rev. Lett.* 118 (21 2017), p. 216402. DOI: 10.1103/PhysRevLett.118.216402 (cit. on p. 42).

[135] Ken Shiozaki et al. "Many-body topological invariants for fermionic short-range entangled topological phases protected by antiunitary symmetries". In: *Phys. Rev. B* 98 (3 2018), p. 035151. DOI: 10.1103/PhysRevB.98.035151 (cit. on p. 42).

[136] Hassan Shapourian and Shinsei Ryu. "Entanglement negativity of fermions: Monotonicity, separability criterion, and classification of few-mode states". In: *Phys. Rev. A* 99 (2 2019), p. 022310. DOI: 10.1103/PhysRevA.99.022310 (cit. on p. 42).

[137] Javier Faba, Vicente Martin, and Luis Robledo. "Two-orbital quantum discord in fermion systems". In: *Physical Review A* 103.3 (2021), p. 032426. DOI: https://doi.org/10.1103/PhysRevA.103.032426 (cit. on p. 43).

[138] M. J. Frisch et al. *Gaussian 09 Revision E.01.* (Gaussian Inc., Wallingford CT). 2009 (cit. on pp. 48, 75).

[139] Hans-Joachim Werner et al. "Molpro: a general-purpose quantum chemistry program package". In: *Wiley Interdisciplinary Reviews: Computational Molecular Science* 2.2 (2012), pp. 242–253. DOI: https://doi.org/10.1002/wcms.82 (cit. on p. 50).

[140] Hans-Joachim Werner et al. "The Molpro quantum chemistry package". In: *The Journal of chemical physics* 152.14 (2020). DOI: https://doi.org/10.1063/5.0005081 (cit. on p. 50).

[141] Justin M Turney et al. "Psi4: an open-source ab initio electronic structure program". In: *Wiley Interdisciplinary Reviews: Computational Molecular Science* 2.4 (2012), pp. 556–565. DOI: https://doi.org/10.1002/wcms.93 (cit. on p. 50).

[142] Daniel GA Smith et al. "PSI4 1.4: Open-source software for high-throughput quantum chemistry". In: *The Journal of chemical physics* 152.18 (2020). DOI: https://doi.org/10.1063/5.0006002 (cit. on p. 50).

[143] Qiming Sun et al. "PySCF: the Python-based simulations of chemistry framework". In: *Wiley Interdisciplinary Reviews: Computational Molecular Science* 8.1 (2018), e1340. DOI: https://doi.org/10.1002/wcms.1340 (cit. on pp. 50, 75).

[144] Qiming Sun et al. "Recent developments in the PySCF program package". In: *The Journal of chemical physics* 153.2 (2020). DOI: https://doi.org/10.1063/5.0006074 (cit. on pp. 50, 75).

[145] Bastian Jungnitsch, Tobias Moroder, and Otfried Gühne. "Taming Multiparticle Entanglement". In: *Physical Review Letters* 106.19 (2011). DOI: https://journals.aps.org/prl/abstract/10.1103/PhysRevLett.106.190502 (cit. on p. 51).

[146] Bastian Jungnitsch. PPTM*ixer: A tool to detect genuine multipartite entanglement*. 2011. URL: https://www.mathworks.com/matlabcentral/fileexchange/30968-pptmixer-a-tool-to-detect-genuine-multipartite-entanglement (cit. on p. 51).

[147] J. Löfberg. "YALMIP: A Toolbox for Modeling and Optimization in MATLAB". In: *In Proceedings of the CACSD Conference*. Taipei, Taiwan, 2004 (cit. on p. 51).

[148] K. C. Toh, M. J. Todd, and R. H. Tütüncü. "SDPT3 – A Matlab software package for semidefinite programming, Version 1.3". In: *Opt. Meth. Softw.* 11.1-4 (1999), pp. 545–581. DOI: 10.1080/10556789908805762 (cit. on p. 51).

[149] R. H. Tütüncü, K. C. Toh, and M. J. Todd. "Solving semidefinite-quadratic-linear programs using SDPT3". In: *Math. Program., Ser. B* 95 (2003), pp. 189–217. DOI: https://doi.org/10.1007/s10107-002-0347-5 (cit. on p. 51).

[150] BA Laws et al. "The dicarbon bonding puzzle viewed with photoelectron imaging". In: *Nature Communications* 10.1 (2019), p. 5199. DOI: https://doi.org/10.1038/s41467-019-13039-y (cit. on p. 54).

[151] Xiaodie Lin, Zhenyu Chen, and Zhaohui Wei. "Quantifying quantum entanglement via a hybrid quantum-classical machine learning framework". In: *Physical Review A* 107.6 (2023), p. 062409. DOI: https://doi.org/10.1103/PhysRevA.107.062409 (cit. on p. 57).

[152] Noa Feldman et al. "Entanglement estimation in tensor network states via sampling". In: *PRX Quantum* 3.3 (2022), p. 030312. DOI: https://doi.org/10.1103/PRXQuantum.3.030312 (cit. on p. 57).

[153] Lexin Ding et al. "Quantum correlations in molecules: from quantum resourcing to chemical bonding". In: *Quantum Science and Technology* 8.1 (2022), p. 015015. DOI: 10.1088/2058-9565/aca4ee (cit. on p. 57).

[154] Mahir H Yeşiller and Onur Pusuluk. "Electron delocalization in aromaticity as a superposition phenomenon". In: *arXiv preprint arXiv:2307.00672* (2023). DOI: https://doi.org/10.48550/arXiv.2307.00672 (cit. on p. 58).

[155] Michael Faraday. "XX. On new compounds of carbon and hydrogen, and on certain other products obtained during the decomposition of oil by heat". In: *Philosophical Transactions of the Royal Society of London* 115 (1825), pp. 440–466. DOI: https://doi.org/10.1098/rstl.1825.0022 (cit. on p. 59).

[156] August Wilhelm Von Hofmann. "I. On insolinic acid". In: *Proceedings of the Royal Society of London* 8 (1857), pp. 1–3. DOI: https://doi.org/10.1098/rspl.1856.0002 (cit. on p. 59).

[157] Auguste Kekulé. "Sur la constitution des substances aromatiques". In: *Bulletin mensuel de la Société Chimique de Paris* 3 (1865), p. 98 (cit. on p. 59).

[158] John Kidd. "XVI. Observations on naphthaline, a peculiar substance resembling a concrete essential oil, which is apparently produced during the decomposition of coal tar, by exposure to a red heat". In: *Philosophical Transactions of the Royal Society of London* 111 (1821), pp. 209–221 (cit. on p. 59).

[159] Eug Bamberger. "Ueber die Constitution fünfgliedriger Ringsysteme". In: *Berichte der deutschen chemischen Gesellschaft* 24.1 (1891), pp. 1758–1764 (cit. on p. 60).

[160] Gilbert N Lewis. "The atom and the molecule". In: *Journal of the American Chemical Society* 38.4 (1916), pp. 762–785 (cit. on p. 60).

[161] Walter Heitler and Fritz London. "Wechselwirkung neutraler Atome und homöopolare Bindung nach der Quantenmechanik". In: *Zeitschrift für Physik* 44.6-7 (1927), pp. 455–472 (cit. on p. 60).

[162] Linus Pauling. "The nature of the chemical bond. Application of results obtained from the quantum mechanics and from a theory of paramagnetic susceptibility to the structure of molecules". In: *Journal of the American Chemical Society* 53.4 (1931), pp. 1367–1400 (cit. on p. 60).

[163] Linus Pauling. "The nature of the chemical bond. II. The one-electron bond and the three-electron bond". In: *Journal of the American Chemical Society* 53.9 (1931), pp. 3225–3237 (cit. on p. 60).

[164] Erich Hückel. "Quantum-theoretical contributions to the benzene problem. I. The electron configuration of benzene and related compounds". In: *Z. physik* 70.3-4 (1931), pp. 204–286 (cit. on p. 61).

[165] Keith Yates. *Hückel molecular orbital theory*. Elsevier, 2012 (cit. on p. 61).

[166] Melvin Calvin and KW Wilson. "Stability of chelate compounds". In: *Journal of the American Chemical Society* 67.11 (1945), pp. 2003–2007. DOI: https://doi.org/10.1021/ja01227a043 (cit. on p. 61).

[167] Junichi Aihara. "Three-dimensional aromaticity of polyhedral boranes". In: *Journal of the American Chemical Society* 100.11 (1978), pp. 3339–3342. DOI: https://doi.org/10.1021/cr000442t (cit. on p. 61).

[168] R Bruce King. "Three-dimensional aromaticity in polyhedral boranes and related molecules". In: *Chemical reviews* 101.5 (2001), pp. 1119–1152. DOI: https://doi.org/10.1021/cr000442t (cit. on p. 61).

[169] E Heilbronner. "Hűckel molecular orbitals of Mőbius-type conformations of annulenes". In: *Tetrahedron Letters* 5.29 (1964), pp. 1923–1928. DOI: https://doi.org/10.1016/S0040-4039(01)89474-0 (cit. on p. 61).

[170] Zin Seok Yoon, Atsuhiro Osuka, and Dongho Kim. "Möbius aromaticity and antiaromaticity in expanded porphyrins". In: *Nature chemistry* 1.2 (2009), pp. 113–122. DOI: https://doi.org/10.1038/nchem.172 (cit. on p. 61).

[171] Xi Li et al. "Observation of all-metal aromatic molecules". In: *Science* 291.5505 (2001), pp. 859–861. DOI: 10.1126/science.291.5505.859 (cit. on p. 61).

[172] Xin Huang et al. "Observation of d-orbital aromaticity". In: *Angewandte Chemie* 117.44 (2005), pp. 7417–7420. DOI: https://doi.org/10.1002/anie.200502678 (cit. on p. 61).

[173] Jörg Grunenberg. "Ill-defined chemical concepts: The problem of quantification". In: *International Journal of Quantum Chemistry* 117.9 (2017), e25359. DOI: https://doi.org/10.1002/qua.25359 (cit. on p. 61).

[174] Gernot Frenking and Andreas Krapp. "Unicorns in the world of chemical bonding models". In: *Journal of Computational Chemistry* 28.1 (2007), pp. 15–24. DOI: https://doi.org/10.1002/jcc.20543 (cit. on p. 61).

[175] Roald Hoffmann. "The many guises of aromaticity". In: *Am. Sci* 103.18.10 (2015), p. 1511 (cit. on p. 62).

[176] Miquel Solà. "Why aromaticity is a suspicious concept? Why?" In: *Frontiers in Chemistry* 5 (2017), p. 22. DOI: 10.3389/fchem.2017.00022 (cit. on p. 62).

[177] Gabriel Merino et al. "Aromaticity: Quo Vadis". In: *Chemical Science* (2023). DOI: https://doi.org/10.1039/D2SC04998H (cit. on p. 62).

[178] Michał Ksawery Cyrański. "Energetic aspects of cyclic pi-electron delocalization: evaluation of the methods of estimating aromatic stabilization energies". In: *Chemical reviews* 105.10 (2005), pp. 3773–3811. DOI: https://doi.org/10.1021/cr0300845 (cit. on pp. 62, 79).

[179] Mercedes Alonso and Israel Fernández. "Quantifying aromaticity according to the energetic criterion". In: *Aromaticity*. Elsevier, 2021, pp. 195–235. DOI: https://doi.org/10.1016/B978-0-12-822723-7.00006-6 (cit. on pp. 62, 64).

[180] Tadeusz Marek Krygowski and Michał Ksawery Cyrański. "Structural aspects of aromaticity". In: *Chemical Reviews* 101.5 (2001), pp. 1385–1420. DOI: https://doi.org/10.1021/cr990326u (cit. on pp. 62, 63).

[181] Tadeusz M Krygowski et al. "Aromaticity from the viewpoint of molecular geometry: application to planar systems". In: *Chemical reviews* 114.12 (2014), pp. 6383–6422. DOI: https://doi.org/10.1021/cr400252h (cit. on pp. 62, 63).

[182] Reginald H Mitchell. "Measuring aromaticity by NMR". In: *Chemical reviews* 101.5 (2001), pp. 1301–1316. DOI: https://doi.org/10.1021/cr990359+ (cit. on p. 62).

[183] Jordi Poater et al. "Theoretical evaluation of electron delocalization in aromatic molecules by means of atoms in molecules (AIM) and electron localization function (ELF) topological approaches". In: *Chemical reviews* 105.10 (2005), pp. 3911–3947. DOI: https://doi.org/10.1021/cr030085x (cit. on p. 62).

[184] Ferran Feixas et al. "Quantifying aromaticity with electron delocalisation measures". In: *Chemical Society Reviews* 44.18 (2015), pp. 6434–6451. DOI: https://doi.org/10.1039/C5CS00066A (cit. on pp. 62, 66, 69).

[185] Linus Pauling and J Sherman. "The nature of the chemical bond. VI. The calculation from thermochemical data of the energy of resonance of molecules among several electronic structures". In: *The Journal of chemical physics* 1.8 (1933), pp. 606–617. DOI: https://doi.org/10.1063/1.1749335 (cit. on p. 62).

[186] Yirong Mo. "The block-localized wavefunction (BLW) perspective of chemical bonding". In: *The Chemical Bond: Fundamental Aspects of Chemical Bonding*. Ed. by Gernot Frenking and Sason Shaik. Wiley Online Library, 2014. Chap. 6, pp. 199–232. DOI: https://doi.org/10.1002/9783527664696.ch6 (cit. on p. 62).

[187] Yirong Mo, Peng Bao, and Jiali Gao. "Energy decomposition analysis based on a block-localized wavefunction and multistate density functional theory". In: *Physical Chemistry Chemical Physics* 13.15 (2011), pp. 6760–6775. DOI: https://doi.org/10.1039/C0CP02206C (cit. on p. 63).

[188] Paul von Ragué Schleyer and Frank Pühlhofer. "Recommendations for the evaluation of aromatic stabilization energies". In: *Organic Letters* 4.17 (2002), pp. 2873–2876. DOI: https://doi.org/10.1021/ol0261332 (cit. on p. 63).

[189] Karl Jug. "A bond order approach to ring current and aromaticity". In: *The Journal of Organic Chemistry* 48.8 (1983), pp. 1344–1348. DOI: https://doi.org/10.1021/jo00156a038 (cit. on p. 63).

[190] J Kruszewski and TM Krygowski. "Definition of aromaticity basing on the harmonic oscillator model". In: *Tetrahedron Letters* 13.36 (1972), pp. 3839–3842. DOI: https://doi.org/10.1016/S0040-4039(01)94175-9 (cit. on p. 63).

[191] Tadeusz Marek Krygowski. "Crystallographic studies of inter-and intramolecular interactions reflected in aromatic character of. pi.-electron systems". In: *Journal of chemical information and computer sciences* 33.1 (1993), pp. 70–78. DOI: https://doi.org/10.1021/ci00011a011 (cit. on p. 64).

[192] Paul von Ragué Schleyer et al. "Nucleus-independent chemical shifts: a simple and efficient aromaticity probe". In: *Journal of the American Chemical Society* 118.26 (1996), pp. 6317–6318. DOI: https://doi.org/10.1021/ja960582d (cit. on p. 64).

[193] Paul von Ragué Schleyer et al. "An evaluation of the aromaticity of inorganic rings: refined evidence from magnetic properties". In: *Journal of the American Chemical Society* 119.51 (1997), pp. 12669–12670. DOI: https://doi.org/10.1021/ja9719135 (cit. on p. 64).

[194] Rainer Herges and Daniel Geuenich. "Delocalization of electrons in molecules". In: *The Journal of Physical Chemistry A* 105.13 (2001), pp. 3214–3220. DOI: https://doi.org/10.1021/jp0034426 (cit. on p. 65).

[195] Eduard Matito and Miquel Solà. "The role of electronic delocalization in transition metal complexes from the electron localization function and the quantum theory of atoms in molecules viewpoints". In: *Coordination Chem-*

istry Reviews 253.5-6 (2009), pp. 647–665. DOI: https://doi.org/10.1016/j.ccr.2008.10.003 (cit. on p. 65).

[196] Yirong Mo and Sigrid D Peyerimhoff. "Theoretical analysis of electronic delocalization". In: *The Journal of chemical physics* 109.5 (1998), pp. 1687–1697. DOI: https://doi.org/10.1063/1.476742 (cit. on p. 65).

[197] Yirong Mo et al. "Electronic delocalization: A quantitative study from modern ab initio valence bond theory". In: *Journal of Theoretical and Computational Chemistry* 1.01 (2002), pp. 137–151. DOI: https://doi.org/10.1142/S0219633602000099 (cit. on p. 65).

[198] Richard FW Bader. "A quantum theory of molecular structure and its applications". In: *Chemical Reviews* 91.5 (1991), pp. 893–928. DOI: https://doi.org/10.1021/cr00005a013 (cit. on pp. 65, 67).

[199] Wolfgang Scherer et al. "Valence charge concentrations, electron delocalization and β-agostic bonding in d0 metal alkyl complexes". In: *Chemistry–A European Journal* 9.24 (2003), pp. 6057–6070. DOI: https://doi.org/10.1002/chem.200304909 (cit. on p. 65).

[200] Erin R Johnson et al. "Revealing noncovalent interactions". In: *Journal of the American Chemical Society* 132.18 (2010), pp. 6498–6506. DOI: https://doi.org/10.1021/ja100936w (cit. on p. 65).

[201] Richard FW Bader and Michael E Stephens. "Spatial localization of the electronic pair and number distributions in molecules". In: *Journal of the American Chemical Society* 97.26 (1975), pp. 7391–7399. DOI: https://doi.org/10.1021/ja00859a001 (cit. on p. 66).

[202] Xavier Fradera, Maggie A Austen, and Richard FW Bader. "The Lewis model and beyond". In: *The Journal of Physical Chemistry A* 103.2 (1999), pp. 304–314. DOI: https://doi.org/10.1021/jp983362q (cit. on p. 66).

[203] Jordi Poater et al. "The calculation of electron localization and delocalization indices at the Hartree–Fock, density functional and post-Hartree–Fock levels

of theory". In: *Theoretical Chemistry Accounts* 107 (2002), pp. 362–371. DOI: https://doi.org/10.1007/s00214-002-0356-8 (cit. on p. 66).

[204] R. F. Bader. "Atoms in molecules". In: *Accounts of Chemical Research* 18.1 (1985), pp. 9–15. DOI: https://doi.org/10.1021/ar00109a003 (cit. on p. 67).

[205] Axel Becke. *The quantum theory of atoms in molecules: from solid state to DNA and drug design*. John Wiley & Sons, 2007 (cit. on p. 67).

[206] I Mayer and P Salvador. "Overlap populations, bond orders and valences for 'fuzzy'atoms". In: *Chemical physics letters* 383.3-4 (2004), pp. 368–375. DOI: https://doi.org/10.1016/j.cplett.2003.11.048 (cit. on p. 67).

[207] Pedro Salvador and Eloy Ramos-Cordoba. "Communication: an approximation to Bader's topological atom". In: *The Journal of Chemical Physics* 139.7 (2013), p. 071103. DOI: https://doi.org/10.1063/1.4818751 (cit. on p. 67).

[208] Mario Giambiagi, Myriam S de Giambiagi, and Kleber C Mundim. "Definition of a multicenter bond index". In: *Structural Chemistry* 1 (1990), pp. 423–427. DOI: https://doi.org/10.1007/BF00671228 (cit. on p. 67).

[209] Patrick Bultinck, Robert Ponec, and Sofie Van Damme. "Multicenter bond indices as a new measure of aromaticity in polycyclic aromatic hydrocarbons". In: *Journal of physical organic chemistry* 18.8 (2005), pp. 706–718. DOI: https://doi.org/10.1002/poc.922 (cit. on p. 67).

[210] Jerzy Cioslowski, Eduard Matito, and Miquel Sola. "Properties of aromaticity indices based on the one-electron density matrix". In: *The Journal of Physical Chemistry A* 111.28 (2007), pp. 6521–6525. DOI: https://doi.org/10.1021/jp0716132 (cit. on p. 67).

[211] Eduard Matito, Miquel Duran, and Miquel Sola. "The aromatic fluctuation index (FLU): A new aromaticity index based on electron delocalization". In: *The Journal of chemical physics* 122.1 (2005), p. 014109. DOI: https://doi.org/10.1063/1.1824895 (cit. on p. 68).

[212] Jordi Poater et al. "The delocalization index as an electronic aromaticity criterion: application to a series of planar polycyclic aromatic hydrocarbons". In: *Chemistry–A European Journal* 9.2 (2003), pp. 400–406. DOI: https://doi.org/10.1002/chem.200390041 (cit. on p. 68).

[213] Bernard Silvi and Andreas Savin. "Classification of chemical bonds based on topological analysis of electron localization functions". In: *Nature* 371.6499 (1994), pp. 683–686. DOI: https://doi.org/10.1038/371683a0 (cit. on p. 68).

[214] Ferran Feixas et al. "Electron localization function at the correlated level: a natural orbital formulation". In: *Journal of Chemical Theory and Computation* 6.9 (2010), pp. 2736–2742. DOI: https://doi.org/10.1021/ct1003548 (cit. on p. 68).

[215] Stephan N Steinmann, Yirong Mo, and Clemence Corminboeuf. "How do electron localization functions describe π-electron delocalization?" In: *Physical chemistry chemical physics* 13.46 (2011), pp. 20584–20592. DOI: https://doi.org/10.1039/C1CP21055F (cit. on p. 68).

[216] Dariusz W Szczepanik et al. "The electron density of delocalized bonds (EDDB) applied for quantifying aromaticity". In: *Physical Chemistry Chemical Physics* 19.42 (2017), pp. 28970–28981. DOI: https://doi.org/10.1039/C7CP06114E (cit. on p. 68).

[217] Ferran Feixas et al. "On the performance of some aromaticity indices: a critical assessment using a test set". In: *Journal of computational chemistry* 29.10 (2008), pp. 1543–1554. DOI: https://doi.org/10.1002/jcc.20914 (cit. on pp. 69, 78–80).

[218] Michal K Cyranski et al. "To what extent can aromaticity be defined uniquely?" In: *The Journal of Organic Chemistry* 67.4 (2002), pp. 1333–1338. DOI: https://doi.org/10.1021/jo016255s (cit. on p. 69).

[219] Jordi Poater et al. "Discrepancy between common local aromaticity measures in a series of carbazole derivatives". In: *Physical Chemistry Chemical Physics*

6.2 (2004), pp. 314–318. DOI: https://doi.org/10.1039/B309965B (cit. on p. 69).

[220] Johan Aberg. "Quantifying superposition". In: *arXiv preprint quant-ph/0612146* (2006). DOI: https://doi.org/10.48550/arXiv.quant-ph/0612146 (cit. on p. 69).

[221] Tillmann Baumgratz, Marcus Cramer, and Martin B Plenio. "Quantifying coherence". In: *Physical review letters* 113.14 (2014), p. 140401. DOI: https://doi.org/10.1103/PhysRevA.105.042410 (cit. on pp. 69, 71).

[222] Alexander Streltsov, Gerardo Adesso, and Martin B Plenio. "Colloquium: Quantum coherence as a resource". In: *Rev. Mod. Phys.* 89.4 (2017), p. 041003. DOI: https://doi.org/10.1103/RevModPhys.89.041003 (cit. on p. 69).

[223] Kavan Modi et al. "The classical-quantum boundary for correlations: Discord and related measures". In: *Rev. Mod. Phys.* 84.4 (2012), p. 1655. DOI: https://doi.org/10.1103/RevModPhys.84.1655 (cit. on p. 69).

[224] Gerardo Adesso, Thomas R Bromley, and Marco Cianciaruso. "Measures and applications of quantum correlations". In: *J. Phys. A: Math. Theor.* 49.47 (2016), p. 473001. DOI: https://doi.org/10.1088/1751-8113/49/47/473001 (cit. on p. 69).

[225] Thomas Theurer et al. "Resource theory of superposition". In: *Phys. Rev. Lett.* 119.23 (2017), p. 230401. DOI: https://doi.org/10.1103/PhysRevLett.119.230401 (cit. on p. 70).

[226] Gökhan Torun, Hüseyin Talha Şenyaşa, and Ali Yildiz. "Resource theory of superposition: State transformations". In: *Physical Review A* 103.3 (2021), p. 032416. DOI: https:https://doi.org/10.1103/PhysRevA.103.032416 (cit. on p. 70).

[227] Hüseyin Talha Şenyaşa and Gökhan Torun. "Golden states in resource theory of superposition". In: *Physical Review A* 105.4 (2022), p. 042410. DOI: https://doi.org/10.1103/PhysRevA.105.042410 (cit. on p. 70).

[228] Onur Pusuluk. "Unified view of quantum superposition and quantum indistinguishability". In: *arXiv preprint arXiv:2210.02398* (2022). DOI: https://doi.org/10.48550/arXiv.2210.02398 (cit. on p. 70).

[229] Dorje C Brody. "Biorthogonal quantum mechanics". In: *Journal of Physics A: Mathematical and Theoretical* 47.3 (2013), p. 035305. DOI: https://doi.org/10.1088/1751-8113/47/3/035305 (cit. on p. 72).

[230] Ali Mostafazadeh. "Pseudo-Hermitian representation of quantum mechanics". In: *International Journal of Geometric Methods in Modern Physics* 7.07 (2010), pp. 1191–1306. DOI: https://doi.org/10.1142/S0219887810004816 (cit. on p. 72).

[231] Chia-Yi Ju et al. "Non-Hermitian Hamiltonians and no-go theorems in quantum information". In: *Physical Review A* 100.6 (2019), p. 062118. DOI: https://doi.org/10.1103/PhysRevA.100.062118 (cit. on p. 72).

[232] Frank Weinhold. "Chemical bonding as a superposition phenomenon". In: *Journal of chemical education* 76.8 (1999), p. 1141. DOI: https://doi.org/10.1021/ed076p1141 (cit. on p. 73).

[233] Frank Weinhold and Roger A Klein. "What is a hydrogen bond? Resonance covalency in the supramolecular domain". In: *Chemistry Education Research and Practice* 15.3 (2014), pp. 276–285. DOI: https://doi.org/10.1039/C4RP00030G (cit. on p. 73).

[234] Gernot Frenking and Sason Shaik. *The chemical bond: fundamental aspects of chemical bonding*. Vol. 1. John Wiley & Sons, 2014 (cit. on p. 73).

[235] Russell D Johnson III. "NIST computational chemistry comparison and benchmark database, NIST standard reference database number 101". In: *Release 22 http://cccbdb. nist. gov/(accessed April 11, 2023)* (2022). DOI: https://doi.org/10.18434/T47C7Z (cit. on p. 75).

[236] Ronald Breslow and John T Groves. "Cyclopropenyl cation. Synthesis and characterization". In: *Journal of the American Chemical Society* 92.4 (1970), pp. 984–987. DOI: https://doi.org/10.1021/ja00707a040 (cit. on p. 75).

[237] Steven R Kass. "Cyclopropenyl anion: an energetically nonaromatic ion". In: *The Journal of Organic Chemistry* 78.14 (2013), pp. 7370–7372. DOI: https://doi.org/10.1021/jo401350m (cit. on p. 75).

[238] Alexandru T Balaban, Daniela C Oniciu, and Alan R Katritzky. "Aromaticity as a cornerstone of heterocyclic chemistry". In: *Chemical reviews* 104.5 (2004), pp. 2777–2812. DOI: https://doi.org/10.1021/cr0306790 (cit. on p. 77).

[239] Jian Wu, T. G. Schmalz, and D. J. Klein. "An extended Heisenberg model for conjugated hydrocarbons. II. Kekulé basis". In: *J. Chem. Phys.* 119.21 (Dec. 2003), pp. 11011–11016. DOI: https://doi.org/10.1063/1.1622659 (cit. on p. 83).

[240] Klaus Hornberger et al. "Colloquium: Quantum interference of clusters and molecules". In: *Rev. Mod. Phys.* 84.1 (Feb. 2012), pp. 157–173. DOI: https://doi.org/10.1103/revmodphys.84.157 (cit. on p. 83).

[241] Christian Brand et al. "Conformer Selection by Matter-Wave Interference". In: *Phys. Rev. Lett.* 121 (17 Oct. 2018), p. 173002. DOI: https://link.aps.org/doi/10.1103/PhysRevLett.121.173002 (cit. on p. 83).

[242] Christian Brand et al. "Bragg Diffraction of Large Organic Molecules". In: *Phys. Rev. Lett.* 125 (3 July 2020), p. 033604. DOI: 10.1103/PhysRevLett.125.033604 (cit. on p. 83).

[243] Ferran Feixas et al. "Patterns of π-electron delocalization in aromatic and antiaromatic organic compounds in the light of Hückel's 4n + 2 rule". In: *Phys. Chem. Chem. Phys.* 12.26 (2010), p. 7126. DOI: https://doi.org/10.1039/b924972a (cit. on pp. 83, 84).

[244] Ceren Dağ et al. "Multiatom Quantum Coherences in Micromasers as Fuel for Thermal and Nonthermal Machines". In: *Entropy* 18.7 (June 2016), p. 244. DOI: https://doi.org/10.3390/e18070244 (cit. on p. 83).